Spatial Transformations in Frontal Cortex During Memory-Guided Head-Unrestrained Gaze Shifts

Amirsaman Sajad

A DISSERTATION SUBMITTED TO THE FACULTY OF GRADUATE STUDIES IN PARTIAL FULFILLMENT OF THE REQUIREMENTS FOR THE DEGREE OF

DOCTOR OF PHILOSOPHY

Graduate Program in Biology

York University

Toronto, Ontario

May 2016

Abstract

We constantly orient our line of sight (i.e., gaze) to external objects in our environment. One of the central questions in sensorimotor neuroscience concerns how visual input (registered on retina) is transformed into appropriate signals that drive gaze shift, comprised of coordinated movement of the eyes and the head. In this dissertation I investigated the function of a node in the frontal cortex, known as the frontal eye field (FEF) by investigating the spatial transformations that occur within this structure. FEF is implicated as a key node in gaze control and part of the working memory network. I recorded the activity of single FEF neurons in head-unrestrained monkeys as they performed a simple memory-guided gaze task which required delayed gaze shifts (by a few hundred milliseconds) towards remembered visual stimuli. By utilizing an elaborate analysis method which fits spatial models to neuronal response fields, I identified the spatial code embedded in neuronal activity related to vision (visual response), memory (delay response), and gaze shift (movement response). First (Chapter 2), spatial transformations that occur within the FEF were identified by comparing spatial codes in visual and movement responses. I showed eye-centered dominance in both neuronal responses (and excluded head- and space-centered coding); however, whereas the visual response encoded target position, the movement response encoded the position of the imminent gaze shift (and not its independent eye and head components), and this was observed even within single neurons. In Chapter 3, I characterized the time-course for this target-to-gaze transition by identifying the spatial code during the intervening delay period.

The results from this study highlighted two major transitions within the FEF: a gradual transition during the visual-delay-movement extent of delay-responsive neurons, followed by a discrete transition between delay-responsive neurons and pre-saccadic neurons that exclusively fire around the time of gaze movement. These results show that the FEF is involved in memory-based transformations in gaze control; but instead of encoding specific movement parameters (eye and head) it encodes the desired gaze endpoint. The representations of the movement goal are subject to noise and this noise accumulates at different stages related to different mechanisms.

Dedication

I dedicate this dissertation

to my mother, my father and my grandmother.

Acknowledgements

First, I would like to express my most sincere gratitude to my supervisor, Prof. Doug Crawford, for his incomparable mentorship during my graduate work. With his vision in science, his effective management, and his continuous support he provided me with an amazing working environment during my PhD. In addition to science and research, in Doug's lab I learned invaluable life lessons that will serve me a lifetime. Doug: you truly are the best scientific father I could have asked for. Thank you!

Furthermore, I would like to thank my committee members, Drs. Kari Hoffman and Thilo Womelsdorf, for their insightful comments and encouragement throughout my PhD. I also want to thank my fellow lab members for the stimulating discussions and all the fun and happy experiences, and especially Drs. Xiaogang Yan, and Hongying Wang, and Mrs. Saihong Sun for their continual help with technical aspects.

I want to take this opportunity to thank my dear parents who have endlessly supported me throughout my life. Despite geographical distance between us I never felt alone because I knew the one thing I could always count on is their love, care and support. Thank you dad for all you have done for me. And thank you mom for having sacrificed beyond imagination for me to be where I am today. Also, a very special thanks to my dear grandmother without whom my life in Canada would have been impossible. No words can fully express how much I appreciate all she has done for me. The years I spent with her have been a precious gift that I will always cherish. Thank you!

And last but not least, I want to thank my brothers, my loved ones, and my friends whose love and support helped me through all the ups and downs in life. Without these incredible people my life just wouldn't be the same.

Candidate Contribution

The candidate (Amirsaman Sajad) was involved in all stages of the experimental work, including experiment design, data acquisition, animal training, data analysis and the write up of the manuscripts presented in this dissertation. This would have not been possible without the help of the co-authors:

Morteza Sadeh and Drs. Xiaogang Yan and Hongying Wang assisted with training the subjects, surgery and early phases of the collection of data that's presented in this dissertation.

Dr. Gerald P Keith contributed to the development of the model-fitting method (Keith et al., 2009; also used in DeSouza et al., 2011 and Sadeh et al., 2015) used throughout these studies. This method was further elaborated by the candidate to consider additional coding schemes critical for the primary conclusions on this dissertation.

Prof J.D. Crawford supervised the project and provided critical input and guidance into designing the studies conducted in this dissertation, presenting the data, and the write up of the manuscripts.

Table of Contents

Table of Illustrations

Chapter 1: General Introduction

Primates constantly sample sensory information in order to interact with the environment. They have evolved to perform complex behaviours which are dissociated both in space and time from those defined by the bottom up sensory input. A central question in sensorimotor neuroscience concerns what sequence of events takes place in order to transform vision into voluntary action. The traditional approach in sensorimotor neuroscience considers the brain as a black box with sensory information (and already acquired information) as input and the behaviour as output. With this approach, the brain is divided into a sequence of distinct functional and/or anatomical nodes. The goal of sensorimotor neuroscience is to use various techniques including (but not limited to) disruption in normal function (by means of lesion, microstimulation, or temporary inactivation) or recording brain activity during normal function (using techniques such as single-unit recording or brain imaging) to attribute function to each node. Once a full understanding of the function of each node is gained the processes within the entire system (i.e., brain) can be understood.

This dissertation describes experiments I performed on one of the nodes in the visuomotor pathway, called the frontal eye field (FEF) located in the frontal cortex (Bruce and Goldberg, 1985). Specifically, I recorded from the activity of single neurons (single-unit recording) in the monkey FEF during head-unrestrained gaze shifts to understand the function of this structure in gaze control. Head-unrestrained conditions enabled me to consider spatial models that have been proposed to exist in the cascade of visuomotor processing but have largely

remained unidentified (see section 1.4). I identified changes in spatial code that occur in the time spanning visual stimulation of the retina and the gaze movement, separated by a short memory interval. This allowed me to characterize the nature of the spatial transformations that take place within the FEF, and to understand the spatial information encoded during the short-term retention interval, temporally separating the input- and output-related signals. The results from these experiments have important implications in understanding the functional role of FEF with respect to the spatial transformations in the gaze control system. Also, it allows us to understand the type of spatial information maintained in spatial working memory. In the following sections of the introduction I will introduce the gaze control system, provide background on the type of spatial codes observed in this system, introduce working memory as a linking bridge between vision and action, and introduce the experimental chapters (2 and 3) of the dissertation.

1. 1. Introduction to gaze control system

One of the best study models in sensorimotor neuroscience is the saccadic system in primates used to reorient the retinal fovea toward visual stimuli in space. A saccadic eye movement is characterized as a fast (200-900 degrees/sec) ballistic movement of the eyes that shifts the line of sight (i.e., gaze) in space (Robinson, 1978). Because of the ballistic nature of saccades the gaze control system cannot benefit from sensory feedback but instead relies on internal forward models that predict the sensory consequences of motor commands (Wolpert and Ghahramani, 2000). Primates on average make 3-4

saccadic eye movements to scan the visual environment. The saccadic system is well characterized partly due to its simple structure: Only three pairs of muscles are involved in generating eye rotations, inertial influences are negligible and the geometry of eye movement is less complex compared to other motor systems (Robinson, 1971).

In natural conditions re-orienting the fovea often involves the coordinated movement of the eyes (saccades), the head, and sometimes even the body. However, most studies have only studied the gaze control system by focusing exclusively on the saccadic component (by immobilizing the head and the body). This is especially because few experimental techniques allow the study of the brain while the subject's head freely moves. A complete understanding of the gaze control system requires studying this system in conditions where the full structural complexity of visual input and behavioural outputs are considered. In this dissertation I will discuss this motor system by considering a more natural output structure compared to most previous studies: gaze shift comprised of both eye and head movements.

1. 2. Behavioural aspects of eye-head gaze shifts

Movements of the eyes and head are described by rotations in three dimensions: horizontal (about the vertical axis), vertical (about the horizontal axis), and torsional (about its orientation axis) (Crawford et al., 2003). One problem the brain deals with is a degree of freedom problem: many combinations of eye and head orientations can result in orienting the line of sight towards the intended object. This is further complicated by the fact that rotations are non-commutative

(i.e., order matters) meaning that in order to get from one orientation to another, it matters what sequence of rotations are implemented (Tweed et al., 1999; Tweed and Vilis, 1987).

Donders showed that in order to orient the line of sight in a given direction, the eye assumes a fixed orientation in space irrespective the pre-saccadic orientation (Donders, 1848). In other words the eye only assumes one three-dimentional orientation for a given horizontal and vertical gaze angle. The vector that describes the rotation of the eye (using right-hand rule conventions) would have zero torsional component (relative to the head) and thus fall on a single plane, known as the Listing's plane (Tweed and Vilis, 1990) (Figure 1.1).

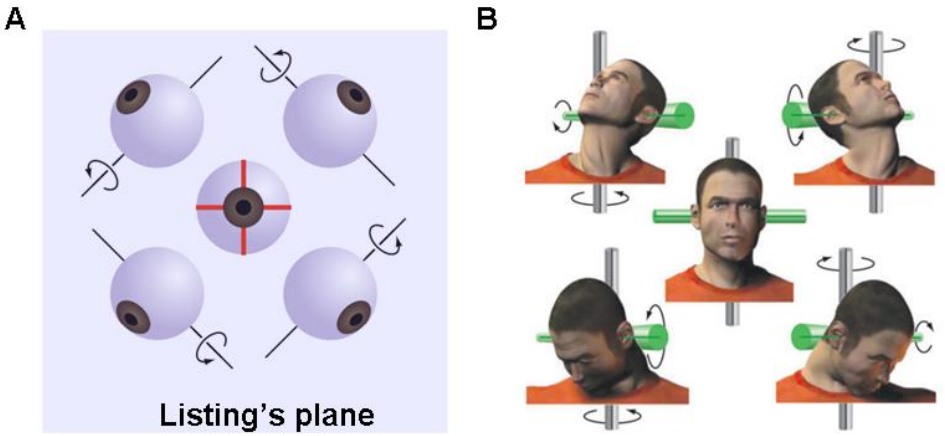

Figure 1.1. Geometric constraints on the gaze control system. A) Listing's law states that the eye assumes only orientations that can be reached from a central primary eye position through fixed-axis rotations about axes within a head-fixed plane. Direction of rotation about four example axes are shown. Torsion is defined as rotation about the axis aligned with gaze at primary eye position—here, orthogonal to the page. B) The Fick strategy states that the head assumes only orientations that can be reached through rotations about a body fixed vertical axis (black lines embedded in gray cylinders) and a head-fixed horizontal axis (green lines and cylinders). (modified from Crawford et al., 2011)

The head also follows Donder's law, but its rotations follow a geometrically different constraint referred to as the Fick strategy in which head rotation vectors are confined to the Fick coordinates (Crawford et al., 2003). According to this strategy, any head rotation is described as a succession of rotations first in horizontal, next in vertical, and finally in torsional components. It has been shown that these constraints are neurally implemented (Radau et al., 1994; Crawford et al., 2003) (Figure 1.1).

A curious thing about gaze shift with coordinated eye and head movement (henceforth referred to as *eye+head gaze shift*) is that although eyes and head follow Donder's law, for the same desired change in line of sight, the relative contributions of the eyes and the head are quite variable (Bizzi et al., 1971; Freedman and Sparks, 1997). The source of this variability is unknown, but it has been shown that it can depend on factors such as initial eye and head position, and even cognitive factors such as urgency and task requirements (Freedman and Sparks, 1997; Fang et al., 2015). Freedman and Sparks have shown that in monkeys, usually for gaze shifts larger than 20 degrees head movement is recruited, and the amount of head contribution on average monotonically increases with the magnitude of the gaze shift (Freedman and Sparks, 1997).

Visually-guided gaze shifts are typically initiated by a saccadic eye-in-head movement, and a head movement that lags behind (Freedman, 2008). However, in cases where the shift of gaze is instructed to be delayed, the onset of eye movement lags behind head movement onset. At the end of the saccadic component of the gaze shift the head normally continues moving due to inertial

effects for an additional 100-300ms. The time of peak head velocity appears to be synchronized with the end of the gaze shift (Chen & Tehovnik 2007). Following the saccadic component of the gaze shift, gaze remains stable on the visual target by a neural mechanism which drives the eyes to counter-roll in the head to compensate for the head rotation (Bizzi et al., 1971). This is known as the Vestibulo Occular Reflex (VOR). So, a complete eye+head gaze shift can be described by an initial saccadic phase, a head movement that starts around the time of saccade onset (but usually a short time after saccade onset), and a VOR phase, in which the head continues moving while gaze remains stable on the target (Figure 1.2).

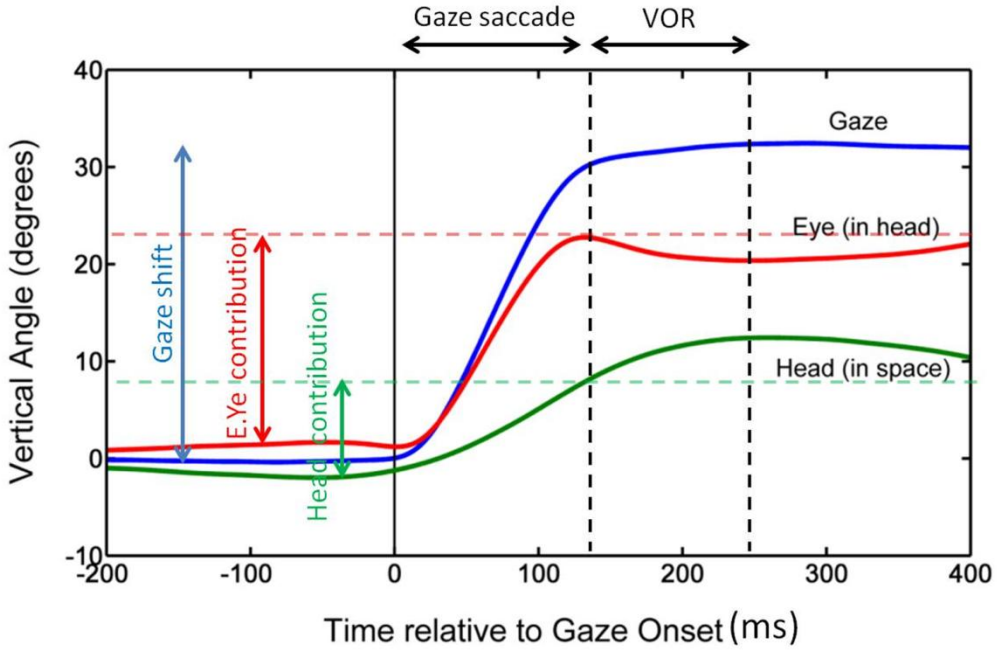

Figure 1.2. 1-D position of gaze effectors before, during and after an eye+head gaze shift. Gaze shift (blue) is contributed by both the eye (red) and the head (green). When the gaze stabilizes on the visual stimulus (end of gaze saccade) the head continues to move, during which time the eye counter-rolls in its orbit to maintain a stable gaze position (during VOR phase).

1.3. Neural Substrates for Saccades and Gaze Shifts

Much of what we understand about primate neurophysiology comes from the study of non-human primates. With the advent of new brain imaging techniques such as magnetoencephalography (MEG) and functional magnetic resonance imaging (fMRI) our understanding of the human brain has grown rapidly, and many homologies have been found between in the two species (Wager and Yarkoni, 2012). Since the experiments presented in this dissertation are on rhesus macaque monkey, much of the neurophysiology explained here will be based on the macaque brain, though similar neural mechanisms exist in the human brain.

The first step in visuomotor processing for gaze control starts from the retina, which contains photoreceptors sensitive to light. This retinal activation activates neurons whose axons cross the midline at the optic chiasm and terminate in the lateral geniculate nucleus (LGN) in the thalamus. The LGN in turn projects to the primary visual cortex, area V1 (Van Essen et al., 1992). Signals from V1 then diverge into two relatively segregated (but interconnected) processing streams: the dorsal stream processes information related to "where" and which concerns "action" and the ventral stream processes information related to "what" which concerns “perception” (Goodale and Milner, 1992; Bullier et al., 1996). Processing in both streams is hierarchical (Felleman and Van Essen, 1991). In the ventral stream, different segments of the visual stimulus are realized into a feature as signals are processed further in the association areas (Lerner et al., 2001). Similarly, the spatial information used for action are processed in a multi-

stage process, starting from the location of the visual stimulus and ending with spatial signals for effective action (Cui, 2014). Since the work in this dissertation focuses on spatial transformations, the remainder of the introduction will be focused on the dorsal stream.

Throughout the dorsal pathway, at least two types of neuronal responses are abundantly observed which are important for sensorimotor processing: Visual response, which is characterized as a burst of action potentials time-locked to visual stimulation (related to retinal input), and the motor response, which is a burst of action potentials time-locked to gaze movement onset (Bruce and Goldberg, 1985; Hikosaka and Wurtz, 1983; Funahashi et al., 1989; Robinson, 1971; Bizzi and Schiller, 1970). It has been shown that the average rate of action potentials (firing rate) of these neuronal responses encode spatial information (Adrian, 1928; Quiroga and Panzeri, 2009). Many neurons in the visuomotor pathway exhibit spatial selectivity such that they show maximal firing in response to a specific patch of space, known as response field (receptive field specifically for visual sensitivity, and movement field for movement-related activity) (Hubel and Wiesel, 1959; Mohler et al., 1973; Sparks et al., 1976). This patch of space can often be approximated by a Gaussian or semi-Gaussian shape representing the average firing rate of the neuron in response to a specific position in space (Bruce and Goldberg, 1985; Platt and Glimcher, 1998). Although activity of single neurons contains spatial information, it is the activity of a population of neurons that encodes a position in space with each neuron only serving as a small

contributor to the encoded information (Georgopoulos et al., 1986; Quiroga and Panzeri, 2009).

After early visual processing in the occipital cortex, visual signals are prominently projected to the posterior parietal cortex (PPC) for additional spatial processing (Mountcastle et al., 1975). The PPC itself is divided into different subregions dedicated to different perceptual and movement-related functions (Andersen 1989). There is some degree of effector specificity within the different parts of the parietal cortex. For instance, three regions namely, the medial- (MIP), anterior- (AIP), lateral- (LIP) intraparietal areas are largely found to encode information related to reach, grasp and saccadic eye movements (Vesia et al., 2012; Andersen et al., 1989). In the gaze circuitry, activity from PPC (mainly LIP) is projected to different parts in the frontal cortex, including the frontal eye field (FEF), dorsolateral prefrontal cortex (dlPFC) and mediodorsal prefrontal cortex, specifically referred to as the supplementary eye fields (SEF) (Schall, 2015). Most areas in the PFC are not implicated in saccade generation per se, but are involved in higher cognitive control of movements (Badre and D'Esposito, 2009; Koval et al., 2011). The FEF however, is implicated as a key frontal area involved in saccade production (Bruce and Goldberg, 1985; Schiller et al., 1980). This structure is located at the apex of cortical motor hierarchy (Tehovnik et al., 2000) and sends signals down to the brain stem nuclei (especially the superior colliculus and saccade generator circuitry) that are critical to gaze movement generation (Kunzle et al., 1976; Segraves, 1992; Schiller et al., 1987).

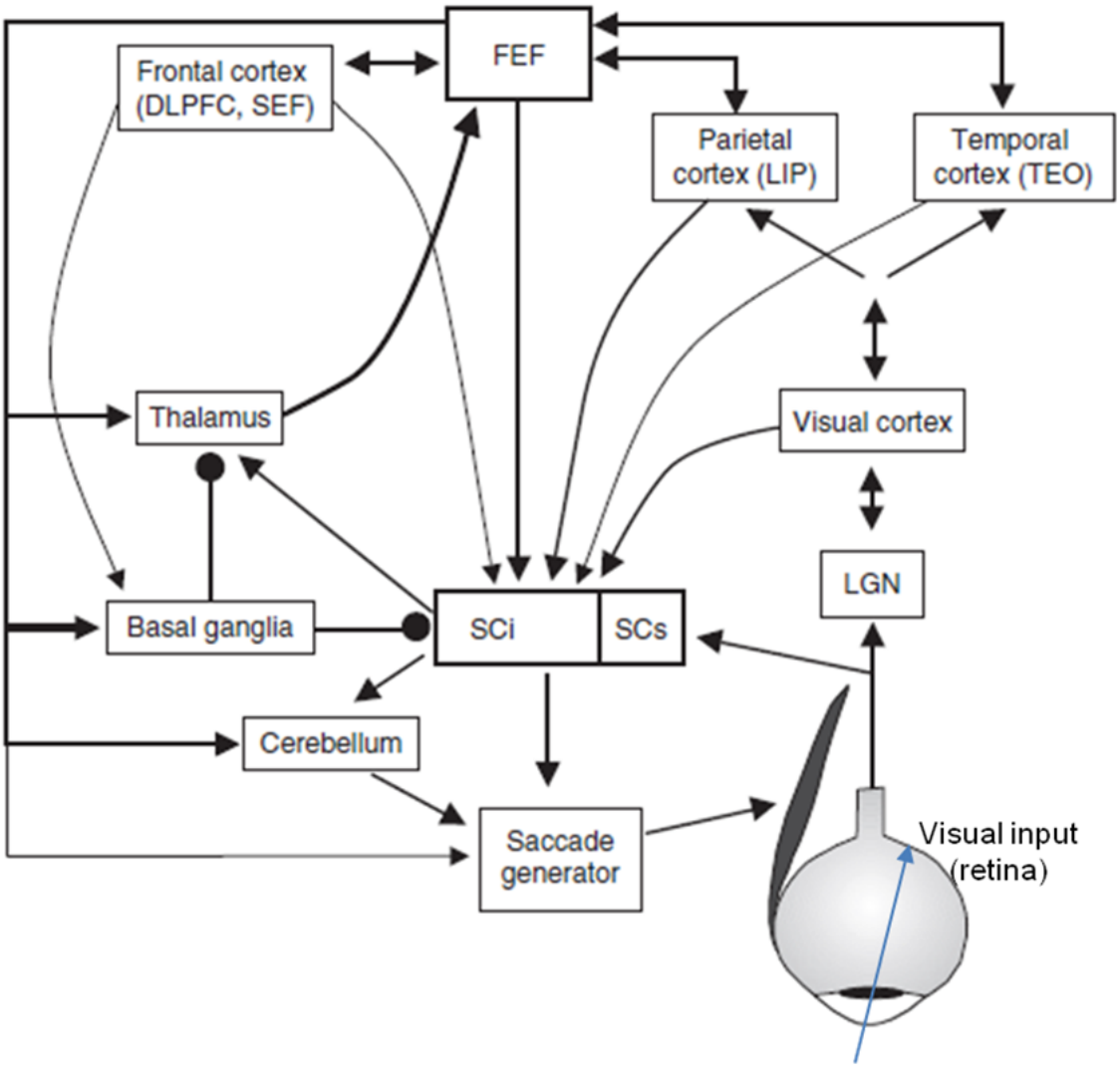

Figure 1.3. Schematic of some brain structures (and anatomical connections) involved in saccade generation. Visual input from the retina is transmitted to the lateral geniculate nucleus (LGN) and the superficial layers of the superior colliculus (SCs). The LGN transmits visual signals to primary visual cortex, where processing proceeds through areas in the ventral stream (areas in temporal lobe - TEO - particularly involved in feature processing) and the dorsal stream (areas mainly in parietal lobe such as area LIP). Extrastriate visual areas are reciprocally connected with the frontal eye field (FEF), although the main projections are from LIP. FEF is also connected with dorsolateral prefrontal cortex (DLPFC) and the supplementary eye field (SEF). FEF influences saccade production through projections to the intermediate layers of the superior colliculus (SCi), the basal ganglia, the cerebellum, and the mesencephalic and pontine brain stem saccade nuclei. (modified from Schall 2009)

As can be noted in this general overview, there appears to be a progression of signals from occipital cortex to parietal cortex, and then to the frontal cortex, down to the brain stem circuitry. However, this is only a simplified scheme, as many of these brain areas mentioned above make reciprocal connections with each other. Also, information processing does not occur sequentially, but rather occurs in parallel across a distributed network (Wurtz et al., 2001).

Since the focus of this dissertation is on the FEF, below I have provided a more detailed review of some of the major nodes along the viosuomotor pathway that are interconnected with the FEF.

1.3.1. Lateral Intraparietal Area

The LIP receives projections from extrastriate visual areas as well as other subregions in the parietal cortex (Blatt et al., 1990). Microstimulation of the LIP evokes saccadic eye movements (Andersen et al., 1992). LIP makes reciprocal connections with the FEF as well as other prefrontal areas, including dlPFC and SEF (Schall, 2015). LIP neurons are particularly responsive to visual stimulation (visual response) but often also respond just before a saccadic eye movement. However, LIP neurons rarely show response exclusively during (or around the time of) movement (Andersen et al., 1992; Bisley et al., 2003). It has been shown that the LIP has spatial representation of the visual world, but one in which static objects with no behavioural relevance are filtered out (Gottlieb et al., 1998). Some studies have suggested that LIP is involved in movement planning (coding intention) while some others have proposed that it encodes attention (Gnadt et al., 1988; Quiroga et al., 2006; Bisley and Goldberg, 2010). Although there is a

tight coupling between attention and movement preparation (as proposed by the premotor theory of attention; Rozzolatti et al., 1987, but also see Smith and Schenk, 2012), the LIP is shown to not be exclusively involved in saccade planning, but serve more as a salience map (Bisley and Goldberg, 2010). When multiple salient stimuli are present LIP salience map shows multiple hills of activity determining the behavioural priority of the various parts of the visual field. In agreement with this, LIP is also known to exhibit activity correlating with reward expectation (Sugrue et al., 2004), decision making (Platt and Glimcher, 1999), and time perception (Leon and Shadlen, 2003; Jazayeri and Shadlen, 2015), and LIP activity is not always congruent with the movement plan. The function of this salience map is defined by its projections. Motor-related outputs of the LIP are mainly sent to two oculomotor structures, FEF and SC (Ferraina et al., 2002; Pare and Wurtz, 1997), both implicated as critical nodes in the oculomotor circuitry. However, the LIP is also connected with other areas in the ventral stream, allowing this saliency map to serve functions related to visual perception (Goldberg et al., 2006).

1.3.2. Frontal Eye Field

The frontal eye field (FEF) is located at the rostral bank of the arcuate sulcus in monkeys (Bruce and Goldberg, 1985). This prefrontal area has been extensively studied as one of the key nodes in the saccade circuitry. The FEF was first discovered by Ferrier who showed that low stimulation currents from this site in the frontal cortex can generate eye movements (Ferrier, 1876). Although FEF lesion or inactivation by itself does not result in permanent loss of saccadic

function (Schiller et al., 1987; Hanes and Wurtz, 2001), it results in significant deficiencies in tasks involving voluntary control of saccades which require a dissociation of the gaze movement from visual stimulus either in the spatial (e.g., anti-saccades which require saccade to position opposite to target location) or temporal (e.g., memory-guided tasks) domains (Guitton et al., 1985; Pierrot-Deseilligny et al., 1991; Dias and Segraves, 1999). FEF receives various inputs from extra-striate visual areas, areas in prefrontal cortex including dlPFC, and SEF, and subcortical structures, and sends projections to the SC and gaze (saccade)-generator circuitry in reticular formation (Schall et al., 1995; Kunzle et al., 1976; Segraves, 1992; Stanton et al., 1988; Lynch et al., 1994). However, the control of saccades by FEF is mainly mediated through the SC (Hanes and Wurtz, 2001). Low current stimulation of the FEF generates saccadic eye movements and eye-head coordinated gaze shifts (Bruce et al., 1985, Monteon et al., 2010). Shorter saccades are represented more laterally in the FEF and longer saccades are represented more medially (Bruce et al., 1985). This is in agreement with the differences in inputs into these subregions of the FEF. Although both the lateral (short-saccade) and medial FEF receive inputs from the extrastriate visual areas in the dorsal pathway, the lateral FEF also receives inputs from areas in the ventral stream which is in agreement with the functional role of short saccades in exploratory behaviour within the visual field. (Schall et al., 1995; Babapoor-Farrokhran et al., 2013).

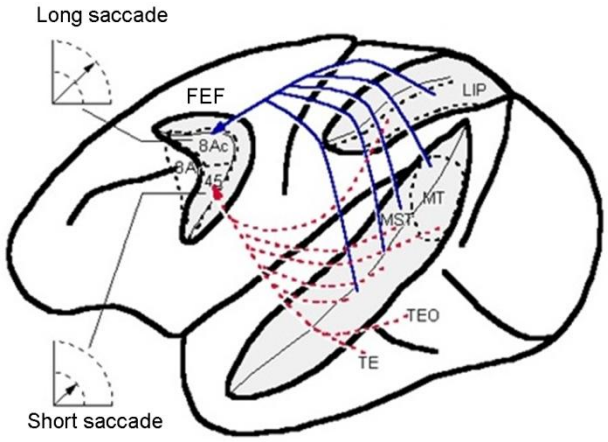

Figure 1.4. Visual input into the FEF. Visual input from dorsal (LIP, MT/MST) and ventral stream (TEO and TE) into lateral (short-saccade) and medial (long-saccade) FEF. Lateral FEF, where smaller amplitude saccades are represented receives more input from ventral areas whereas the medial FEF receives signals almost exclusively from the dorsal stream (modified from Schall et al., 1995).

There is a gradient of visual-to-motor responsiveness of pre-saccadic neurons: some neurons only respond to the visual stimulation of the retina (visual neurons), some contain both visual and motor responses (visuomovement neurons), and some only fire prior to (and during) saccade (movement neurons) (Bruce and Goldberg, 1985). Similar to LIP, activity in the FEF has been described as a priority or salience map of space (Thompson and Bichot, 2005). It influences attention through its projections to extrastriate visual areas (Moore and Armstrong, 2003; Moore and Fallah, 2004).

Visual activity in the FEF is involved in visual detection as well as processes such as target selection (Schall and Hanes, 1993), movement detection (Ferrera et al., 2009), and even feature detection (only acquired after training; Bichot et al. 1996). The movement response in the FEF is tightly coupled with saccade generation towards the contralateral hemifield. It has been shown that once the pre-saccadic movement activity in the FEF reaches a fixed threshold a saccade is generated; though it has been shown that this threshold is flexibly controlled, possibly through subcortical influences (Hanes and Schall, 1996; Jantz et al.,

2013). With clear visual and motor functions of the FEF, this structure is implicated as one of the critical nodes (and thus a great study model) for visuo-motor transformations for gaze control. As most experiments on FEF have been performed in head-restrained conditions the function of the FEF in the control of coordinated eye+head gaze shifts remains largely unknown. (but see sections 1.4 and 1.5).

1.3.3. Supplementary Eye Field

The SEF is located in the dorsomedial frontal cortex just anterior to the supplementary motor area (Schlag, and Sclag-Rey, 1987). This area has been largely implicated as a brain area involved in aspects related to saccadic eye movements and eye-head coordinated gaze shifts (Martinez-Trujillo et al., 2003). Similar to LIP and FEF, SEF neurons exhibit both visual and movement responses (Schlag, and Sclag-Rey, 1987).

SEF makes reciprocal connections with the FEF, PPC, and anterior cingulate cortex, an area in the prefrontal cortex involved in performance monitoring (Schall, 2015; Carter et al., 1997). The visual response in SEF has a later latency compared to FEF visual response (Schmolesky et al., 1998) and although it is implicated as a salience map it is functionally distinct from the FEF (for instance it is not critically involved in target selection for saccades unlike the FEF) (Purcell et al., 2012).

Unlike the FEF, inactivation of this area does not compromise saccade production in simple oculomotor tasks (Schiller & Chou 2000). In agreement with this, it has been shown that SEF activity does not directly control the production

of single saccades, but is crucial to the production of sequential saccades (Isoda & Tanji 2002, Lu et al. 2002,). SEF is suggested to contribute to abstract representations that are involved in performance in complex tasks (Amador et al. 2004, Moorman & Olson 2007, Stuphorn et al. 2010) to a greater extent than the FEF (Middlebrooks & Sommer 2012).

1.3.4. Superior Colliculus

The superior colliculus (SC) (homolog of optic tectum in non-mamalians), located in the roof of the brain stem is the most conserved structure in the visuomotor pathway and its Lesion can have detrimental effects on saccadic behaviour (Schiller et al., 1980; Wurtz and Goldberg, 1972). Reversible inactivation of the SC transiently impairs production of the saccades even when FEF is stimulated (Hanes and Wurtz, 2001). The SC is the point of convergence of signals across many modalities (visual, auditory, tactile) and in addition to the FEF it receives input from many cortical structures in occipital, parietal, and frontal areas (Meredith and Stein, 1986; Fries, 1984). SC also receives direct visual input from the retina, enabling the sensorimotor cascade to bypass cortical processing in certain conditions (Robinson and McClurkin 1989; Sparks, 1986; Isa and Kobayashi, 2004; Takura et al., 2011).

The SC contains three main layers divided based on cytoarchitectural properties of the neurons: superficial, intermediate and deep layers. The superficial layer contains neurons which are responsive almost exclusively to visual stimuli (appearing in the contralateral hemifield), and the main projection site for retinal input. Neurons in the intermediate and deep layers on the other hand receive

inputs from various cortical areas (including the FEF) and are responsive to multiple modalities with some that discharge a burst prior to orienting movement (Wurtz et al., 2001; Sommer and Wurtz, 2000; Ferraina et al., 2001; Gandhi and Katnani, 2011). Neurons in the SC that serve orienting behaviour (neurons with motor activity) are structured along a caudal-rostral axis, with the caudal regions for longer saccades and the rostral regions for shorter saccades (Schiller and Stryker, 1972). Similar to the FEF, the population activity in the SC can provide a saccade vector coordinates and once the discharge rate of neurons reaches a threshold a saccade is initiated (Paré and Hanes 2003; Zandbelt et al., 2014). SC population activity can also contribute to the kinematics of the movement as the frequency of action potentials of burst neurons are correlated with peak velocity of the saccade (Waitzman et al., 1991); a feature that is not observed in FEF movement activity (Segraves and Park, 1993).

At the pole of the rostral end, neurons that respond during active fixation of gaze (fixation neurons) are also identified (Munoz and Wurtz, 1993). Models of gaze control suggest that gaze movement initiation depends on the balance of activity between the "go" and "stop/ No-go" signals that originate from motor neurons and fixation neurons respectively (Munoz et al., 2000). These two signals project to the gaze-related nuclei in the brainstem that in turn project to motor neurons driving eye and head movement (Scudder et al., 2002).

1.3.5. Gaze (and saccade) generator circuitry:

The brainstem circuitry involved in generation of eye and head movements receives direct inputs from both the SC and (to a lesser extent) the FEF. These

brainstem nuclei in turn project to motorneurons that innervate eye and head (neck) muscles. The mechanisms by which the gaze command is dissociated into separate eye and head signals, and the coordination of the two effectors is largely unknown (Chen and Tehovnik, 2007). Compared to the oculomotor system, much less is known about the neural circuits for head control. Therefore, here, I will largely focus on the saccade generator circuitry; but it has been suggested that the head generator circuitry may follow the same principles as those in the oculomotor circuitry (Isa and Sasaki, 2002).

The eyes rotate by the action of three pairs of muscles. Horizontal rotations are produced by medial and lateral rectus muscles. Vertical rotations are produced by superior and inferior rectus and superior and inferior oblique muscle pairs and torsional movements are produced by contractions of combinations of superior/ inferior rectus and superior/inferior oblique muscle pairs (Robinson, 1971). Different motor neurons innervate each muscle (Fuchs and Luschei, 1971). The neural signal necessary to drive a saccadic eye movement requires two distinct phases: a pulse of activation, required to move the eye against the viscous drag, followed by a step signal to maintain muscle activation to keep eye in the desired orientation (against the tendency of eyes to move back due to elasticity) (Robinson, 1964). Importantly, the horizontal, vertical, and torsional movements of the eyes are controlled by distinct neural mechanisms.

Neurons in paramedian pontine reticular formation (PPRF) and in the medulla show horizontal saccade-related activity (Cohen et al., 1972; Sparks and Travis, 1971). The medium-lead burst neurons (MLBN) provide the pulse signal just

before ipsilateral saccades. Their activity is temporally locked to saccade onset and is hypothesized to originate from long-lead burst neurons (LLBN) who show a build-up of activity prior to saccade onset. MLBNs make monosynaptic connections to cranial motor neurons and thereby provide the main source of excitatory drive for saccade-related activity (Scudder et al., 2002). The number of spikes, burst duration, and peak firing rate of these neurons are coupled to amplitude, duration and velocity of saccade respectively. The step signal (horizontal eye position) is provided by neurons in the nucleus prepositus hypoglossi (NPH) and the medial vestibular nucleus (MVN) (Sparks, 2002).

For vertical movements excitatory burst neurons in the rostral interstitial nucleus of medial longitudinal fasciculus (riMLF) generate a high frequency burst which determine the kinematics of the saccade in vertical direction, similar to MLBNs in PPRF for horizontal direction (Buttner et al., 1977; Sparks 2002). The step signal (vertical eye position signal) is provided by the interstitial nucleus of Cajal (INC) and the vestibular nuclei (King et al., 1981; Klier et al., 2002). Burst neurons in the riMLF also provide monosynaptic excitatory input to the motor neurons that are involved in torsional rotations of the eye. The right and left riMLFs both contain burst neurons with up and down direction selectivity, but the right riMLF has preference for clockwise movements whereas left riMLF has preference for counter clockwise movements (Vilis et al., 1989; Crawford et al., 2003). Therefore, torsional eye movements can be generated by a balance of activity between up and down neurons with the same rotational preference.

Although the commands for horizontal and vertical components are generated in different regions of the brainstem (and are seemingly independent), during oblique saccades with both vertical and horizontal components, the onsets and the duration of the two components are synchronized (Guitton and Mandl, 1980). This is done by omnipause neurons which discharge tonically during fixation but stop just before, and during saccades in all directions (both horizontal and vertical) (Pare and Guitton, 1994).

Unlike the oculomotor pathway which is tightly gated through a threshold gating mechanism orchestrated by omnipause neurons (disallowing premature movement of the eyes) the pathway innervating the neck muscles is less strictly controlled (Pare and Guitton, 1990; 1998; Gandhi and Sparks 2007). This explains why the temporal control of head movements exhibits idiosyncrasies that are not observed in eye movement control (Freedman and Sparks, 1997).

1.4. Spatial Models of Gaze Control System

The main focus of this dissertation is to characterize spatial transformations that occur within the FEF. For this, we compared the spatial information encoded by the signals that represent the input (visual response) and the output (movement response) to this node. To characterize spatial information it is not sufficient to determine what is being encoded, but it is also required to specify the frame of reference used. This is because spatial information are defined differently with respect to different frames of reference, especially when different frames of reference are constantly moving relative to each other. For instance, the location of the document you are currently reading is most likely straight ahead (with

respect to your body) and remains at this relative position regardless of where you read it in your room. However, as you change your position in the room the location of the document changes relative to the coordinates of the room and in relation to other objects within it. In the gaze control system, because the eyes, head and body continuously move (rotate) relative to each other and the external world, it is important to characterize spatial information not only by answering what is encoded but also what reference frame is used. Below provides a review of the different coding schemes (both sensory-motor and reference frame transformations) that have been characterized in the visuomotor pathway and touch on some of the mechanisms by which these transformations are believed to be achieved.

1.4.1. Frames of Reference in gaze control system

In visually-guided gaze control, visual information (registered in the reference frame defined by the retina; i.e., retinal or eye-centered coordinates), need to be transformed into a sequence of muscle contractions that results in the movement of the eye (with respect to the head; hence head-centered) and the movement of the head (with respect to the body; hence body-centered). But gaze movements can also be driven by other sensory modalities (Maxier and Groh, 2009). However, sensory input from other modalities are encoded in different formats (Lee and Groh, 2014). For example auditory stimuli are encoded by cues that depend on the spatial relationship between the ears, which are fixed to the head (hence head-centered). The dominant viewpoint is that, in order for sensory signals from different modalities to be 1) effectively processed and integrated,

and 2) result in muscle contractions that drive appropriate movements of the end-effectors (eye rotation described in head-frame, and head rotation described in body-frame) the brain needs to have a mechanism to interconvert between different frames of reference (Wallace et al., 1998; Lee and Groh, 2012; Mullette-Gillman et al., 2005; Crawford, 1994; Soechting and Flanders, 1992).

Spatial information can either be encoded relative to self (egocentrically) or relative to external objects in the visual field (allocentrically) (Olson and Gettner, 1995; Chen et al., 2014; Ekstrom et al., 2014) . Because the eyes, head and body can move relative to one another and gaze movements are accomplished by these effectors, egocentric representations are described in three coordinate frames, namely, eye-centered, head-centered, or body-centered (Crawford et al., 2011). Although allocentric representations play an important role in spatial processing in natural conditions (where several visual objects are present in the visual field), in the studies presented in this dissertation the focus is mainly on egocentric representations especially because here, (as in similar studies) only single visual stimuli are presented in the periphery.

1.4.1.1. Egocentric representations in the visuomotor pathway

Much of the evidence regarding the reference frames used in the oculomotor centers of the brain come from head-restrained studies. These studies show a prominence of eye-centered representations in the major oculomotor centers in the parietal (such as LIP) and frontal cortex (FEF and SEF), as well as the SC (Cohen and Andersen, 2002; Bruce and Goldberg, 1985; Russo and Bruce, 2000; DeSouza et al., 2011; Medendorp et al., 2003; O'Dhaniel et al., 2009).

However, just having an eye-centered representation is not sufficient to drive appropriate actions. For instance, with each movement of the eyes the retinal input changes (so retinal input is unstable) yet we perceive our world as stable. Also, as described above, our movements are defined in other coordinate frames. How are these problems dealt with in the brain?

For the first problem (visual constancy), Duhamel et al., (1992) showed that even though neurons have eye-centered representations of the world, before eye movements, the receptive field of neurons transiently "shift" to their eye-centered post-saccadic location. It has been proposed that it is through this remapping mechanism that a percept of stable world is achieved. Similar mechanism for eye-centered updating of movement goals is shown in humans and in other motor systems (Medendorp, 2010; Henriques et al., 1998).

For the second problem (transforming vision into action) the spatial relationship of the movement effectors with respect to each other and the world is also required. It has been shown that neurons in many visuomotor areas show position-dependent modulations that provide this information in the form of gain fields (Andersen et al., 1985; Snyder et al., 1998). Gain fields were first discovered by Andersen and colleagues who showed that even though a neuron responds to a visual stimulus appearing in a certain patch of the retina (hence eye-centered), the response strength is “gain” modulated depending on where the eye is oriented in the head (eye-position dependent modulation) (Andersen et al., 1985). The source of this implicit eye position signal remains unknown, but

evidence suggests that it is at least partly dependent on the proprioceptive afferents from somatosensory cortex (Wang et al., 2007).

Andersen and Zipser, showed that such gain field effects can provide the underlying mechanism by which the transformation between frames of reference can occur (Zipser and Andersen, 1988). Later computational models have used basis functions to show that such implicit gain field codes can be utilized such that multiple frames of reference could be read out from a given population (Pouget and Sejnowski, 1997; Pouget and Snyder, 2000). Head- and body-position-dependent gain fields have also been identified, which in theory can be utilized to transform head- and body-centered representations into world-frame of reference (Snyder et al., 1998; Brotchie et al., 1995).

Curiously, only a few areas thus far are shown to have neurons with explicit representations in head- or space-centered (or allocentric) coordinates (Olson and Gettner; 1995; Stricanne et al., 1996; Avillac et al., 2005; Chen et al., 2013; Snyder et al., 1998). For instance, explicit head-centered codes are observed in a minority of neurons in area V6A, VIP and premotor cortex (Galletti et al., 1995; Duhamel et al., 1997; Fogassi et al., 1992) but, even these cells show gain-field modulation effects. The fact that head-centered signals are represented both implicitly and explicitly even within the same neurons brings up the question of whether both representations are related to the same function. In fact, it has been proposed that gain fields may have functions beyond reference frame transformations, possibly related to attention, spatial updating, navigation and decision making (Andersen and Buneo, 2002; Xu et al., 2012). These functions of

gain fields will not be described further as they are beyond the scope of this dissertation.

Unlike the robotics approach to reference frame transformations, where transformations take place discretely from one coordinate frame to another, neurons in the visuomotor pathway often exhibit codes described in intermediate frames of reference. One of the first to show evidence for such intermediate frames of reference was Jay and Sparks who showed that auditory receptive fields are best represented in a frame of reference hybrid between eye- and head- frames (Jay and Sparks, 1984). Evidence for such intermediate frames have also been shown in other brain areas in both the gaze control system (Avillac et al., 2005; Mullette-Gillman and Groh, 2005) and other movement systems (Pesaran et al., 2006; Bremner et al., 2014).

1.4.1.2. Evidence from microstimulation studies

In addition to the studies reviewed above, which recorded from neuronal responses to identify the reference frames used in different areas of the brain, many studies have used microstimulation to address this question (Bruce and Goldberg, 1985; Schall et al., 1993; Martinez-Trujillo et al., 2004; Tehovnik et al., 2000). Specifically, the researcher stimulated a specific node along the visuomotor pathway and analyzed the output behaviour. These studies are complementary to studies that investigate the reference frame of neuronal response fields because they show how the output of a population (which is artificially activated through stimulation) is read out to drive behaviour (Monteon et al., 2013; Smith et al., 2005; Blohm et al., 2009).

In head-restrained conditions the stimulation of most cortical areas and the superior colliculus evoke fixed-vector saccadic eye movements relative to the fixation point, though stimulation of some sites in the dorsomedial prefrontal cortex (in particular SEF) evokes goal-directed saccades to fixed positions on the screen (Tehovnik and Lee, 1993; Bruce et al., 1985; Robinson, 1972). Only recently these visuomotor areas have been investigated in head-unrestrained conditions in which head-centered and body/space-centered coordinates are also dissociated. They show that the results are not as trivial as those observed in head-restrained conditions. In a series of studies, Crawford and colleagues showed that microstimulation of SEF, FEF, and LIP, which typically evoke eye-centered fixed vector saccades when the head is immobilized, evokes gaze shifts that are often described in hybrid frames of reference (Martinez-Trujillo et al., 2004; Constantin et al., 2007; Monteon et al., 2013). This suggests that even though these neurons have response fields described in eye-centered coordinates (at least based on head-restrained results) the output of these structures could undergo further coordinate transformations. What is especially missing in the literature is an understanding of the frame of reference neurons in these brain areas use in head-unrestrained conditions.

As reviewed above, we can see that neurons with various frames of reference are observed throughout the visuomotor pathway even within single functional nodes). This could suggest that these different spatial representations may be used concurrently for different functional purposes (Lappe, 2001; Monteon et al., 2012).

1.4.2. Sensory vs. movement (Gaze / eye / head) codes in gaze control system

An important goal of studies on spatial transformations is to understand where and how spatial signals that determine sensory parameters are transformed into signals that determine the metrics of the movement of these effectors, namely gaze and its independent eye and head components.

1.4.2.1. Separation of sensory and movement parameters in oculomotor studies

One of the challenges faced with in the gaze control system is that unlike the reach system in which the sensory and motor parameters are easily disentangled in the spatial domain, in the gaze control system sensory and motor parameters are often difficult to separate out as they are highly correlated (Snyder, 2000). This is especially in head-immobilized conditions in which motor parameters are simplified down to eye rotations in head. For instance a target 20 degrees to the left would also require an eye movement 20 degrees to the left. Of course, gaze behaviour is not perfectly accurate. So, in theory, one could use errors in behaviour to dissociate sensory and motor parameters. In fact, psychophysics and some neurophysiology experiments have used such errors to understand transformations in the visuomotor pathway (Flanders et al., 1992, ; Vesia et al., 2010; Platt and Glimcher, 1998; Krappmann, 1998). But this is not easily accomplished in neurophysiological studies that rely on average firing rate and position data across multiple trials (Snyder 2000, Platt and Glimcher, 1998). Therefore, oculomotor studies that aim at answering questions regarding sensory vs. motor coding often use non-spatial parameters (e.g., temporal parameters) or

employ tasks that spatially dissociate sensory and movement directions via an instructed mapping rule (Sato and Schall, 2003; Hanes and Schall, 1996; Zhang and Barash, 2000; 2004, Funahashi et al., 1993; Gottlieb and Goldberg, 1999; Everling and Munoz, 2000). These "visuo-motor dissociation studies" show that, especially in areas closer to the motor-end of the visual-to-motor hierarchy, there is a general tendency for the visual response to encode the sensory direction and the motor response to encode the direction of the movement (Sato and Schall, 2003; Munoz and Everling, 2004). However, these results cannot be generalized to sensori-motor transformation in every task condition mainly because in the visual-motor dissociation tasks the movement direction is separated from sensory direction by virtue of cognitive operations that are specific to that task (Fernandez-Ruiz et al., 2007; Sato and Schall, 2003; Hawkins et al., 2013; Johnston et al., 2009; Krappman, 1998). Therefore, neural correlates for movement direction coding could simply be related to the cognitive transformations and thus not present in standard visually-guided tasks which are devoid of such cognitive manipulations.

1.4.2.2. Codes related to intended gaze position, or actual rotations of the eyes and head?

Note that most studies on sensorimotor transformations in gaze control system (including the ones described in previous section) have only been performed in head-restrained conditions. Therefore, it remains unclear the movement of which gaze effector (if any at all) is encoded by the movement response. Unfortunately

very few studies have recorded from neurons in head-unrestrained conditions, but those that have done so generally suggest that neurons in the motor areas of the cortex, and the superior colliculus encode gaze displacement vector independent of its eye and head components (Guitton, 1992; Freedman and Sparks 1997b; DeSouza et al., 2011; Sadeh et al., 2015). Consistent with this, microstimulation of these areas has been shown to evoke kinematically natural gaze shifts with coordinated eye and head movement (Harris, 1980; Monteon et al., 2010; Martinez-Trujillo et al., 2003; Knight and Fuchs, 2007; Tu and Keating, 2000; Klier et al., 2001) while the stimulation of the downstream nuclei in reticular formation often results in independent movement of the eyes and the head, and rotations about specific cardinal axes (horizontal vs. vertical, vs. torsional) (Klier et al., 2002; 2003; Farshadmanesh et al., 2007; Sparks, 2002). However, some studies have provided evidence for independent eye and head movement codes even at the level of the cortex (Chen 2006, Chen and Tehovnik 2007, Knight 2012). Bizzi and colleagues have shown that some neurons in the FEF fire exclusively during head turning (Bizzi and Schiller, 1970). Microstimulation of certain cortical areas in head-unrestrained conditions, particularly certain sites in the SEF and FEF evoke either gaze shifts with larger than normal head movements, or head-only movements (Chen and Walton, 2005; Chen 2006). Also, studies that have inactivated these areas have shown unnatural eye-head coordination, pointing to the importance of these areas in generating coordinated gaze shifts (Van der Steen et al., 1986). In the only head-unrestrained study to consider spatial codes in the cortex (specifically the FEF) it

was shown that neurons in the FEF often encode the magnitude of the head or eye component of the gaze shift separately (Knight 2012). On the other hand studies on the SC (which is a structure located downstream of FEF) which have employed similar methods have shown that spatially-tuned neurons do not encode independent eye or head movements (Freedman and Sparks, 1997). Also, Walton et al., (2007) have shown that during head movements that do not change the line of sight (i.e., eye movement in head counters the head movement to keep gaze stable), certain neurons in the SC do fire. But these neurons showed different properties to the typical gaze shift cells found in the SC as they lacked spatial tuning (Walton et al., 2007). Therefore, the degree to which these head-related neurons contribute to natural head-unrestrained gaze shifts remains unclear (Walton et al., 2007; Knight 2012; Bizzi and Schiller, 1970). Certainly more studies in head-unrestrained conditions are required to gain a full understanding of the underlying mechanisms for coordinated eye and head movements during gaze behaviour.

1.4.3. Investigating spatial models of gaze control

As can be noted from the review above, in the gaze control system still much remains unclear about where sensory signals are transformed into movement signals (in their appropriate coordinate frame), and where and how movement signals are split into independent effector signals.

To address these question, the following needs to be determined for the input and output signals for every node in the visuomotor pathway:

1) What reference frame is the information encoded in? (and is there evidence for intermediate frames of reference?)
2) Is there evidence for position-dependent modulations?
3) What spatial parameters are encoded (sensory location? Or metrics of the movement (eye/head/gaze)?

The work in this dissertation contributes to this question by fitting a comprehensive list of spatial models to neural data from single FEF neurons to examine these questions.

1.5. Introduction to delay activity

In the review on gaze control system (section 1.3), two type of neuronal responses were described, namely the visual (temporally aligned with input) and movement / motor responses (temporally aligned with output). To make inferences about the transformations that occur within a brain structure many studies (as the studies in this dissertation) compare and contrast information encoded in these neuronal responses. These studies often temporally separate these neuronal responses by virtue of memory-delayed response tasks (Hikosaka and Wurtz, 1983) that require a delayed movement to a location defined by the visual stimulus (that is no longer present). One important requirement in performing these tasks is a short-term retention of information (short-term memory). Many visuomotor areas exhibit neuronal activity during this delay period (Fuster and Alexander, 1971; Gnadt and Andersen, 1988; Funahashi et al., 1989; Hikosaka and Wurtz, 1983). Since this delay temporally

connects the visual and motor responses, it has often been regarded to as the linking bridge between vision and action (Goldman-Rakic, 1987).

1.6. Functions of delay activity

The first evidence for the delay activity was provided by Fuster and Alexander (1971) in the dlPFC. This activity was suggested to be a neural correlate of short-term memory (Fuster and Alexander, 1971). Further investigations of delay activity showed that it reflected not just a passive sensory memory but it maintained information necessary to guide the upcoming action (Goldman-Rakic, 1995). Therefore, the delay activity was suggested to be the neuronal correlate for a specific form of memory known as working memory, which is the temporary storage (and manipulation) of information for the purpose of performing a task (Miller et al., 1960; Goldman-Rakic, 1995). One of the most successful models (Baddeley and Hitch, 1974) of working memory is the multicomponent model which states that there are two independent storage compartments: one for verbal information, and one for visuospatial information, which is further subdivided into a “visual cache” which concerns with “what”, and the “inner scribe” which concerns with “where” information (Baddeley and Logie, 1999; Logie, 1995). These two main storage buffers are interconnected with a third compartment (referred to as central executive) which serves to control attention and manage/manipulate information in each of the storage compartments. The delay activity observed during working memory tasks was interpreted as the neuronal manifestation of the storage buffers (and the interactions with the central executive) in the multicomponent system (Goldman-Rakic, 1987). In fact,

similar compartmentalization of visuospatial working memory was found in the prefrontal cortex as that suggested by the model (Wilson et al., 1993).

Despite the great amount of evidence linking delay activity with working memory, in the past few decades the idea of whether delay activity is exclusively related to working memory (and not such things as attention and movement planning) has been challenged (Postle, 2006; Courtney, 2004; Awh and Jonides, 2001; Funahashi, 2015; Tsujimoto and Postle, 2012; Lara and Wallis, 2015). This is mainly because most experimental paradigms to date have failed to disentangle the locus of the attention from the location of the remembered object and the location of the upcoming movement. In order to address this question some studies (mostly using fMRI brain imaging) designed experimental tasks in which these functions are (at least partially) separated (Ikkai and Curtis, 2011; Awh et al., 2006; Funahashi et al., 1993). These studies have shown that similar functional networks are activated for these different functions. This is in agreement with the theories that link attention with movement planning and / or working memory (Rizzolatti et al., 1987; Awh et al., 2001; 2006). According to these theories it is the loci of attention that are maintained in working memory, and planning an action is both necessary and sufficient for a shift of spatial attention (Courtney, 2004; Postle, 2006). On the other hand, some neurophysiological studies have shown that individual neurons are differentially activated depending on how attention, memory, and movement are dissociated (Sommer and Wurtz, 2001; Lebedev et al., 2004). Therefore, to what degree

these functions are segregated in the brain still remains an active area of research.

Regardless of the extent to which attention, movement planning, and working memory are functionally segregated, there is plethora of evidence linking delay activity to mnemonic functions (see Funahashi, 2015 for review on this). The amount of delay activity in working memory network is shown to be proportional to the performance level in memory-guided tasks in both humans and monkeys (Todd and Marois, 2015; Reinhard et al., 2012). Also, lesion or inactivation of the PFC is shown to specifically impair performance in working memory tasks while it has no influence on visually-guided behaviour (Dias and Segraves, 1999; Funahashi et al., 1993). Therefore, although the delay activity may serve different functions, its functions related to working memory cannot be dismissed (Funahashi, 2015).

1.7. Working Memory – behavioural limitations

Maintenance is a key function of working memory, but in order to perform any working memory task there is need for three distinct processing steps: 1) encoding into working memory, 2) maintenance of information and 3) retrieval / decoding of working memory information into action. (Woodman and Vogel, 2005; Ma et al., 2014; Chatham and Badre, 2015).

One of the important characteristics of working memory is that it is limited in capacity to 3-5 items at any given time (Miller, 1956; Luck and Vogel, 1997; Irwin, 1992). Studies have shown that as the number of items maintained in

working memory increases, errors in recall also increase. Several different models have been proposed to explain this capacity limitation (which will not be reviewed here). Some of the most popular models are the resource models which attribute this capacity limit to limited resources that has to be shared among all the items in working memory (Cowan, 2010; Ma et al., 2014). These models are based on the presumption that the internal representations (or measurements) of sensory stimuli are noisy. The level of this noise increases with the number of items in memory due to limitations in resources (Todd and Marois, 2004). Therefore, the precision with which an item can be recalled depends on the quantity of resource allocated to it. This noise, which results in behavioural errors (also in the form of spatial inaccuracy) is present even when a single object is maintained in working memory (such as the studies in this dissertation). It is important to note that these errors can arise at all the three processing stages (Faisal et al., 2008; Bays et al., 2011; Ma et al., 2014; Todd et al., 2011). In neuropsychiatric patients with possibility of impairments at any of these processing stages, the performance in memory-guided tasks involving single objects is significantly compromised confirming the contribution of these processing stages to behavioural errors (Ketcham et al., 2003; Avery and Krichmar, 2015). Therefore, in order to effectively treat delay activity as a linking bridge between vision and action (Goldman-Rakic, 1987), considering all these processing stages is essential. As we shall see in Chapter 2, our results provide neurophysiological evidence for multi-stage accumulation of noise during a

simple memory-guided gaze tasks which may be related to these distinct processing stages.

1.8. Functional networks subserving working memory

Since the discovery of delay activity in the PFC many studies have shown that the delay activity is ubiquitous throughout the visuomotor pathway. This activity has been observed in parietal areas (Barash et al., 1991), frontal areas such as dlPFC and FEF (Funahashi et al., 1989; Goldberg and Bruce, 1990), early sensory areas (Pasternak and Greenlee, 2005) as well as subcortical structures such as basal ganglia (Hikosaka and Wurtz, 1983; Levy et al., 1997), thalamus (Watanabe et al., 2009), and even the superior colliculus (Sommer and Wurtz, 2001). Therefore, working memory involves the interaction between several brain areas part of different functional networks differentially activated depending on the type of information maintained or processed (Baddeley, 2002; Wang et al., 2004, Linden, 2007). The activation of these networks are not only dependent on the type of task but also depend on the distinct processing stages including encoding, maintenance, and decoding (i.e., retrieval). (Badre and D'Esposito, 2009; Markowitz et al., 2015; Brown et al., 2004; O'Reilly and Frank, 2006; Ma et al., 2014). Below I will provide a brief overview of two pathways that are particularly involved in maintenance and executive functions of spatial working memory: the parieto-frontal network and the fronto-striato-thalamic loop.

Studies that have recorded simultaneously from both frontal and parietal cortex (Salazar et al., 2012) or frontal and sensory areas (Liebe et al., 2012), have shown that there are increased functional interactions between these regions

during working memory tasks and the strength of these interactions predicted performance. In the parieto-frontal network, whereas parietal areas often represent recent visual stimuli irrespective of their lack of relevance to the upcoming task (Constantinidis and Steinmetz, 2005; Bisley and Goldberg, 2003) the PFC largely encodes task-relevant information (McKee et al., 2014; Postle, 2006; Sreenivasan et al., 2014). Therefore, it has been suggested that the PFC is more closely associated with controlling lower-level visual areas and the gating of access to task-relevant information in working memory (Anderson and Green, 2001; Feredoes et al., 2011; Curtis and D'Esposito, 2003; Postle, 2005). This function of the PFC has been verified by studies on monkeys and humans showing that subjects with lesioned PFC (in particular dlPFC and FEF) show a significant inability to resist distracting stimuli (Guitton et al., 1985; Suzuki and Gottlieb, 2013; Chao and Knight, 1995).

Although the parieto-frontal network has been implicated in working memory tasks, the specific contribution of specific nodes within the frontal and parietal regions remain largely unknown (Fuster, 2001; Badre and D'Esposito, 2009). For instance although both dlPFC and FEF exhibit delay activity in working memory tasks (Funahashi et al., 1989; Sweeney et al., 1996; Gaymard et al., 1999; Curtis, 2006) there is evidence suggesting that their contributions to performance in memory-guided tasks might be different, though these differences are yet not fully understood (Ploner et al., 1999).

One of the major outputs of the frontal cortex is the basal ganglia, which is known to send signals back to cortex via the thalamus (McFarland and Haber, 2002). It

has been shown that the basal ganglia plays a critical role as it offers flexibility to the working memory system through an adaptive gating mechanism which can switch between new information and existing information in memory (Goldman-Rakic and Selemon, 1990; O'Reilly, 2006). It is believed to perform this dynamic gating through disinhibition mechanisms, thereby allowing only information relevant to upcoming behaviour to be maintained in PFC. Details on function of basal ganglia will not be reviewed here, but suffice it to say that this gating function of basal ganglia is reminiscent to its function in disinhibition of the motor circuitry for execution of intended actions: the "Go" neurons in the striatum inhibit substantia Nigra (SNr) and result in a disinhibition of thalamic neurons, which in turn project back to the cortex (O'Reilly and Frank, 2006). This therefore, results in transfer of activity from one population of neurons in PFC to another population (when necessary), or in some cases diminished activity (Figure 1.5). Using a similar mechanism the fronto-striato-thalamic loop is suggested to take part in input gating into working memory (encoding) and output gating from working memory to action (decoding/retrieval) (Chatham and Badre, 2015). It remains a question how the basal ganglia "knows" what information is task relevant and how and when it should be manipulated and used (O'Reilly, 2006; Fuster and Bressler,2012).

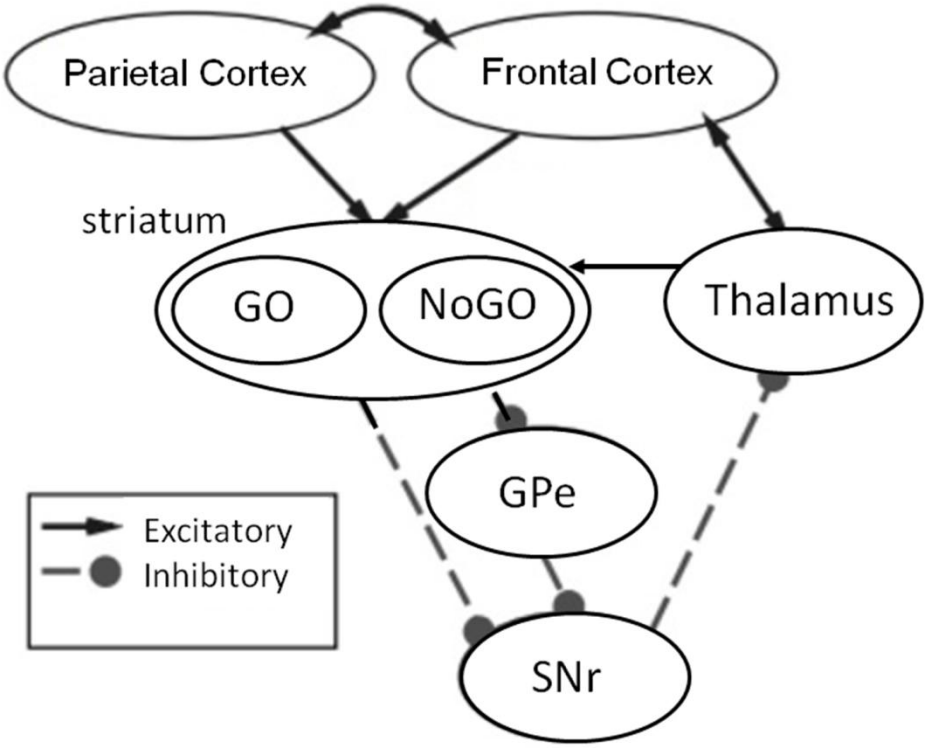

Figure 1.5. Schematic of the fronto-striato-thalamic loop. In the base state the fronto-parietal network maintains information while the SNr (substantia nigra pars reticulata) exhibits tonic activity inhibiting thalamic neurons (NoGo-unit more active than Go-unit). When there is need for activity switching (for executive functions) the SNr neurons are inhibited (By increased Go-unit activation), thereby opening the thalamocortical loop resulting in an updating/transfer of PFC activity to a new set of neurons in the PFC including those involved in maintenance of the new information. This mechanism is identical to that for gating motor actions via basal ganglia interactions with motor areas resulting in action control. (modified from O'Reilly, 2006)

1.9. Spatial models of Working Memory

With the idea that delay activity is a linking bridge between vision and movement many investigators interested in spatial processing have investigated what information is encoded during this period: is it retrospective sensory information, or prospective movement information (Curtis and D'Esposito, 2003; Rainer et al., 1999; Fuster, 2000)? The answer to this question can shed light on the boundary between "visual" and "motor" and identify the series of processes that take place to get from one to the other (Postle, 2006; Fuster 2009). Here I will explain some of the literature on the kinds of spatial information proposed to be encoded during delay activity.

Delay activity in many visuomotor areas represents spatial information in eye-centered coordinates (at least in simple oculomotor tasks used in neurophysiological experiments) (Duhamel et al., 1992; Mazzoni et al., 1996; Dash et al., 2015; Snyder, 2000; Medendorp et al., 2003). Delay activity is also gain- modulated suggesting that the prerequisite information for coordinate transformations resides in this activity (Andersen et al., 1990; Snyder, 2000; Cui, 2014). Evidence for movement-related coordinate frames has been shown during the delay period. For instance, in a recent study by Bremner and Andersen (2014) it was shown that in area 5d (which is a parietal area involved in reach control) as neuronal activity progressed further in time (away from visual presentation time, towards the movement time), the strength of hand-centered coding of target increased (Bremner and Andersen, 2014). This showed that the representations in delay activity in some brain areas may dynamically change

into coordinate frames more closely related to the upcoming motor behaviour (Gnadt et al., 1988). Other studies have also shown that delay activity can contain intermediate frames of reference, as well as allocentric codes (Stricanne et al., 1996; Postle and D'Esposito, 2003; Chen et al., 2014). Therefore, although there is a predominance of eye-centered codes in the delay activity in gaze control system, both sensory and movement-related reference frames related to different stages of sensorimotor processing are shown to be represented during the delay period (Pesaran et al., 2010; Bremner and Andersen, 2014; Snyder, 1998).

Several psychophysics experiments have used behavioural errors in memory-guided gaze movement to make inferences about spatial transformations in working memory tasks (e.g., Gnadt et al., 1991; White et al., 1994; Toni et al., 2002). These studies have systematically varied the duration of the memory delay period and showed that for the range of delay durations tested, the variability in behaviour monotonically increased with delay duration. Also, they often characterized the inaccuracies in gaze end point as a combination of systematic (usually upward) and variable errors possibly arising due to memory-dependent transformations.

A few studies exploited these behavioural errors to understand the transformations that take place during memory-guided task (Standford and Sparks, 1994; Opris et al., 2003; Ploner et al., 1999; Krappmann 1998). They concluded that systematic errors arise independently from variable errors, and downstream from the spatial memory maintenance network. However the

underlying mechanism for these two error components still remains unknown. A recent study by Wimmer et al. (2014) provided the first neurophysiological evidence for the accumulation of variable errors during the delay period. They showed that the eventual deviation of gaze endpoint from target could be predicted based on the changes in firing rate of PFC neurons during the delay period. Their results were consistent with the models of memory maintenance in which spatial representations drift continuously due to the accumulation of correlated noise in the recurrent memory network (Wimmer et al., 2014).

Although behavioural errors can be used to separate sensory and motor parameters, as explained in the section on spatial models of gaze control (section 1.4.2.1) many studies instead have used visual-motor dissociation tasks. Some of these studies specifically investigated the spatial information encoded during the delay period. These studies often assumed static spatial codes in individual neurons (either sensory and motor) or characterized the delay code as either a retrospective sensory or a prospective motor code. One of the first studies to employ such tasks was conducted by Niki and Watanabe (1976) who trained monkeys to perform two spatial delayed-response tasks with either left vs. right or up vs. down visual target positions. They also trained the monkeys to perform a task in which the monkey had to press the left button for upward position and the right button for downward position. They recorded from neurons while the monkey performed these tasks and showed that the majority of neurons encoded the position of the visual cue (i.e., retrospective spatial information), irrespective of the response (Niki and Watanabe, 1976). In the

oculomotor version of this task Funahashi et al. (1993) was the first to use memory-guided pro- and anti-saccade task to dissociate sensory and motor parameters. As later corroborated by many similar studies on PFC and LIP (Takeda and Funahashi 2002; Zhang and Barash, 2004), they found that a large majority of PFC neurons (both dlPFC and FEF) encoded the direction of the visual cue and only a small proportion of neurons encoded prospective movement information during the delay period. They further showed that neurons that exhibit spatial codes related to upcoming movement showed accelerating firing rates through the delay period (progressively more dominant in the population activity) while the neurons that exhibit spatial codes related to sensory information showed decelerating firing rates (Takeda and Funahashi, 2007). A spatiotemporal analysis of the population vector in both dlPFC and LIP revealed that the population code gradually changed from the sensory direction to the movement direction (Takeda and Funahashi, 2004; Zhang and Barash, 2004). Interestingly, similar analyses on mediodorsal thalamus, which is reciprocally connected with dlPFC, revealed that the population delay code changed rather abruptly and early on in the delay (Watanabe et al., 2009). They interpreted these results as thalamus driving the changes in spatial code in dlPFC (Watanabe and Funahashi, 2009). As can be noted, delay activity in different brain areas contribute differently to spatial processing in working memory.

The sensory vs. motor nature of working memory signals has also been investigated by studies that used other kinds of spatial tasks or tasks that do not involve spatial processing at all (Curtis and D'Esposito, 2006; Romo et al., 1999;

Barak et al., 2010; Rainer et al., 1999; Funahashi, 2013; Gaymard et al., 1999; Gnadt et al., 1988; Mars et al., 2008; Constantinidis et al., 2001; Wang et al., 2015). Curiously, however these studies have provided conflicting results, even within the same area. One influential idea that has been relatively successful in reconciling the differences across these studies proposes that working memory represents relevant information necessary to perform the task (Curtis et al., 2004; Postle, 2006; Sreenivasan et al., 2014). According to this idea differences between studies could be due to differential levels of reliance on sensory (or transformed) information to perform the experimental task.

1.10. Introduction to the experiments presented in this dissertation

The purpose of the research in this dissertation is to investigate the spatial code in the visual, delay, and motor activity of the FEF and characterize the transformations that take place within the FEF. The nature of the spatial transformations in the FEF are not fully understood especially because almost every study on FEF thus far has been in head-immobilized subjects, leaving many questions related to spatial coding in FEF unanswered. Also very few studies have investigated FEF delay activity. Here are the objectives of my PhD work:

1.10.1. Experiment 1. **To characterize the spatial transformations in the FEF in head-unrestrained conditions (Sajad et al., 2015):** This was done by comparing and contrasting the spatial code embedded within the visual and movement responses in the FEF while the subjects made head-unrestrained gaze shifts. In order to temporally separate these neuronal responses, we trained

the subjects to perform memory-guided gaze shifts towards briefly flashed visual stimuli in the periphery (details are presented in the methods section of each experimental chapter). As we shall see in the next chapter, 1) we compared between spatial models related to various egocentric frames of reference (eye-, head-, and body/space-coordinates) and their related intermediate frames of reference 2) We differentiated between sensory (target) coding and movement coding by considering spatial models based on target position, final gaze position, and eye and head components of gaze shift.

Given that the visual response is tightly linked with perceptual processes (Bichot et al., 1996; Thompson et al., 1996) and arises relatively early on after target presentation (Schmolesky, 1998), we hypothesized that the visual response will encode a spatial code closely described by target position relative to the eye. With the tight coupling between FEF movement activity and gaze movement generation (Bruce and Goldberg, 1985; Hanes and Schall, 1996; Woodman et al., 2008; Schall, 2011) we expected that, unlike the visual response, the movement response will encode spatial codes more closely related to specific movement parameters. Previous microstimulation studies have evoked kinematically normal eye+head gaze shifts when the head was allowed to freely move (Monteon et al., 2010; Tu and Keating, 2000; Knight and Fuchs, 2007) or evoked saccades paired with neck muscle contractions in head-restrained conditions (Elsley et al., 2007; Guitton and Mandl, 1978) which suggest the FEF output is a gaze command (i.e., how much should the gaze shift)? However, a few head-restrained studies have suggested the possibility for independent eye

and head movement codes (Chen, 2006; Knight, 2012) or the existence of hybrid head-centered and / or body-centered codes in addition to eye-centered codes in the FEF (Monteon et al., 2013). Therefore, with respect to the movement response, we expected to observe some degree of heterogeneity in the spatial codes. Our results showed that as expected, the visual response was best described by the target location while the movement response (separated by a memory delay period) preferentially encoded final gaze position. Both of these codes were predominantly in eye-centered coordinates and this difference between visual and movement codes was even observed at the level of individual neurons (see next chapter for results).

1.10.2. Experiment 2 (Sajad et al., 2016): The type of transformation observed in experiment 1 (target-to-gaze coding between visual and movement response) prompted a new study aiming at characterizing the underlying processes leading to this transition: In order to do this we analyzed the evolution of spatial code through the entire duration of the memory-guided task, especially the delay activity intervening visual and movement responses. By devising a novel spatial continuum spanning the two spatial codes observed in visual and movement response (i.e., target position and final gaze position, see chapter 1. 4. 2.1), and by tracing the code through time, we were able to identify the evolution of spatial code through the entire visual-memory-motor extent of neuronal responses of individual neurons. Because the delay activity intervenes the visual and movement responses, we hypothesized that this transition would be reflected in this spatiotemporal analysis of FEF neuronal code. As described in section 1.9,

there is conflicting evidence for the sensory vs. motor nature of representations in delay activity. So, in this study, we examined whether the target-to-gaze transition occurs early on during the delay (motor code, i.e., gaze end point, maintained in memory), late in the delay (sensory code, i.e., target location, is maintained in memory) or gradually evolves throughout the delay? We observed evidence for all of these transition schemes contributing to the overall transition in the FEF population code.

1.10.3. Experimental approach:

All the methods are explained in detailed in the following chapters (sections 2.2 and 3.2). But before I proceed with the experimental chapters I will provide a basic introduction to the conceptual rationale behind the spatial analysis method used and the spatial models investigated throughout this dissertation.

Previous studies that have addressed the reference frame problem have immobilized the head and systematically varied initial eye position relative to the head, resulting in the systematic misalignments of the eye-coordinates from head-coordinates.

In head-unrestrained conditions, this cannot be easily achieved. Although gaze (eye position in space) can be controlled by the location of the presented visual stimulus, the head orientation cannot be easily controlled (esp. in situations where natural behaviour is reinforced). Keith, DeSouza, and Crawford were the first to come up with an analysis method that exploited the random variability and misalignments in the orientations of the head and eye during initial fixation

relative to the body/space to differentiate between eye-, head-, and body-coordinates (Keith et al., 2009).

Through a rigorous model-fitting approach (explained in detail in the following chapters) the spatial model that best described the variability in the firing rate of each sampled neuronal activity was identified as the coding scheme of the neuron at that time interval. This is based on the presumption that activity of neurons are described as coherent maps in space (i.e., response fields): If the response field of an “ideal” neuron is represented in its intrinsic spatial model, it should exhibit perfect spatial organization. Accordingly, any representation based on other spatial parameters which deviate from the best-fit model should be spatially less organized depending on the degree of variable differences from the best-fit spatial model (the intrinsic code of the neuron). DeSouza et al. (2011) were the first to apply this method on SC visuomotor responses to show that in head-unrestrained conditions SC neurons preferentially encode information in eye-centered coordinates. They also exploited the natural variability in final gaze position (relative to the target) in order to differentiate between target coding and final gaze position coding. Because sensorimotor transformation has been suggested to be a progression and intermediate frames of reference had been proposed before, intermediate spatial models between eye-, head-, and space-centered coordinates were also considered (DeSouza et al., 2011).

In the current dissertation I further advanced this method to differentiate between spatial codes related to the final gaze position from those related to either eye or head movement. Although intermediate spatial models are typically described as

the representation of a position in intermediary frames of reference, in these studies I also considered intermediate codes between different effector-related codes. More importantly, I considered the possibility for spatial codes intermediate between target position and gaze position, which allowed us to examine whether or not there is any preference for positions between the visual stimulus and where the eventual gaze lands. As we shall see in the experimental chapters, this spatial representation provides the most insight into explaining the types of spatial transformations that take place within the FEF in the memory-guided task which form the basis for the main conclusions of this dissertation.

Chapter 2:

Visual-Motor Transformations within Frontal Eye Fields During Head-Unrestrained Gaze Shifts in the Monkey

(Sajad et al., 2015)

Amirsaman Sajad [1,2,3,4], Morteza Sadeh[1,2,3,5], Gerald P. Keith[1,2,6], Xiaogang Yan[1,2], Hongying Wang[1,2], and John Douglas Crawford[1,2,3,4,5,6]

[1]Centre for Vision Research,

[2]Canadian Action and Perception Network (CAPnet)

[3]Neuroscience Graduate Diploma Program,

[4]Department of Biology,

[5]School of Kinesiology and Health Sciences,

[6]Department of Psychology,

York University, Toronto, Ontario, Canada M3J 1P3,

Corresponding Author:

Name: Prof. J.D. Crawford

2.1. Abstract

A fundamental question in sensorimotor control concerns the transformation of spatial signals from the retina into eye and head motor commands required for accurate gaze shifts. Here, we investigated these transformations by identifying the spatial codes embedded in visually-evoked and movement-related responses in the frontal eye fields (FEF) during head-unrestrained gaze shifts. Monkeys made delayed gaze shifts to the remembered location of briefly presented visual stimuli, with delay serving to dissociate visual and movement responses. A statistical analysis of non-parametric model fits to response field data from 57 neurons (38 with visual and 49 with movement activity) eliminated most effector-specific, head-fixed, and space-fixed models but confirmed the dominance of eye-centered codes observed in head-restrained studies. More importantly, the visual response encoded target location, whereas the movement response mainly encoded the final position of the imminent gaze shift (including gaze errors). This spatio-temporal distinction between target and gaze coding was present not only at the population level but even at the single-cell level. We propose that an imperfect visual-motor transformation occurs during the brief memory interval between perception and action, and further transformations from the FEF's eye-centred gaze motor code to effector-specific codes in motor frames occur downstream in the subcortical areas.

2.2. Introduction

One of the most fundamental, yet illusive, questions in sensorimotor neuroscience concerns where, and how, signals defined in sensory space become spatially-tuned commands for motor effectors (Sparks 1986; Flanders et al. 1992; Andersen et al. 1993; Pouget and Snyder 2000; Wurtz et al. 2001; Kakei et al. 2003; Smith and Crawford 2005; Crawford et al. 2011). This question has proven particularly difficult to answer in the gaze control system because of the normally high spatial correlation between gaze parameters, such as target location versus gaze end-point location (Platt and Glimcher 1998; Snyder 2000), retinal coordinates versus gaze displacement coordinates (Crawford and Guitton 1997; Klier et al. 2001), and (in the head-unrestrained condition) gaze, eye, and head motion (Guitton 1992; Freedman and Sparks 1997a,b; Gandhi and Katnani 2011; Knight 2012). This leaves three computational questions unanswered: When and where does the spatial transformation from coding stimulus location to coding movement-related parameters occur? When and where is visual information transformed from retinal coordinates into motor coordinates? And how and where are gaze commands split into signals that result in the coordinated movement of the end-effectors, namely, eye and head?

One way to approach these general questions is to establish the specific signals encoded in key gaze control areas. One such area is the frontal eye fields (FEF), a dorso-lateral frontal lobe structure with reciprocal projections to many striate and extrastriate cortical areas including area V4, the lateral intraparietal cortex (LIP), supplementary eye field (SEF), and the prefrontal cortex (PFC). The FEF

also makes reciprocal connections with sub-cortical areas involved in rapid gaze shifts, including the superior colliculus (SC) and brainstem reticular formation (Schiller et al. 1979; Stanton et al. 1988; Dias et al. 1995; Schall et al. 1995; Dias and Segraves 1999; Summer and Wurtz 2000; Munoz and Schall 2004). Low current stimulation of the FEF in alert cats and monkeys evokes short-latency saccades in head-restrained conditions (Robinson and Fuchs 1969; Guitton and Mandl 1978; Bruce et al. 1985), and eye-head gaze shifts in head-unrestrained conditions (Ferrier 1876; Tu and Keating 2000; Chen 2006; Knight and Fuchs 2007; Monteon et al. 2010). Like most gaze control areas, FEF neurons show responses that are time-locked to visual stimuli (visual response) and/or saccade onset (movement response) (Bizzi 1968; Mohler et al. 1973; Bruce and Goldberg 1985). Further, these responses are spatially selective, i.e., plotting them in two-dimensional (2-D) spatial coordinates often yields well-organized visual and / or movement response fields (RF) (Mohler et al. 1973; Bruce and Goldberg 1985). However, it is unknown exactly what spatial codes are embedded within these FEF responses. Specifically, does FEF visual / movement activity encode visual target locations, or desired gaze end-points? What frames of reference are used to represent such codes? Is the FEF further involved in dividing these signals into specific eye and head commands?

The question of target location versus gaze end-point coding has been addressed in the FEF (and other oculomotor structures interconnected with the FEF) using tasks in which the saccade end-point is spatially incongruent from the visual stimulus. For example, monkeys can be trained to make saccades

opposite to the visual stimulus (anti-saccades; Everling and Munoz 2000; Sato and Schall 2003), or in a direction rotated 90º from the target (Takeda and Funahashi 2004). Such studies suggest that FEF visual responses are generally tuned to the direction of the visual stimulus and movement responses are tuned for saccade direction (Everling and Munoz 2000; Sato and Schall 2003; Takeda and Funahashi 2004). However, it is not certain whether these movement responses encode saccade metrics, or a spatially reversed / rotated representation of the target (Everling and Munoz 2000; Zhang and Barash 2000; Medendorp et al. 2004; Munoz and Everling 2004; Amemori and Sawaguchi 2006; Fernandez-Ruiz et al. 2007; Collins et al. 2008). Consistent with the second possibility, it has been suggested that the movement responses in the FEF may code for the saccade goal rather than the metrics of the movement (Dassonville et al. 1992). Other methods to spatially separate the target from the gaze end-point involve saccadic adaptation (Frens and Van Opstal 1997; Edelman and Goldberg 2002), weakening eye muscles (Optican and Robinson 1980), or the natural variability in gaze end-points relative to the target (Stanford and Sparks 1994; Platt and Glimcher 1998; DeSouza et al. 2011), but to date, these techniques have not been applied to the FEF.

Frames of reference have been tested by recording from visual or movement RFs from several different eye positions to see which spatial frame (eye or head) yields the most spatially *coherent* RF, i.e. with the least variability in activity for the same spatial coordinates (e.g., Jay and Sparks 1984; Avillac et al. 2005). Head-restrained FEF studies tend to support an eye-fixed coding scheme (Bruce

and Goldberg 1985; Russo and Bruce 1994; Tehovnik et al. 2000). However, the spatial frames for RFs in the FEF have not been tested with the head unrestrained. This is not a trivial step, because in head-unrestrained conditions more frames are discernible (eye, head, and space), torsion (rotation about the visual axis) is much more variable (Glenn and Vilis 1992; Crawford et al. 1999), and inclusion of head motion can alter the codes observed in head-unrestrained conditions (Pare and Guitton 1990; Cullen and Guitton 1997). The reference frames for gaze have also been studied by analyzing the dependence of stimulation-evoked eye movements on initial eye position. Head-restrained stimulation studies have favored eye-centered codes with minor eye position modulations (Bruce et al. 1985; Tehovnik et al. 2000). Some head-unrestrained stimulation studies also favored eye-centered movement coding for gaze (i.e., final gaze direction relative to initial eye orientation; Tu and Keathing 2000; Knight and Fuchs 2007), but others have favored intermediate (eye-head-space) reference frames (Monteon et al. 2013).

Finally, the role of the FEF in coding gaze direction, as opposed to eye and/or head movement signals, also remains controversial. To date, only one study has investigated this question by recording single-unit activity in the FEF during head-unrestrained gaze shifts, using regressions between FEF movement activity along the peak ‘on-off’ axis of each neuron’s directional tuning and behavioral data obtained from 2-D behavioral recordings (Knight 2012). This study confirmed the role of the FEF in the production of coordinated eye-head gaze shifts, but also suggested that the movement responses of individual FEF

neurons possess separate codes for gaze, eye, and head motion. Head-unrestrained stimulation of the FEF produces different results depending on the details of stimulation site, stimulus parameters, initial eye/head orientation, and behavioral state. In brief, FEF region stimulation can produce naturally coordinated gaze shifts (Monteon et al. 2010, 2013), saccades followed by head movements or head movement alone (Chen 2006), or different amounts of eye and head movement, depending on initial eye position (Tu and Keating 2000; Knight and Fuchs 2007), as often observed in normal behavior (Guitton and Volle 1987; Freedman and Sparks 1997a,b).

In short, controversies and / or gaps in knowledge continue to exist with respect to nearly every question that has been asked about the role of the FEF in spatial transformations for gaze. Further, it is often difficult to cross-reference previous results because each experiment focused on a subset of these questions in a different experimental preparation. In particular, to date there has not been a comprehensive attempt to compare all of these questions in the visual versus movement responses of FEF neurons.

In the current study, we addressed these issues by fitting spatial models corresponding to *all* of the options described above to FEF visual *and* movement responses recorded in head-unrestrained monkeys (a more detailed description of these models is provided in Figure 2.4 and accompanying text). Rather than using 1-D regressions, we made non-parametric fits to the visual and / or movement RFs of FEF neurons, and determined which spatial coordinates (i.e. corresponding to the possibilities discussed above) gave the most coherent

representation. Importantly, these coordinates were derived from 3-D behavioral recordings, where the explained variance originated from untrained variations in behavior (Keith et al. 2009; DeSouza et al. 2011). The results show that FEF visual and movement responses encode different physical parameters (i.e., target position versus gaze displacement) often within the same neurons, but always in eye-centered coordinates. This suggests a role for the FEF in eye-centered visual-to-motor transformations, with other spatial transformations implemented downstream.

2.3. Methods

2.3.1. Surgical procedures and 3-D gaze, eye, and head recordings

All protocols were in accordance with the Canadian Council on Animal Care guidelines on the use of laboratory animals and approved by the York University Animal Care Committee. The data were collected from two female *Macaca mulatta* monkeys. Animals were prepared for chronic electrophysiological recordings and 3-D eye movement recordings. Each animal underwent surgeries described previously (Crawford et al. 1999; Klier et al. 2003). We implanted the recording chamber, which was centered in stereotaxic coordinates at 25mm anterial for both monkeys, and 19mm and 20mm lateral for monkeys S and A respectively. A 19-mm-diameter craniotomy covered on the base of the chamber allowing access to the right FEF. A recording chamber was attached over the trephination with dental acrylic. Two 5-mm-diameter sclera search coils were implanted in one eye of each animal.

During experiments, animals were seated within a primate 'chair' modified to allow free motion of the head near the centre of three mutually orthogonal magnetic fields (Crawford et al. 1999). This, in combination with the scleral coils, allowed for 3-D recordings of eye (i.e., gaze) orientation (horizontal, vertical, and torsional components of eye orientation relative to space). During experiments two orthogonal coils were also mounted on the skull to provide similar 3-D recordings of head orientation in space. Other variables such as the eye orientation relative to the head, eye and head velocities, and accelerations were calculated from these quantities (Crawford et al. 1999).

2.3.2. Basic Behavioral paradigm

Visual stimuli were laser projected onto a flat screen, 80cm away from the animal. To separately analyze visually-evoked and movement-related responses in the FEF, monkeys were trained to perform a standard memory-guided gaze task, which imposes a temporal delay between target presentation and movement initiation. In this task, the animal fixated on an initial central target position for 500ms, before a single visual stimulus was briefly flashed for 80-100ms on the screen serving as the gaze target. After the disappearance of the gaze target, the animal maintained fixation on the initial target for 400-800ms until it was extinguished, cueing the animal to make a gaze shift (with the head completely unrestrained) to the remembered location of the target (Fig. 2.1*A*). If the gaze shift started after the go-signal, and the final gaze position fell within the spatial acceptance window for at least 200ms, a juice reward was given to the animal via a tube fixed to the head. A relatively large acceptance window (~5-10°

in radius proportional to the eccentricity of the centre of the target array) was set to allow for the variability of memory-guided gaze shifts (Gnadt et al. 1991; White et al. 1994) which in turn was used in our analysis (see below). Further details of initial and final target placements, and gaze/eye/head kinematics are shown in Figure 2.1 *B*-*C*, and described in the following sections.

2.3.3. Experimental procedures

We recorded extracellular activity from single FEF neurons using tungsten microelectrodes (0.2-2.0 mΩ impedance, FHC). The neural activity was amplified, filtered, and stored for offline cluster separation applying principal component analysis with the Plexon MAP system. The recorded sites were confirmed to be within the low-threshold FEF (<50 μA) using microstimulation criteria defined by Bruce and Goldberg (1985) in *head-restrained* conditions. Every effort was made to sample evenly from the entire medio-dorsal extent of the FEF in both animals. Consistent with previous studies (Stanton et al. 1989) we found a few sites outside of the arcuate sulcus, but most of these were excluded from analysis (see Fig. 2.2). In most recording sessions, the search for neurons was conducted when the animal was freely scanning the environment in a lighted room with the head free to move. Once a neuron had clear and stable spiking activity the experiment began. In the first step of the experiment the neuron's visual and / or movement RF was characterized while the monkey made memory-guided gaze shifts from a fixed central fixation location to a randomly presented target within an array of targets (5-10° apart) covering +/-40° visual angle in all directions. Once the spatial extent of the visual and movement RFs were roughly

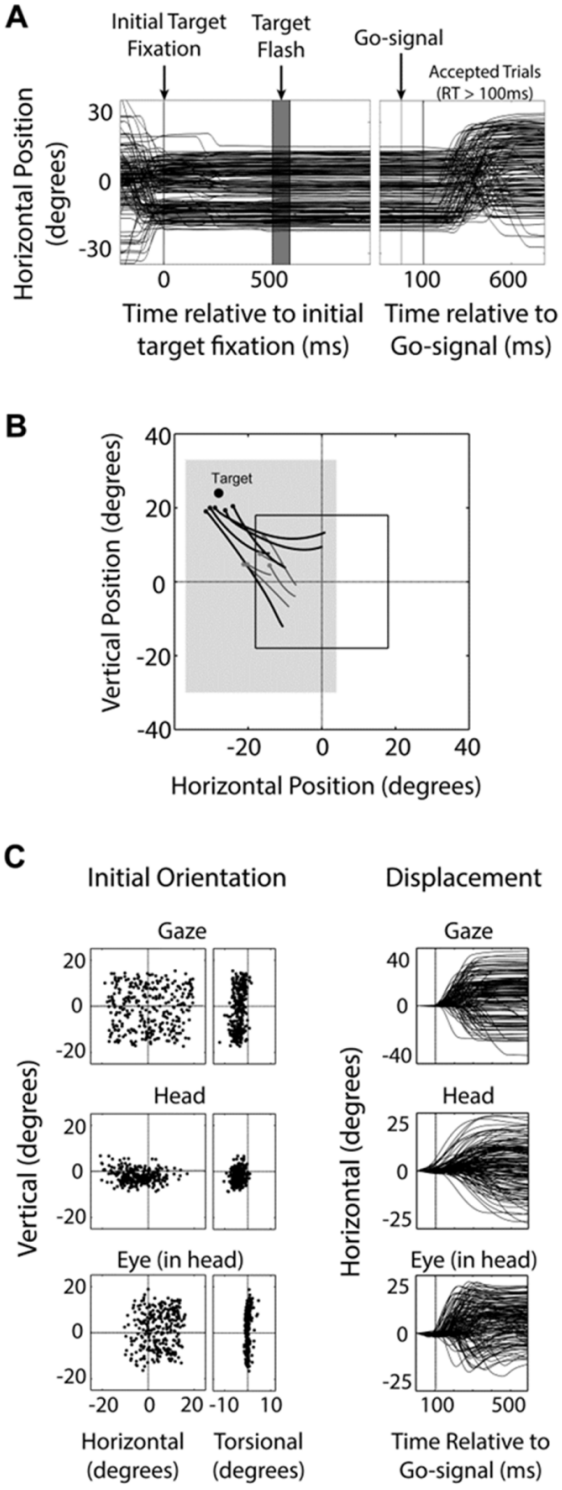

Figure 2.1. Behavioral paradigm and example movement kinematics associated with one neural recording session (see Methods for explanation). (*A*) The temporal and spatial parameters of the memory-guided paradigm used in this experiment. Each trial began with the appearance of the initial fixation target. After 500ms of fixation, a visual target briefly flashed (for 80-100ms) in the periphery serving as the gaze target. After a variable delay period (400-800ms) the initial fixation target disappeared (go-signal) instructing the monkey to make a gaze shift to the remembered location of the target. Gaze movement traces in the horizontal component are depicted (black lines), showing a large distribution of initial (left panel) and final (right panel) gaze positions. (*B*) Variability of gaze accuracy and two dimensional distributions of initial / final target positions. Gray Rectangle: zone where targets might appear (in this case an 8 X 5 grid covering 60° x 40°). Black outlined box: zone where initial gaze fixation targets might appear. Five example gaze trajectories (black lines) are shown with their corresponding head trajectories (gray lines), and their endpoints indicated by small dots (•), for a single example target position (large dot ●). (*C*) Kinematics of gaze (upper row), eye (middle row), and head (lower row). The left and middle columns of the panels show the distributions of initial orientations for all targets (vertical x horizontal on left, and vertical x torsional on right). The right column shows horizontal displacement of gaze, eye (in head), and head from the time of go-signal presentation till 600ms after. By this time the gaze shift and the related head movement are over.

characterized, in the second step an array of gaze targets were set to cover within and just outside of the RF of the neuron. Gaze targets were typically positioned in 4X4 to 8X8 arrays (5-10° apart) depending on the size and shape of the RF. Initial fixation target positions were randomized within a square window with width size ranging from 10-40° proportional to the size of the RF (Fig. 2.1*B*). For most neurons with RF that extended beyond 40°, the range of initial fixation targets was shifted from the centre by up to 10° away from the RF to allow for larger retinal eccentricities. Importantly, the variability in initial target positions helped to increase the variability in initial 3-D gaze, eye, head, distributions and displacements (Fig. 2.1*C*) for our analysis (see below).

2.3.4. Data inclusion Criteria

We only analyzed neurons that were clearly isolated and task-modulated. This included cells with clear visually-evoked and/or pre-saccadic movement activity (Fig. 2.3). Cells that only exhibited anticipatory, post-saccadic (activity starting after saccade onset) or delay activity were excluded. This stage of neuron inclusion was based on the qualitative examination of post-stimulus time histogram plots of individual neuronal responses.

In addition, individual trials were excluded offline based on three behavioral criteria: First, a spatial criterion that included all trials (irrespective of whether or not final gaze position fell in the acceptance window during online monitoring of behavior) with the exception of trials with final gaze position falling in the opposite direction of the gaze target or with gaze error exceeding 2 standard deviations

beyond gaze error versus retinal error regression line (gaze errors were larger for larger retinal errors). Furthermore, trials were excluded based on a temporal criterion which excluded trials in which the subject made anticipatory gaze shift, either before or within 100ms after the go-signal. Finally, trials in which gaze, eye, and head were not stable during the delay period were eliminated. Given that in head-unrestrained conditions despite stable gaze on fixation target, the eye and the head could move (vestibulo-ocular reflex, VOR), the few trials (less

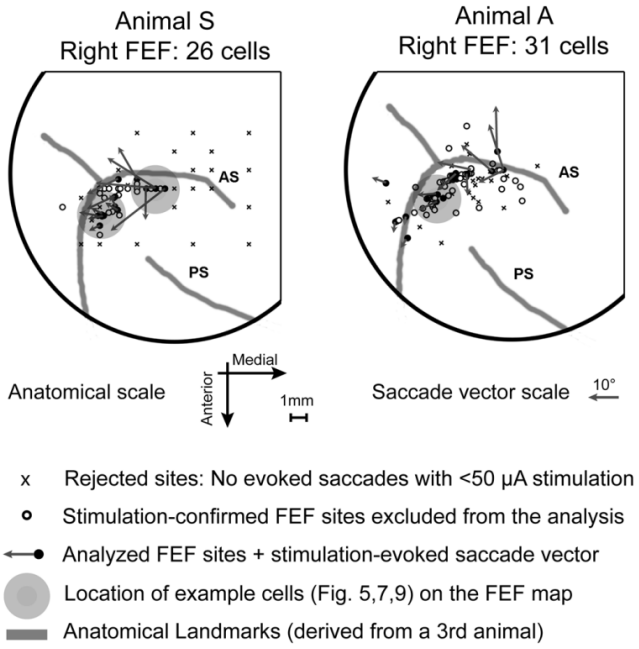

Figure 2.2. Reconstruction of the map of the explored and recorded sites. A schematic of recording chamber (edge shown by the large semi-circle) and penetrated sites for both subjects (S and A) are depicted. Gray lines are an estimate of the anatomical landmarks obtained from a previously euthanized monkey, overlaid on the sites map based on the stereotaxic coordinates and the distribution of the confirmed FEF sites. (o): sites which were confirmed to be within the FEF using standard stimulation criteria (Bruce and Goldberg 1985), but either no cell was recorded from, or recorded cells were rejected based on the exclusion criteria. (●): sites which were confirmed to be within the FEF from which the analyzed neurons (n = 57) were recorded; (ß): Vector of the saccades evoked by < 50μA current at the recorded sites as projected on the screen (see the scale in the legend). (x): sites which were rejected as FEF sites based on the stimulation criteria. AS: arcuate sulcus; PS: principal sulcus.

than 3%) in each session in which the head was clearly moving (velocity > 10 °/sec) during the delay period were excluded. After applying all of these criteria, on average, 221 (median= 198; SD = 132; min = 59; max = 657) trials per neuron were used for analysis.

2.3.5. Sampling Windows for Visual and Movement Activity Analysis

The 'visual epoch' was defined as a fixed temporal window of 80-180ms after target onset, corresponding to the early stages of sensory processing (i.e., the visual transient; Fig. 2.3, Left column). The 'movement epoch' was defined as a 100ms peri-saccadic period, ranging from -50 to +50ms relative to gaze onset (Fig. 2.3, Right column). This fixed window was chosen because it contained the high frequency peri-saccadic burst ramping up to the peak of movement activity (see Fig. 2.3) and therefore 1) provided a good signal-to-noise ratio for our analysis method, and 2) most likely represented the period in which FEF activity influenced gaze shifts (the saccadic component of our gaze shifts on average lasted 140 ms and it takes about 20-30ms for FEF signals to reach eye muscles; Hanes and Schall 1996). However, the full movement burst of the neurons in our sample on average started from 98ms before saccade and lasted 85ms after the end of the saccade, well into the VOR / head movement period. Therefore, we also did our analysis using the full movement burst to fully test the possibility that the movement signal was coding for head movement. The full-burst window was selected from the time point at which the spike density profile started to ramp up (at the inflection point on the spike density plot) till the time point at which the activity subsided to its lowest level (Fig. 2.3, Right column; Fig. 2.9*A,F*).

2.3.6. Neuron Classification and Calculation of Visuomovement Index

Since some of our trials involved eccentric positions outside of visual / movement RF, and since we did not know *a priori* which spatial model to use for measuring the RF hot-spot activity, we characterized our neurons based on trials that showed the top 10% of activity in the fixed sampling windows, which we called Vis10% for the visual response and Mov10% for the movement response (red lines in Fig. 2.3). This roughly corresponds to trials toward the peak of the RF when represented in the correct spatial model. A neuron was considered to have either visual or movement response (or both) if the Vis10% or Mov10% activity exceeded the firing rate in the 100ms pre-target baseline by at least 25 spikes/sec.

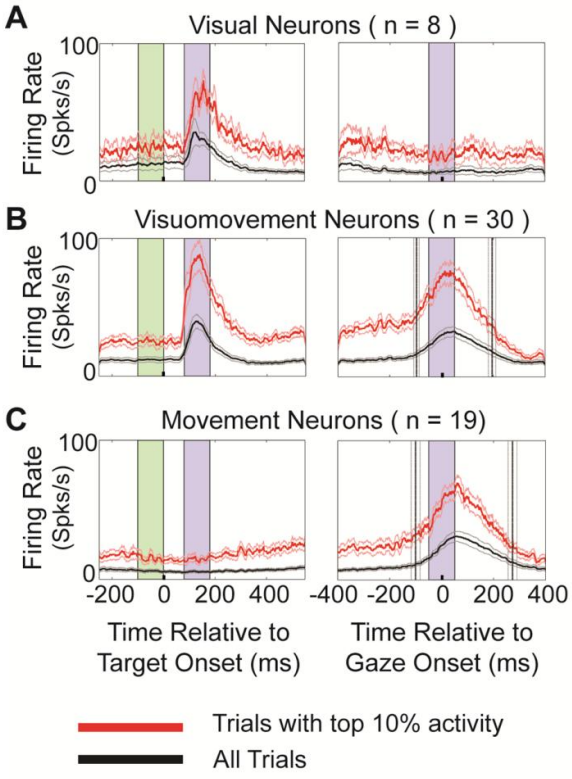

Figure 2.3. Spike density plots for the 57 analyzed task-related FEF neurons. Target-aligned- (left) and gaze-aligned- (right) population spike density plots for visual (*A*), visuomovement (*B*), and movement (*C*) neurons are shown. The spike density plots are shown based on *all* trials (black trace), and for 10% of trials with the highest firing rate in the activity-matched time epoch (red trace). The 'visual epoch' is 80-180ms after target onset (left, mauve shade) and the 'movement epoch' is -50 to +50ms relative to gaze onset (right, mauve shade). The pre-target baseline is 0-100ms before target onset (left, green shade). For visual RF analysis activity in the visual epoch and for movement RF analysis activity in both the movement epoch and the entire movement burst were used. On average, the full movement burst spanned -97+/-11ms (mean +/- SEM) to 195+/-14ms for the VM population (*B*, right panel; vertical black lines), and -101+/-17ms to 272+/-17ms for M population (*C*, right panel; vertical black lines).

In order to quantify the relative strength of visually-evoked versus gaze movement-related activity for some analyses, we calculated a visuomovement index (VMI) for each neuron as the difference of Vis10% and Mov10% divided by their sum, after subtracting off their trial-matched baseline activity. In the rare case where the pre-target baseline activity exceeded either Vis10% or Mov10% a value of 0 was assigned. Thus, VMI was bound between -1 (pure vision) and +1 (pure movement).

2.3.7. Sampling gaze, eye and head positions for analysis

Eye and head orientations (relative to space) were recorded with a sampling rate of 1000Hz and other variables such as the eye orientation relative to the head and eye and head velocities were calculated from these quantities. For movement analysis, the onset of gaze (movement of eye in space) was selected at the time when gaze velocity exceeded 50 °/sec and gaze offset was marked as time point when velocity declined below 30 °/sec. Head movement was marked from the onset of gaze, till the time point at which head velocity declined below 15 °/sec. For trials in which the head velocity never exceeded 15 °/sec the head position was sampled at the time of the gaze marks.

2.3.8. Canonical Spatial models considered in this study

Figure 2.4 *A-C* graphically illustrates how we derived the 11 ‘canonical’ models tested in this study. These models provide a formal means for testing between target versus gaze position coding, and gaze versus eye versus head displacement/position, with each expressed in several possible frames of reference. Figure 2.4A shows the different spatial parameters involved in a

memory-guided gaze shift. Most importantly these include Target position (T) and final Gaze position (G). In our preparation, T and G could be expressed in three different reference frames, i.e., relative to initial eye (e), head (h) or space/body (s) coordinates (Fig. 2.4*B*), resulting in 6 possible *Target* (Te, Th, Ts) and *Gaze* (Ge, Gh, Gs) models, as illustrated in Figure 2.4*C*. Other possible effector-specific *Displacement* or *Position* codes in our preparation include Gaze Displacement (dG: final – initial gaze position in space coordinates), Eye Displacement (dE: final – initial eye orientation in head coordinates), Head displacement (dH: final – initial head position in space coordinates), final eye position in head coordinates (Eh), and final head position in space coordinates (Hs). The eye models were based on eye positions sampled at the end of the gaze shift (and thus did not include the VOR phase), whereas the head models included the entire head movement.

Note that some of these models are identical or linearly summate in a 1-D analysis, but these mathematical relationships become more complex in 3-D, head-unrestrained gaze shifts where one must account for both torsional variations in position (Fig. 2.1*C*) and the non-commutativity of rotations (Tweed and Vilis 1987; Crawford et al. 1999; Martinez-Trujillo et al. 2004; Keith et al. 2009). For example, in 3-D, Te (i.e., target in eye coordinates) and Ge (i.e., final gaze position in eye coordinates) are computed by rotating space-fixed vectors by the inverse of 3-D eye orientation in space, rather than subtraction. Nevertheless, some of our models made similar predictions, e.g., Ge and dG are nearly identical for gaze shifts up to 30º (Crawford and Guitton 1997; see

discussion), and all were inter-related in some way, so we obtained the largest dataset that we could for each neuron and employed the most powerful statistical approach that we could find to discriminate these models (Keith et al. 2009).

2.3.9. Intermediate Spatial Models

It has been suggested that visual-to-motor transformations may occur across neurons and through stages that involve intermediate (or hybrid) frames of reference (Stricanne et al. 1996; Avillac et al. 2005; Mullette-Gillman et al. 2005; Snyder 2005). Therefore, in addition to the 11 canonical spatial models described above, we also considered the possibility for FEF neurons coding for intermediate spatial models. Figure 2.4*D* provides a visualization of intermediate frames of reference (for a mathematical description of how these models were derived see Keith et al. 2009). It shows the intermediate models between the eye-centered and head-centered frames with 9 intermediary frames of reference between the two canonical models, Te and Th (Fig. 2.4*D*, Gray dotted axes between eye- and head-frame), and two (of the 10) additional steps on either side beyond the canonical models (Fig. 2.4*D*, yellow dotted axes). These additional steps were included 1) to allow for the possibility that individual neurons might encode such abstract spatial codes outside the canonical range (Pouget and Snyder 2000; Blohm et al. 2009), and 2) to avoid misleading edge effects where the best-fit models might incorrectly cluster at the canonical models. Just as for Te and Th models in which the activity of the neuron is plotted on all trial-matched target positions relative to eye and head respectively, in each intermediate model, the activity profile of the neuron is plotted on all trial-

matched positions corresponding to that intermediate model (for 50-50 hybrid model, the position relative to the black axis in Figure 2.4*D* is used for the presented trial). Similar intermediate spatial models were calculated for each pair of target models (Te-Th shown in Fig. 2.4*D*, Th-Ts, Te-Ts; Fig. 2.10*A,E*), gaze models (Ge-Gs, Gs-Gh, Gh-Ge; Fig. 2.10*B,F*), displacement models (dG-dE, dE-dH, dH-dG; Fig. 2.10*C,G*), and position models (Gs-Eh, Eh-Hs, Hs-Gs; Fig. 2.10*D,H*). Each pair is depicted as one of the sides of the triangular representations in Figure 2.10. Important to note that unlike target- and gaze-related intermediate models which are describing intermediate frames of reference, the intermediate models between displacement and position models (Fig. 2.10 *C,D,G,H*) are rather abstract and do not have a physically intuitive description and have not been proposed before; nevertheless we tested them here for the sake of completion.

In addition to the intermediate model continua described above, we extended our analysis to a continuum between the eye-centered target and gaze models: Te and Ge. Models along this continuum represented intermediate spatial models (same way as the intermediate models described before) between target and gaze models in eye-centered coordinates (see Results; Fig.10). For instance, the RF model midway between Te and Ge was derived by plotting the trial-matched mid-points between target and gaze positions, as measured from our behavioral data and transformed into eye-centered coordinates.

2.3.10. Experimental Basis for Distinguishing the Models

In order to test between the models described above, they must be spatially separable, and this must be reflected somehow in neural activity. In our experiment spatial separation of the models was provided by the natural (i.e. untrained) variations in the monkey's gaze behavior. For example, the natural variability in accuracy of gaze shifts, especially in memory-guided movements (Fig. 2.1*B*), allowed us to distinguish between target coding versus coding for final gaze position. The variable contributions of eye and head movement to the gaze shift (Fig. 2.1*C*, Right panels) allowed us to distinguish between effector-specific parameters (both displacement and final positions), and the distribution of initial 3-D gaze, eye, and head orientations allowed us to distinguish between different egocentric frames of reference (although we could not distinguish between the body and space in our body-fixed experimental preparation). The models described in the previous section were computed from target locations and 3-D coil signals using mathematical conventions that have been described previously (Tweed and Vilis 1987; Crawford et al. 1999; Martinez-Trujillo et al. 2004; Keith et al. 2009). We then assumed (as in most previous studies) that this spatial variability would be reflected in different neural activity if one plots that activity against the correct spatial parameters (Jay and Sparks 1984; Avillac et al. 2005). The logic behind this approach, and the conventions we used to illustrate neural activity from individual trials, are schematically illustrated in Figure 2.4*E*. A target (red dot) at the ‘hot spot’ of hypothetical neuron’s RF is shown in the left panel, surrounded by 9 hypothetical gaze end-points (black/gray dots).

Corresponding neural responses (firing rate represented by the size of circle) are shown in the rightward table, plotted relative to target position (upper row) or relative to final gaze position (lower row). If a neuron is coding for this target location (left column), it would give the same response for each trial and these responses would coherently align in target coordinates (Fig. 2.4*E*; upper-left table cell) but would spread apart in gaze coordinates (Fig. 2.4*E*; lower-left table cell). If the neuron coded for gaze location, it would produce a different response for each trial, resulting in different (i.e., *spatially incoherent*) responses when plotted in target coordinates (Fig. 2.4*E*; upper-right table cell) but a graded 'hill-like' RF when plotted in gaze coordinates (Fig. 2.4*E*; lower-right table cell). If a variety of different target positions and gaze end-points were illustrated, these would yield four different RFs, with coherent maps in the upper-left and lower-left cells and incoherent maps in the other cells. Similar schematics can be constructed for any of the models considered here, with the prediction that one of these would yield the most coherent RF for the corresponding spatial code. Next we describe a formal method for testing this in real data.

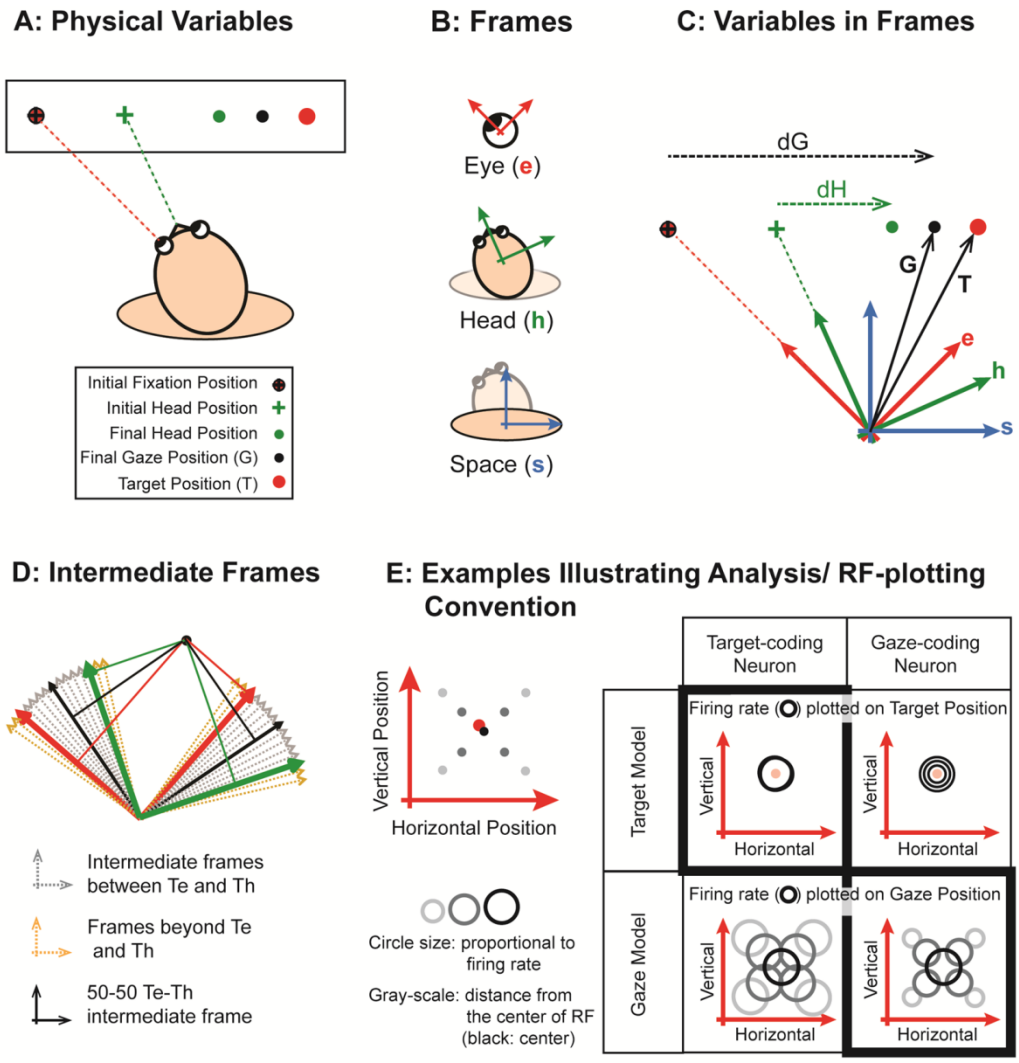

Figure 2.4. Description of the spatial models considered in this study (A-D) and a qualitative description of the logic behind the analysis method (E). The spatial parameters for a single trial are depicted in (*A*). The projections of initial gaze (black cross), initial head (green cross), final gaze (black dot) and final head (green dot) orientations on the screen are depicted. Here, final gaze position deviates from target location (red dot). In head-unrestrained conditions positions can be encoded relative to three egocentric frames of reference (*B*) namely, eye (e), head (h), and space/body (s). Given that the target was sufficiently far from the head to minimize the effects of translation, and that our analysis method is insensitive to such biases, we approximated the centre of these frames to be aligned as shown in (*C*). (*C*) shows the canonical models that result from plotting parameters in *(A)* in reference frames from (*B*). dG: gaze displacement; i.e., final gaze position with respect to the fixation point (not the eye). dH: displacement of head in space coordinates. dE (eye displacement; not shown) is the displacement of eye in the head that accompanies the gaze shift (*D*) Shows the intermediate reference frames between (dashed gray axes) and beyond (yellow axes) eye (red) and head (green) frames of reference in a single trial. (*E*) Is a schematic showing the logic behind the response field (RF) analysis in this study. Left panel: represents a single visual target (red dot) and final gaze positions (black/gray dots) for 9 gaze shifts made to this target (each with a different magnitude and direction of error). Right panel: depicts the RF plots of two 'ideal' neurons represented in Target and Gaze models. Each circle represents a data point on the RF plot with size proportional to the firing rate of the neuron. The gray-scale coloring scheme represents the distance from the centre of the RF (black is at the centre). The Target model is preferred for that target-coding neuron and the Gaze model is preferred for the gaze coding neuron (bolded table cells).

2.3.11. Spatial model analysis for single neurons

Our method was an extension of the schematic shown in Figure 2.4*E*: we plotted visual and movement RFs from our neurons in the spatial coordinates of each of the canonical (and intermediate) models tested, positioning the neural responses according to the spatial coordinates of the corresponding behavioral data. For visual RF mapping, we used eye and head orientations taken at the time of visual stimulus presentation, whereas for movement RF mapping we used behavioral measurements taken at the start of the gaze shift. (Actual examples of such plots are shown in Figures 2.5, 2.7, 2.9 of the results section.) We then computed residuals between the data points and the model fit using Predictive Residuals Sum or Squares (PRESS) statistics (described below) and compared the residuals to determine which model provided the best overall fit (i.e., the best RF representation). The detailed steps of this analysis follow.

Step 1: Non-parametric fitting of the RFs: Since we did not know *apriori* the shape of the RF, we used non-parametric fitting to fit the data points. Since the size of the RFs were not known and the spatial distribution of the sampled data points was different for different spatial models (e.g., smaller range for head models as opposed to target/gaze models) the non-parametric fits were obtained using Gaussian kernels with different sizes ranging from 2 -15° bandwidths (14 different fits obtained for each model). This ensured that we are not biasing our fits in favor of a particular size and spatial distribution. Spatial models with smaller spread of positions (e.g., head models) would be fitted better using smaller kernels in comparison to spatial models with larger spread of positions.

Furthermore, by virtue of employing a non-parametric fitting approach, the analysis was relatively insensitive to unusual biases and spatial distributions in either behavioral or neural data, or to differences in uniformity of spatial sampling of these data in different coordinate frames (see Keith et al. 2009 for further explanation) though in our dataset most RF representations had a relatively continuous spread of data points due to the variability in our behavioral paradigm.

Step 2: Calculating PRESS residuals: Once the fits were made to activity profile distributed in different models, the quality of the fit in each model (at all kernel bandwidths) was quantified using PRESS statistics, which is a form of cross-validation (Keith et al. 2009; DeSouza et al. 2011). In short, the PRESS residual for each trial was obtained by removing that trial's data point from the dataset, obtaining a fit using the remaining data points, and then taking the residual between the fit and the data point. The model (at the kernel bandwidth) that yielded the smallest mean PRESS residuals (which we referred to as the '*best-fit model'*) was identified as the best candidate for the neuron's spatial coding scheme. The assumption here was that if a neuron's activity is represented in a model based on the neuron's intrinsic code, the RF should be spatially more coherent than if represented in any other spatial model.

Step 3: comparison between different spatial models: Once the best-fit model was identified, its mean PRESS residuals were then statistically compared with the residuals for other spatial models fitted at the same kernel bandwidth using a two-tailed Brown-Forsythe test (see Keith et al. 2009). Spatial models that had significantly higher mean PRESS residuals compared to the best-fit model were

excluded as candidate coding schemes for that neuron. Similar procedures were used to test for best-fits along the intermediate model continua (Fig. 2.4*D*) generated for individual neurons.

2.3.12. Population analysis

For population analysis we did a statistical comparison of the mean PRESS residuals across the entire neuronal population for different spatial models. For each neuron PRESS residuals were normalized such that one of the models (here we took Th) had a mean PRESS of 1, so this way the relative goodness of fit between spatial models was preserved across all neurons (DeSouza et al. 2011). Although for some neurons more trials were used for RF analysis, we assigned an equal weight for each neuron for our population analysis, as we did not want the population results to be skewed in favor of neurons with higher number of trials. As for the single-neuron analysis, the spatial model with the smallest population mean PRESS residuals was the best candidate spatial model describing the population activity. A two-tailed Brown-Forsythe test was performed between the population mean PRESS residuals for this model and the population mean PRESS residuals from other models, and any model with significantly higher mean PRESS residuals ($p<0.05$) was excluded as candidate coding scheme for the population activity. Population analysis for the intermediate frames was done in a similar fashion.

2.4. Results

We recorded from over 150 sites within the FEF of two rhesus macaques during head-unrestrained gaze shifts. Of these, 64 task-related neurons showed good isolation, and were confirmed to be in the FEF using previously established head-restrained stimulation criteria (Bruce and Goldberg 1985). Of those, 57 met all of our criteria for analysis; 8 of which were classified as visual (V; Fig. 2.3*A*), 30 were classified as visuomovement (VM; Fig. 2.3*B*), and 19 were classified as movement (M; Fig. 2.3*C*) neurons. Figure 2.2 illustrates the anatomic extent of our included sites (●), corresponding head-restrained saccade vectors evoked by head-fixed stimulation of these sites (→), other sites also identified as FEF through recording / stimulation (○), and the remaining sites that we explored (x). Similar to previous studies, we found that our stimulation-confirmed FEF sites fell along an arc corresponding to shape and stereotaxic coordinates of the Arcuate Sulcus. In the majority of stimulation sites the evoked saccades resembled a fixed vector to the contralateral side relative to the point of fixation. Stimulation at the most lateral sites ('small-saccade FEF') evoked saccades as small as 2 degrees, whereas at the most medial sites ('large-saccade FEF') evoked saccades as large as 20-25 degrees, which would likely correspond to much larger gaze shifts in the head-unrestrained condition (Martinez-Trujillo et al. 2004; Monteon et al. 2010). Also, as shown previously, we found that neurons on the lateral end of the FEF typically had small, bound (closed) RFs and neurons on the medial end of the FEF typically had large, unbound (open) RFs. Of the 38 neurons with visual responses, 23 had closed RFs and 15 had open RFs.

Movement RFs were generally broader than visual RFs even within single VM neurons. Of the 49 neurons with movement responses 30 had open RFs, and 19 had closed RFs (15/19 M-cells had open RFs).

We separately analyzed visual and movement responses. For visual analysis we fitted the activity during the visual epoch (Fig. 2.3, mauve window, on the left) and for movement analysis we fitted the activity during the movement epoch (Fig. 2.3, mauve window, on the right) and full movement burst (Fig. 2.3, vertical lines, right column). Since we have variable initial gaze positions in our experimental paradigm we also tested for gaze position-dependent modulation (i.e., gain field) effects so we could remove them before performing our residual analysis. However, in this study we did not find significant gain field effects unlike the only other study that used this method in the SC (DeSouza et al. 2011). The following sections describe our results first for the visual, and then movement fits.

2.4.1. Analysis of canonical models

2.4.1.1. Visual activity

The RF analysis for an example V neuron is depicted in Figure 2.5. As described in methods, the activity profile of the neuron (spike count in sampling window; Fig. 2.5*A*) was plotted in all 11 canonical representations and then fitted using different Gaussian kernels ranging from 2-15° bandwidths and the quality of fit in each representation (at each kernel bandwidth) was quantified using PRESS residuals (Fig. 2.5*B*). For this neuron, the lowest PRESS residuals were obtained when the activity profile was distributed across target positions in eye-centered coordinates (i.e., Te), fitted with a Gaussian kernel of 4° bandwidth. Therefore,

Te was the best-fit model for this neuron. Statistical testing (Brown Forsythe test) between the PRESS residuals of Te and PRESS residuals of all remaining models at this kernel bandwidth (*p*-values shown in Fig. 2.5*C*) showed that all remaining models have significantly higher PRESS residuals compared to Te, leaving Te as the only candidate coding scheme and reference frame for this neuron.

It is also possible to visualize these trends intuitively. The RF plots of this V neuron are shown in three of the 11 representations: Ts, Te and Ge (Fig. 2.5*D*-*F*). In Ts model the activity profile of the neuron (firing rate in the sampling window for each trial is represented by size of circle) is distributed on a map determined by the angular direction of the *targets* as appeared on the screen (i.e., space-centered). The color-field represents the non-parametric fits made to these data for the optimal kernel bandwidth. Note that the Ts model provides a rather poor description of variability in neuronal activity as indicated by a high degree of activity variability (circle size) for a given point on the map (i.e., low coherence), and also by the relatively large size of the residuals shown at the bottom of the panel (Fig. 2.5*D*, similar to Fig. 2.4*E*, top-right cell in the right panel). In contrast, when the RF was represented in its eye-centered counterpart (Te; best-fit model), like-sized circles clustered together (i.e., high coherence) and the residuals were much smaller (Fig. 2.5*E*). Note than Ts and Te are both spatial models based on target position and only differ in their frame of reference (eye versus space). Putting the data in the 'correct' frame of reference was not enough to obtain these results: for example, when the same data are mapped

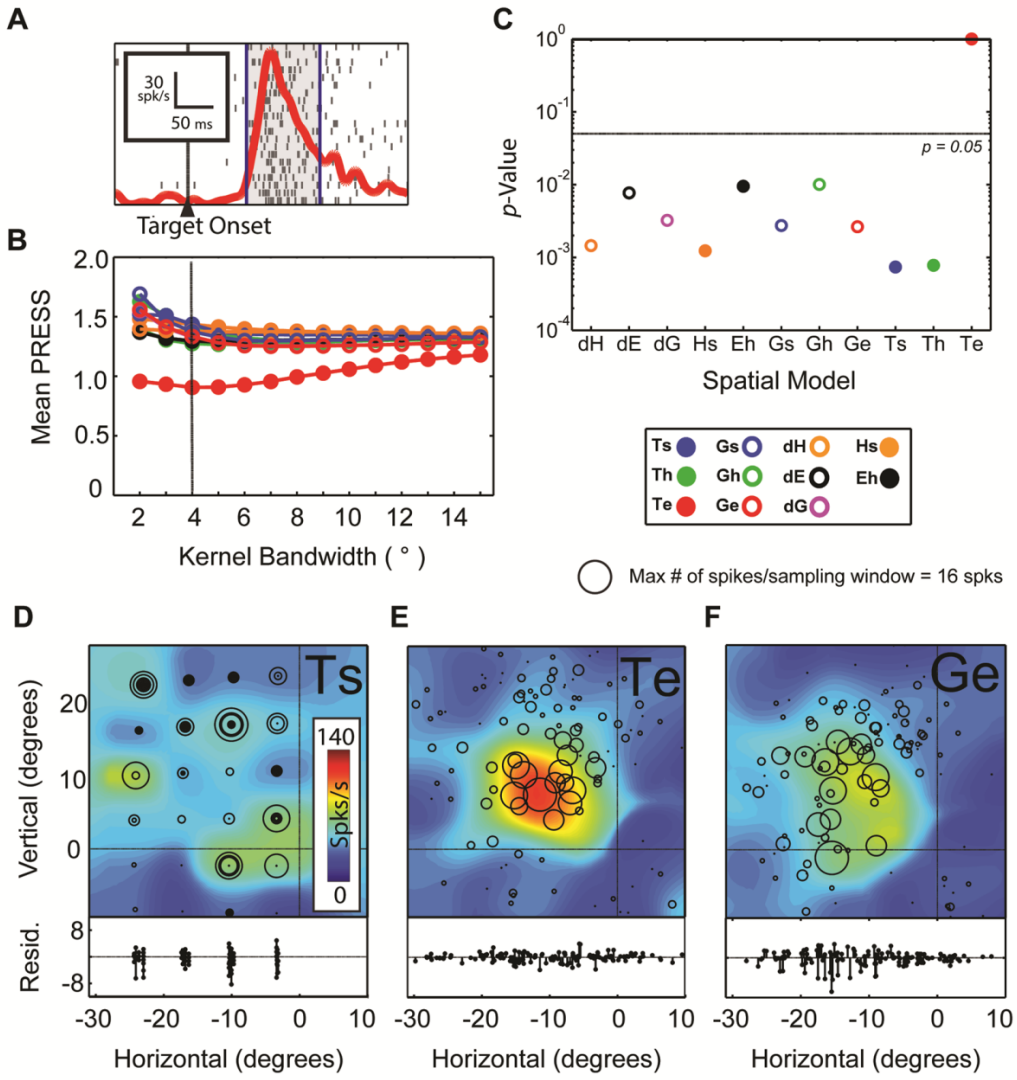

Figure 2.5: Example RF analysis for the visual activity of a representative V neuron. Visual activity was sampled at the visual epoch: 80-180ms after target onset (*A*). The mean residuals from PRESS statistics are shown for all canonical models, fitted using Gaussian kernels with bandwidth ranging from 2-15° (*B*). For this neuron, the lowest mean PRESS was obtained for the eye-centered target model (Te), when fitted using a Gaussian kernel of 4° bandwidth. (*C)* shows the *p*-values for the statistical comparison between Te ($p = 10^0$; the best-fit model, with smallest mean PRESS residuals) and each of the remaining 10 canonical models (Brown-Forsythe test). Models (i.e., circles) falling below the horizontal line ($p = 0.05$) have significantly higher residuals compared to best-fit model and are thus excluded. (*D-F)* show the representation of the activity profile in three spatial models. Ts: activity profile spread over target positions defined relative to space, i.e., the screen; Te: activity profile spread over target positions relative to the eye; and Ge: activity profile spread over final gaze positions relative to the eye. Each circle represents a trial, placed at the appropriate location in the spatial model, with size proportional to the corresponding firing rate (similar to Fig. 2.4*E*). The color-field in each plot represents the non-parametric fit to the RF of the neuron at the best kernel bandwidth (4° here). PRESS residuals obtained for the three models are depicted below each RF plot. When activity is plotted in Te, the RF is spatially more organized (i.e., more coherent) and the residuals are smaller compared to either the Ts (same spatial code, but different reference frame) or Ge (different spatial code, but same frame of reference). This neuron was recorded from a lateral site in the FEF of animal A (see Fig.2, gray circle shades).

according to the Ge model (Fig. 2.5*F*), which is an eye-centered RF map based on gaze end-points, the RF again becomes incoherent and the residuals are higher. Thus, the optimal RF map of a neuron is only obtained when the correct spatial code (e.g., target as opposed to gaze) *and* the correct frame of reference (e.g., eye- as opposed to space-frame) are used.

Figure 2.6*A* summarizes these results for all 8 of our V neurons, showing the per cent of neurons with only a particular model as the sole candidate for the spatial code (black), neurons for which a particular model was the best model but at least one other model was not significantly ruled out (red), neurons for which a particular model was not preferred but was also not significantly excluded (yellow), and neurons for which a particular model was statistically eliminated (gray). As one can see, most V neurons showed a preference for Te, and in two (25%) of these neurons all models including eye-centered gaze models, dG and Ge, which are spatially similar to Te were significantly eliminated. In another 2 of the 8 neurons eye (in head) displacement (dE) or Ge were preferred, though Te remained as the candidate coding scheme. Therefore, in our visual population there was a relatively strong preference for Te as compared to other models while the head-related models (dH and Hs) and Gs were eliminated for most neurons even at the individual-neuron level.

Figure 2.7 illustrates our analysis for an example VM neuron using the same conventions as Figure 2.5, except this time only showing RF maps in the original spatial target (Ts) frame (Fig. 2.7*D*) and the model that provided the best fit (Fig. 2.7*E*). The representation that yielded the best fit (i.e. smallest PRESS residuals)

was the Te model fitted with a Gaussian kernel of 3° bandwidth, but for this neuron the two eye-centered gaze models (Ge and dG) were not statistically ruled out (Fig. 2.7*C*). Te was the best-fit model for most (23/30) of our VM neurons, but only for one of these neurons all other models were eliminated. A few (7/30) neurons preferred other models that were spatially similar to Te (i.e., dE, Ge, dG, Th), but the remaining models (dH, Hs, Eh, Gs, Gh, Ts) were never preferred (Fig. 2.6*B*).

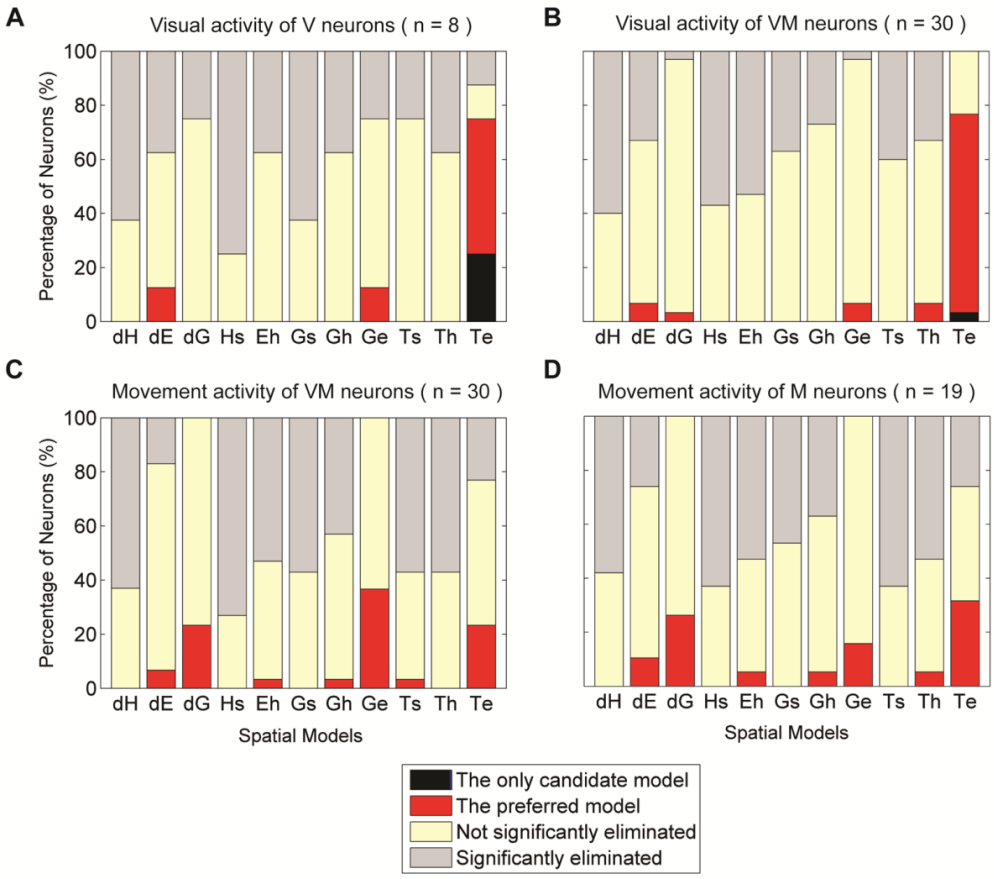

Figure 2.6: Distribution of goodness of fit (vertical axis) to each model (horizontal axis) across neurons for the visual activity of the V neuron population (*A*), the visual activity of the VM population (*B*), the movement activity of the VM population (*C*) and the movement activity of the M neuron population (*D*). Each vertical bar is color-coded to show the % neurons that showed a fit that was statistically preferred (black), non-significantly preferred (red), neither preferred or significantly eliminated (yellow), or significantly eliminated (gray).

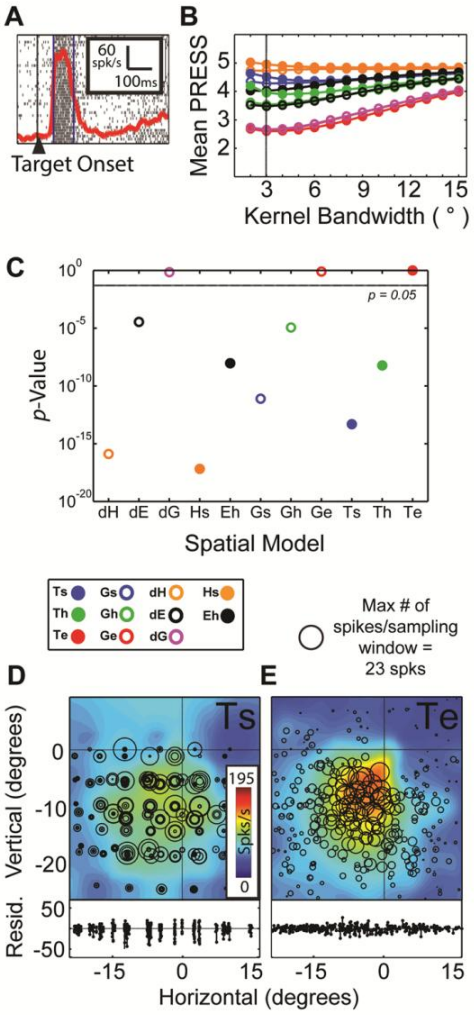

Figure 2.7: Example RF analysis for the visual activity of a representative VM neuron. Similar conventions to Figure 2.5 are used. (*A*) shows the visual sampling window: 80-180ms after target onset. (*B*) shows the mean residuals from PRESS statistics for all canonical models for all tested kernel bandwidths: 2-15°. The lowest mean PRESS was obtained for the eye-centered target model (Te) when fitted using a Gaussian kernel of 3° bandwidth. (*C*) shows the *p*-values for the statistical comparison between Te ($p = 10^0$) and the other canonical models. (*D and E*) are the representation of the activity profile in the Ts (depicting the distribution of targets on the screen), and the Te (best-fit) models. This neuron was recorded from a lateral site in the FEF of animal S (see Fig.2, gray circle shades).

The results reported so far are for single neurons; however, it is important to know how neurons behave as a population. For visual population analysis, V and VM populations were separately analyzed (Fig. 2.8*A,B*). In both populations Te was the best model describing population activity as the population mean PRESS residuals were the lowest for this model. However, more movement codes (Ge and dG) were significantly ruled out in the V compared to VM population. Due to similarity in the overall trend between the two visual populations we also

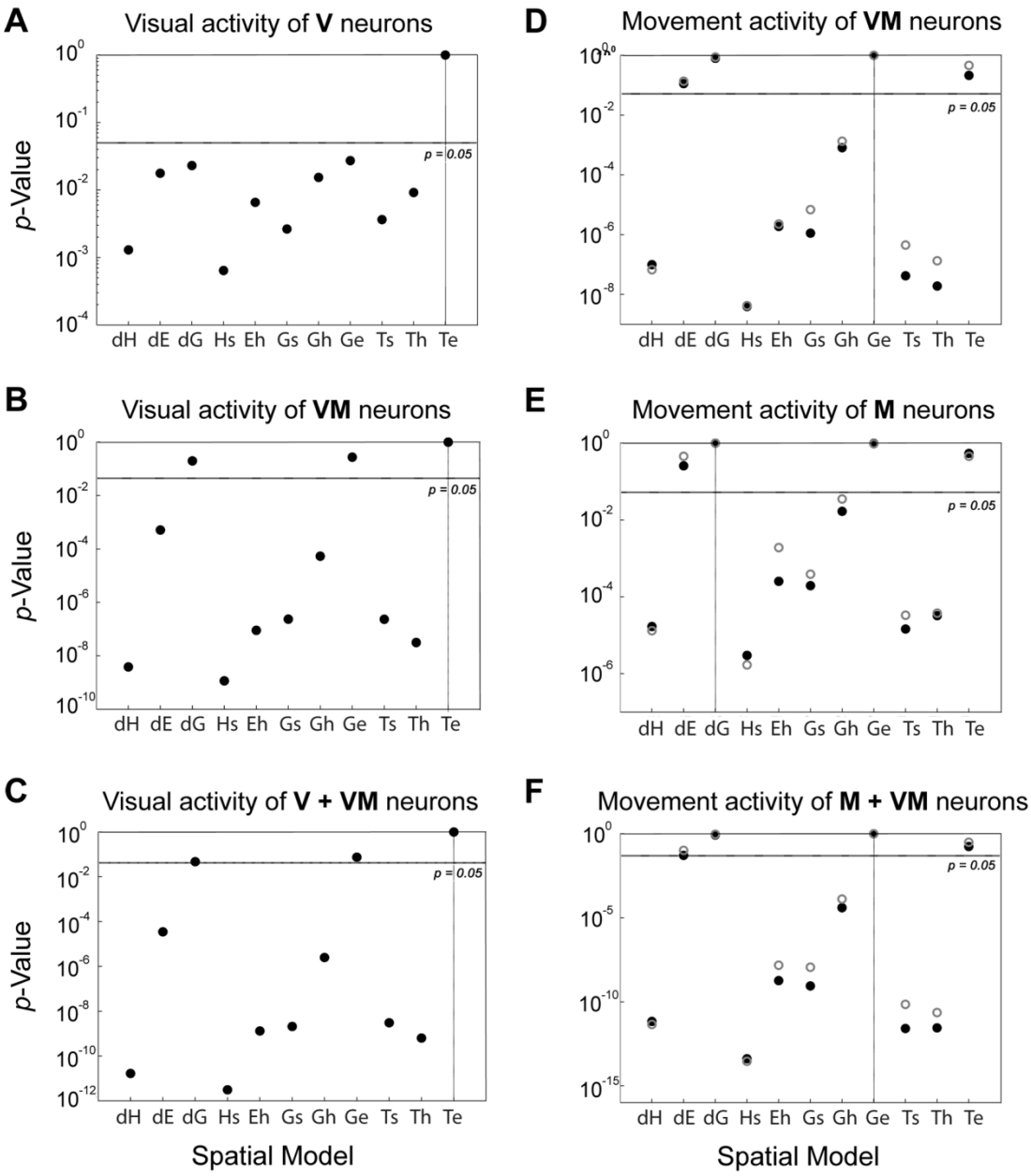

Figure 2.8: Population statistics for visual and movement responses in different neuronal subpopulations. The *p*-value results for the population analysis of the visual response of V neurons (*A*) and VM neurons (*B*) and entire visual population (V + VM) (C), and the movement activity of VM neurons (*D*) and M neurons (*E*) and entire movement population (VM + M) are depicted. For each subpopulation, the model with the lowest mean normalized PRESS residuals (averaged across all neurons) is the best model describing the population coding scheme. ($p = 10^0$). Models (i.e., circles) falling below the horizontal line ($p = 0.05$) have significantly higher mean PRESS compared to best model and thus are excluded as candidate coding schemes for the population. Open circles: *p*-values for visual (*A*-*C*) or movement (*D*-*F*) analysis based on a fixed 100ms sampling window used for all neurons with head effector models based on head contribution to gaze. Filled black circles: *p*-values for movement analysis (*D*-*F*) based on full-burst sampling window (set on a neuron-specific basis) with head effector models based on the complete head movement.

combined them for the statistical analysis illustrated in Figure 2.8*C*. This analysis confirmed the preference for Te that was observed in many individual neurons. All other models were significantly excluded as candidate coding schemes for the visual population ($p < 10^{-4}$, Fig. 2.8*C*) with the exception of the two eye-centered gaze models (Ge and dG, $p = 0.075$ and $p = 0.051$, respectively, Brown-Forsythe test). Thus, we have eliminated space-centered and head-centered models as well as eye or head movement-related models for visual responses.

2.4.1.2. Movement activity

Movement activity was quantified using both a neuron-specific window that included the full movement-related burst as well as a fixed temporal window (-50 to +50ms relative to gaze saccade onset; rationale for this window described in methods). Since (as we shall see) the full burst sometimes provided better separation between models, but otherwise both analyses yielded very similar results, the full burst was used as our default (i.e., in Fig. 2.6,9,10,11).

Figure 2.9 shows the RF analysis for two example movement responses, one VM neuron (with a small and closed RF) and one M neuron (with large and open RF), using the same conventions used in Figure 2.5. For the VM neuron, the best-fit model was Ge fitted with a Gaussian kernel of 4° bandwidth. Once again, in Ts plot, which shows the activity profile distributed over targets as appeared on the screen (i.e., space-coordinates), there is a huge variability in neural activity for a given location for both neurons. But this time, unlike the visual response examples, the neuron's movement activity was best described by Ge: a model based on final gaze positions relative to the initial 3-D eye orientation (i.e., eye-

coordinates; Fig. 2.9*E*). Statistical comparison between the best model (Ge) and all remaining models (Brown-Forsythe test) for the VM neuron (Fig. 2.9*C*), eliminated most models as candidate coding schemes ($p < 10^{-5}$) with the exception of Te, dE, and dG. The dG RF plot (not shown) looked very similar to the Ge plot shown in Figure 2.9*E*, whereas the others diverged commiserate with their statistical ranking.

This example neuron was representative of most of the movement responses in our 30 VM neurons (Fig. 2.6*C*), which showed a distribution of preferences mainly amongst the eye-centered gaze (dG and Ge), and target (Te) models. Occasionally, other models were preferred but this preference was never significantly greater than the gaze-related models. In some cases Ge and dG were the only two candidate models, but these two models could not be separated from each other. The head-related models (dH and Hs), space-centered models (Gs and Ts), and head-centered target model (Th) were significantly eliminated in most neurons.

Similar trends were observed for M neurons, which often showed large open RFs. Figure 2.9*F-J* shows the RF analysis for a M neuron with such a field (incidentally, the behavioral data corresponding to this neuron is presented in Figure 2.1*B,C*). Once again, the representation resulting in the lowest PRESS residuals and the most coherent RF map was the Ge representation (fitted with a Gaussian kernel of 5° bandwidth) though Te and dG (which both were very similar to Ge) remained as candidate coding schemes. In contrast, head-centered and space-centered models, as well as eye and head movement-

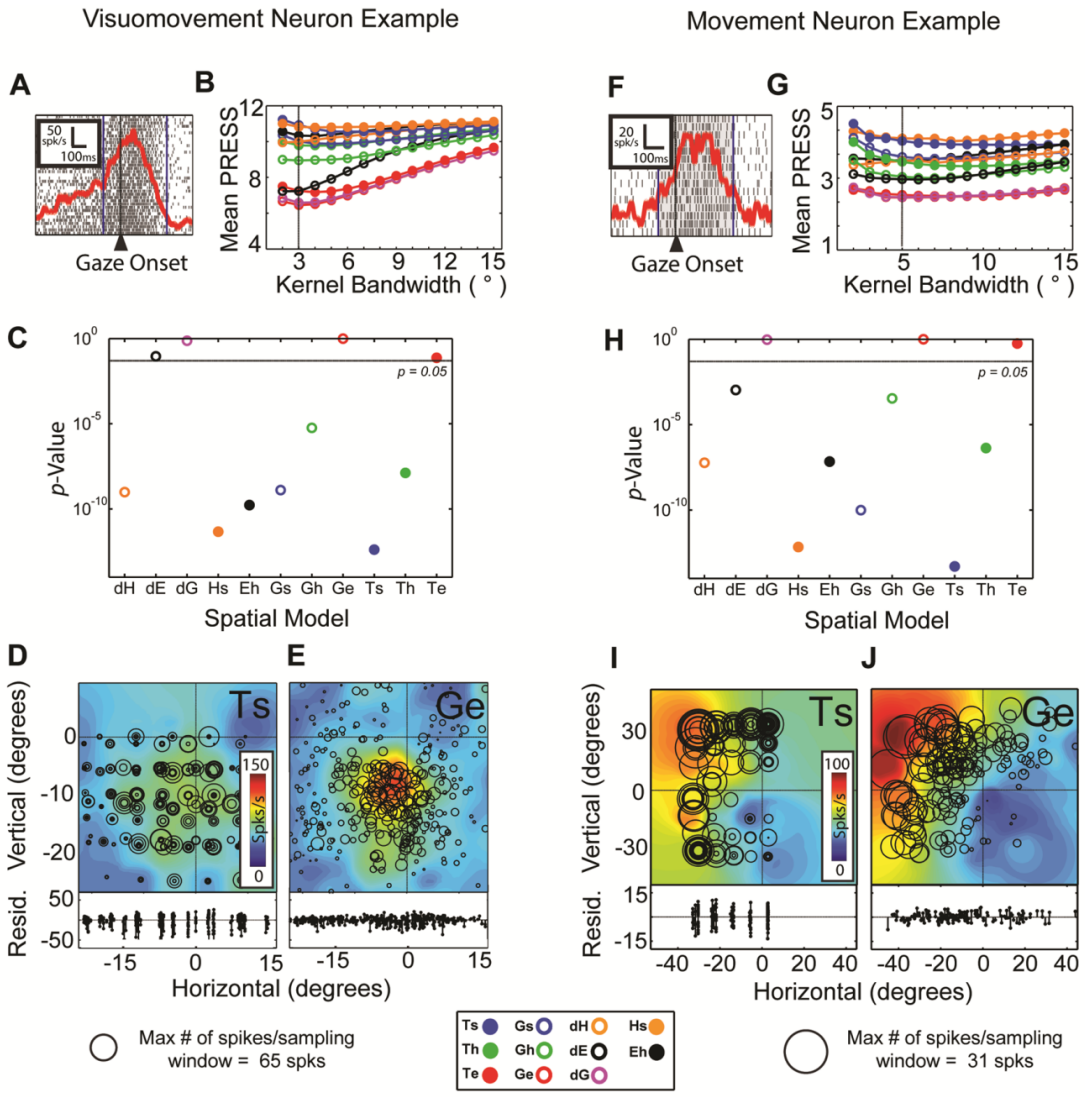

Figure 2.9: Example RF analysis for the movement activity of representative VM and M neurons. Similar conventions to Figure 2.5 are used. For the VM neuron (same neuron as in Fig. 2.7) activity was sampled from -100ms to +270ms relative to gaze onset (*A*). (*B*) shows the mean residuals from PRESS statistics for all canonical models for all tested kernel bandwidths: 2-15°. The lowest mean PRESS was obtained for Ge fitted using a Gaussian kernel of 3° bandwidth. (*C*) shows the *p*-values for the statistical comparison between Ge ($p = 10^0$) and the other canonical models (Brown-Forsythe test). (*D and E)* show the representation of the activity profile in the Ts (depicting the distribution of targets on the screen), and the Ge models. When represented in Ge, the neuron has a small, closed (i.e., bound) RF. (*F-J*) show the similar analyses but for a representative M neuron. The sampling window for this neuron was from -50ms to +270ms relative to gaze onset (*F*). The lowest mean PRESS was obtained for Ge when fitted using a Gaussian kernel of 5° bandwidth (*G*). (*H-J*) same as (*C-E*) but pertains to the M neuron. For this neuron when the activity profile is represented in Ge, the neuron has a large, open (i.e., unbound) RF (*J*). The behavioral data pertaining to the M neuron is presented in Figure 2.2.1*B,C*. The M neuron was recorded from a medial site in the FEF of animal S (see Fig.2, gray circle shades).

related models were eliminated as candidate coding schemes for this neuron (Fig. 2.9*H*). Across our 19 M neurons (Fig. 2.6*D*), dG, Ge, and Te were most preferred whereas the head models (dH, Hs) were eliminated in most neurons (even with the prolonged burst accompanying the full head movement included in the analysis). Importantly, the gaze models (Ge and dG) were never excluded for any movement response even if these models did not yield the best fit.

When the two movement populations were pooled together (Fig. 2.8*F*), Ge and dG provided the best fits, whereas all other models (with the exception of Te and dE; $p = 0.17$ and $p = 0.051$ respectively, Brown-Forsythe test) were eliminated . Separate population analysis of VM and M neurons also provided very similar results (Fig. 2.8*D,E*). Similar to the visual population, all head-centered and space-centered models, as well as head displacement, and effector position models were significantly ruled out ($p < 0.0001$, Brown-Forsythe test). Noteworthy that we obtained essentially the same results using the fixed window in our movement epoch (-50 to +50ms relative to gaze onset) with head-models based on head movement during the gaze saccade (Fig. 2.*8D-F*, grey open circles) and full-burst window with head-models based on full head movement (Fig. 2.*8D-F*, black circles).

Several other variations of the analysis were attempted. We categorized our neurons based on whether they had open or closed movement RFs, but did not find any notable difference between these subpopulations. We also repeated our analysis for each neuron only on the subset of trials in which the head contribution to gaze was at least 2° visual angle. This served to account for the

possibility that some cells may exhibit different spatial codes depending on whether the head contributes to the gaze shift or not. In this analysis, once again Ge and dG were among the best models while head-centered and space-centered models, and head-related models (dH and Hs) were amongst the poorest models both at the single neuron and population levels (results not presented).

2.4.2. Intermediate spatial models

So far, we have only tested between the 11 canonical spatial models described above. However, we also performed an intermediate model analysis to account for the possibility of spatial coding in intermediate frames of reference. Figure 2.10 depicts the distribution of the best-fit intermediate models (denoted by circles with diameter corresponding to the neuron count) for visual (Fig.10, left column) and movement (Fig.10, right column) activities across the tested intermediate models. (see methods for description of these models).

The results from this analysis revealed that there was a tight clustering of best-fit models (i.e., circles) around the Te model for visual activity, irrespective of neuron type (i.e., V versus VM). Specifically, in 32/38 RFs, the intermediate models spatially closest to Te were the best-fit (Fig. 2.10*A*). The overall best-fit model for the visual population (i.e., the model giving rise to the lowest overall residuals) was located at an intermediate model near Te. None of the other canonical spatial models were contained within the 95% confidence interval (Fig. 2.10*A-D,* yellow highlights). However, there were several 'outliers' from this

range: some neurons showed their best-fit model closer to other canonical models, and some had best-fit model that was drawn away from head- and

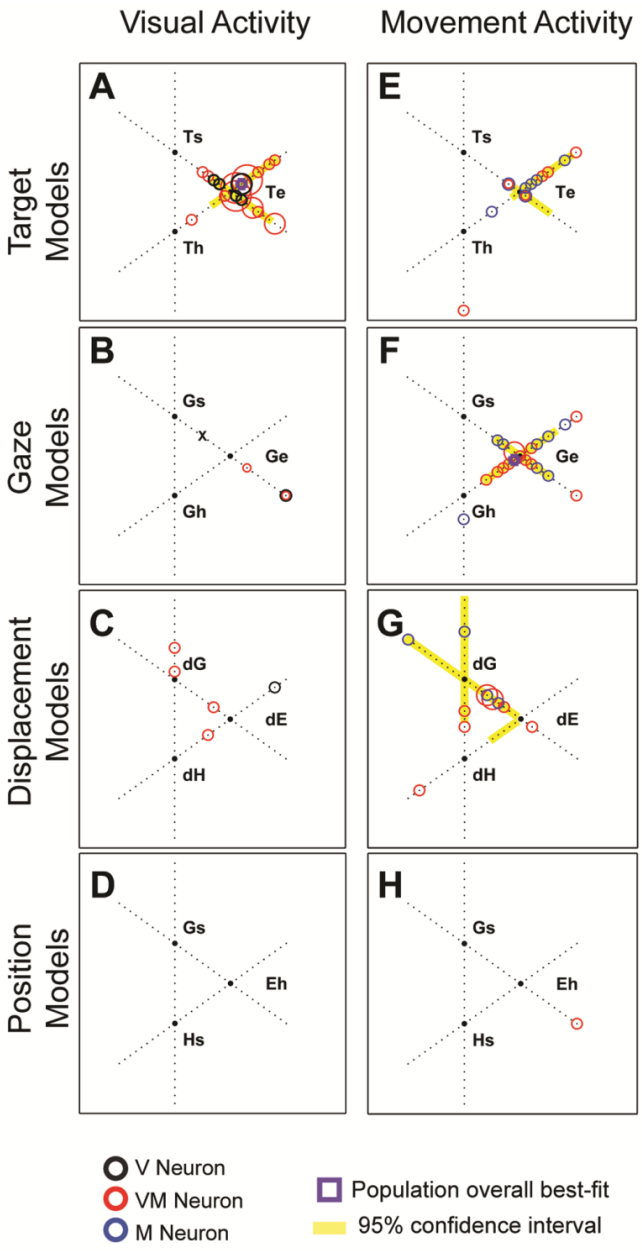

Figure 2.10: Analysis of intermediate (hybrid) spatial models for visual and movement-related activities. Each node at the apex of the triangles represents one of the 11 canonical models considered in this study. Intermediate models were defined at equally spaced intervals between two canonical models. For instance, the model lying between Ge and Gs ("x" on panel *B*) denotes a model based on final gaze positions in an intermediate frame between eye- and space-coordinates (see Fig. 2.4*D* for another example). Intermediate models between the three target models (*A, E*), three gaze models (*B, F*), three displacement models (*C, G*), and three position models (*D, H*), for both visual and movement activities were considered. For each neuron, the intermediate spatial model that yielded the lowest PRESS residuals across all these intermediate models (i.e., best-fit model) was identified. Each circle denotes the best-fit model, with the diameter of circle representing the number of neurons with that best-fit. (*A-D*) shows the best-fit distribution for visual activity of V (black) and VM (red) neurons. (*E-H*) shows the best-fit distribution for movement activity of both M (blue) and VM (red) neurons. The overall best-fit for the overall visual population (purple square in panel *A*) was in close proximity to Te model with the 95% confidence interval (yellow highlight) tightly around Te model, but not including any of the remaining 10 canonical models. The overall best-fit for the movement population (purple square in panel *F*) was in close proximity to Ge model with the confidence interval including only dG and Te models but not containing any of the remaining canonical models.

space-centered models even more than Te (so the best-fit fell beyond Te away from Th and Ts) (Fig. 2.10*A*). This is thought to arise when behavior is determined by the overall balance between members of the neuronal population, rather than individual neurons (Pouget and Snyder 2000; Blohm et al. 2009).

The movement responses did not show as tight clustering as the visual responses, showing a confidence interval spread across several of the intermediate frame continua that we constructed (Fig. 2.10 *E-G*), and again with some individual 'outliers' placed either in other continua or beyond these intermediate continua. But in contrast to visual responses the majority of movement responses had their best RF representation (i.e., best-fit) among the gaze-related intermediate models and largely clustered around the Ge model (Fig. 2.10*F*). Some neurons however, had their best-fit model around Te (Fig. 2.10*E*) or along the dG-dE continuum (Fig. 2.10*G*). Neurons with best-fit models near dG tended to be shifted toward dE, most likely because of the high degree of similarity between eye and gaze displacement in gaze shifts from a central range (Freedman and Sparks 1997a). VM and M neurons had a similar distribution of best-fits along these continua. In confirmation of the aforementioned results for canonical models, none of the neurons had their best-fit around dH or any effector position model (Fig. 2.10*G,H*). The overall best-fit for the movement population fell around Ge, and head-centered and space-centered canonical models, as well as dH and effector position models were not contained within the confidence interval (i.e., these were significantly ruled out).

In summary, our intermediate model analysis showed that despite variability in the position of the best-fit models within the population, they are not distributed haphazardly throughout this map (in Fig.10) but are rather clustered around the eye-centered canonical models, namely Te or Ge/dG in agreement with the population analysis shown for the canonical spatial models (Fig. 2.6 and 8). Importantly, there is an overall shift from Te clustering in the visual response (Fig. 2.10*A*) towards clustering about the eye-centered models derived from final measured gaze position (Ge and dG) in the movement response (Fig. 2.10*F,G*). These analyses suggests that 1) all neuronal populations in the FEF show a clear preference for an eye-centered code, and 2) visual and movement responses are not only temporally locked with the stimulus and gaze shift (by definition), they also show different spatial codes; specifically, target versus gaze coding.

2.4.3. Target-Gaze Continuum Analysis

To summarize the results so far, most of the candidate spatial models (e.g., all models involving head control and all head-centered and space-centered models) have been eliminated. The dominant models at the population level –Te for the visual response (Fig. 2.8*C*) and Ge/dG for the movement response (Fig. 2.8*F*) – were all eye-centered and suggest a shift from target coding to gaze coding in the visual-to-movement responses. However, we have not yet demonstrated this distinction at a statistical level, or examined whether it also emerges at the level of individual neurons with both visual and movement responses. Also we wanted to investigate whether neurons in the population exhibit a graded, as opposed to bimodal, preference for target versus gaze

coding. To address these questions, we elaborated our intermediate model analysis to include a new continuum between (and beyond) target and gaze models (Fig. 2.11). We chose Te to represent target models because it was the clear 'front-runner' for the visual response analysis, and we chose Ge to represent the gaze models because it uses the same frame of reference as Te and yields the same results as the other 'front runner' (i.e., dG). The resulting Te-Ge continuum was constructed based on 10 equally-spaced intervals between Te and Ge (in eye coordinates), and 10 intervals extended on either end (see methods). As an example of an intermediate model between Te and Ge, the RF plot based on the model denoted as '0' along this continuum would be obtained from activity profile distributed across the mid-points between target and final gaze positions.

First, we plotted the VMI (see methods for calculation) of each neuron as a function of best-fit location along the Te-Ge continuum described above (Fig. 2.11*A*, top panel). There was no significant correlation between VMI and spatial coding of FEF neurons within visual responses (R = 0.63 ; p = 0.08, linear regression) or movement responses (R = -0.15; p = 0.28, linear regression); however, when examined across the range, one can see a trend for responses from V neurons (red) to mainly fall in the lower-left corner (preference for a model close to Te) and responses from M neurons (black) to mainly fall in the upper-right corner (preference for a model close to Ge), with VM responses (pink and gray) perhaps falling in the intermediate region.

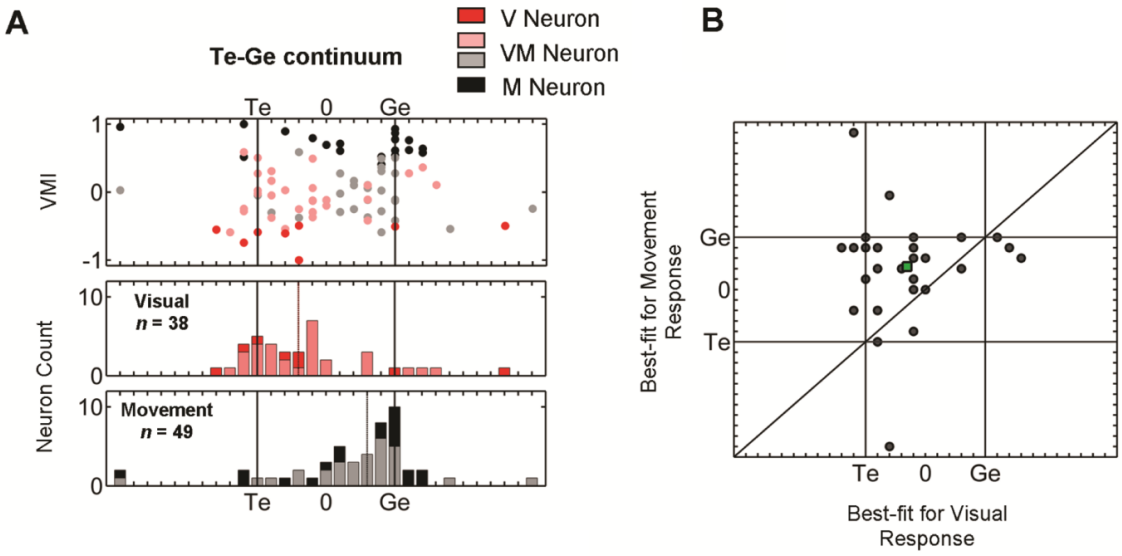

Figure 2.11: Distribution of best-fit intermediate models across the Te-Ge continuum for visual and movement responses and its relationship to visuomovement index (VMI). For each neuron, the fits based on intermediate spatial models between (and beyond) target and gaze models (in eye-coordinates) were considered. As an example the in-between model (denoted as '0') would be a model in which the activity profile is spread over the mid-point between visual target and final gaze positions for all trials. (*A*, top panel) For each neuron (and activity type) VMI is plotted against best-fit location along the Te-Ge continuum. The frequency distributions of best-fits along Te-Ge continuum are plotted for the visual activity of V (red) and VM neurons (pink) (A, middle panel) and the movement response of VM (gray) and M (black) neurons (A, lower panel). There is a significant difference between the distribution of best-fits for combined visual and combined movement responses (p = 0.000134, Mann-Whitney U test). This difference is also significant for the population of VM neurons (pink versus gray; p = 0.0016, Wilcoxon test). The medians of best-fit locations for all visual (*A*, middle panel, vertical red line) and all movement (*A*, lower panel, vertical black line) responses are shown. (*B*) The horizontal (x) and vertical (y) axes represent the Te-Ge continuum for visual and movement responses respectively. Black dots with coordinate (x,y) represent neurons with visual best-fit model at x and movement best-fit model at y. Any dot above the line of identity signifies a VM neuron with the movement best-fit moved towards the Ge-end of the continuum compared to its visual response. The majority of dots appear above the line of identity suggesting a transformation from target coding to gaze coding occurring within *individual* cells. Green square represents the mean across the population of best-fit locations for the movement response versus the best-fit locations for the visual response.

Figure 2.11*A* also provides frequency histograms showing the distribution of best-fits for visual responses (middle panel) and movement responses (lower panel) along the Te-Ge continuum. The distribution of best-fits along this continuum was compared for each cell population and subpopulation (Kruskal-Wallis test followed by Mann-Whitney U test with BonFerroni correction). There

was no significant difference between the two visual populations (p = 0.67) or between the two movement populations (p = 0.57). However, comparison between the best-fit distributions across activity types revealed a significant difference between the best-fit distributions of visual and movement responses in the FEF (p = 0.000134, Mann-Whitney U test).

This difference was also evident when paired comparisons were made between the visual and movement activity of *single* VM neurons. This was tested by performing a neuron-by-neuron comparison of visual versus movement best-fit locations along Te-Ge continuum (Fig. 2.11*B*). Most individual VM neurons showed a shift along the Te-Ge continumum (toward Ge) between their visual and movement responses. This shift was statistically significant for the population (p = 0.0016, Wilcoxon test). Thus, this analysis provided a neuronal correlate for sensorimotor transformation not between population of neurons within the FEF, but also within individual VM cells.

2.5. Discussion

This study is the first to directly test between the entire possible set of visuospatial and gaze movement representations within the FEF in the same dataset during naturally variable head-unrestrained gaze shifts. Our results eliminate a number of candidate models (at least within the task parameters that we used), and provide clear evidence for the FEF being involved in a spatiotemporal transformation of sensory into movement representations, within an eye-centered coordinate frame. Specifically, we have shown that in the temporal gap between its visual and movement responses, the FEF (in

conjunction with its network connections) transforms the location of visual targets into gaze movement commands, both at the cell population level, and at the single-neuron level.

2.5.1. Visual versus movement spatial coding in the FEF

Our results suggest that early visual activity (80-180ms after target onset) in the FEF codes for the spatial location of visual stimuli in eye-centered coordinates (Te). This fits well with the documented literature on visually-evoked responses in the FEF that suggests the early visual response in the FEF is involved in visual detection of stimuli regardless of their task relevance (Thompson and Schall 1999), and the FEF serving as an attention priority map (Thompson and Bichot 2005). These factors were not directly tested in our paradigm, but it makes sense that these target-related computations would be done with target represented in an eye-centered reference frame (Te), rather than a movement code in some other frame. V and VM sub-populations show similar projections to their downstream structures including the SC and the pons (Segraves 1992; Sommer and Wurtz 2000) and overall showed similar results in our analysis. However, these sub-populations have different biophysical and morphological properties (Cohen et al. 2009), and so might be expected to show different codes. When they were separately analyzed (Fig. 2.8*A,B*), the V population showed a stronger preference for Te, perhaps suggesting a more direct or exclusive visual input.

Sato and Schall (2003) showed that in an anti-saccade task (where the gaze is opposite to target location), the visual response of about one third of visually-responsive FEF cells (type II cells; Sato and Schall 2003) codes for the location

of the saccade rather than the visual target. We found a minority of individual visually-responsive neurons (22%) that showed a preference for gaze parameters, but this preference over target coding never reached significance; so we cannot claim that this explains Sato and Schall's (2003) results. The other explanation, which we prefer, is that all FEF visual cells encode Te, but in some (type II), this can undergo a cue-dependent transformation to encode a mentally reversed target representation (Zhang and Barash 2000; Medendorp et al. 2004; Amemori and Sawaguchi 2006; Fernandez-Ruiz et al. 2007; Collins et al. 2008).

In contrast to the clear-cut visual target code observed in FEF visual activity, the movement activity of both VM and M neurons showed a somewhat more distributed coding scheme (Fig. 2.10) but overall preferentially coded for final gaze position relative to initial eye orientation (Fig. 2.8; 10) with a significant shift away from a target code toward a gaze scheme (Fig. 2.11). It has been shown that the FEF predominantly projects to subcortical structures in the brainstem (mainly SC and pons) (Schiller et al. 1979; Stanton et al. 1988; Dias et al. 1995) but also sends projections to the early visual areas (such as area V4) (Stanton et al. 1995; Moore and Armstrong 2003). We did not test where these neurons project to, so we cannot be certain that all FEF movement signals analyzed in this study represent the output of the FEF to downstream brainstem structures that in turn drive the gaze shift. But given that the majority of movement responses in our sample preferred gaze coding, it is fair to assume that the subcortical projection also predominantly contains a gaze code.

Similar to previous studies in head-unrestrained conditions (Bizzi and Schiller 1970; DeSouza et al. 2011; Knight 2012) the movement responses in some of our neurons were relatively prolonged compared to head-restrained conditions. Although we cannot preclude the possibility that some of this late movement response contained efference copy signals from downstream structures (Bruce and Goldberg 1985; Sommer and Wurtz 2004), we took several precautions to minimize the inclusion of such signals and to mainly include signals that are more likely to contribute to the gaze movement. First, we only included cells with clear pre-saccadic activity, and eliminated neurons with activity starting after saccade onset. Second, we also did our analysis on a peri-saccadic time window that only included responses up to 50ms after saccade onset. Since the latency for FEF signals arriving at eye muscles is 20-30ms (Hanes and Schall 1996), and saccades in our dataset were on average 140ms long, it is likely that at least this early movement activity of these neurons directly contributed to the gaze shift. Importantly, we did not see a change in the preferred coding scheme when this 'earlier' peri-saccadic window was used instead of the full movement burst.

The preference for a gaze code in the movement response is consistent with previous anti-saccade studies which suggested that movement activity of FEF neurons mainly codes for the direction of the saccadic eye movement rather than the location of the visual stimulus (Everling and Munoz 2000). Our study strengthens this conclusion because it does not have the interpretive limitations of the anti-saccade task. First, although the anti-saccade task is successful in introducing a spatial dissonance between the sensory and movement

components of the task, it requires non-standard spatial transformations that have been shown to engage quite different patterns of neural activity throughout cortex (Sweeney et al. 1996; Grunewald et al. 1999; Matthews et al. 2002; Brown et al. 2007; Hawkins et al. 2013). Furthermore, it is possible that in this task at some point within the visuomotor pathway the representation of the target is reversed before generating a gaze command (Zhang and Barash 2000; Medendorp et al. 2004; Fernandez-Ruiz et al. 2007). Therefore, this technique by itself does not allow for the distinction between gaze and target coding. In this study, using our RF mapping method, we dissociated between the sensory and movement coding in a task that involved standard spatial transformations, and we found that the movement response preferentially codes for the final location of the gaze. There was no notable difference in spatial coding between the movement responses of VM and M populations. This however does not suggest that these neuron types necessarily have the same function in the gaze system (Ray et al. 2009).

It is often assumed that gaze inaccuracies can be attributed to noise arising somewhere within the visuomotor pathway (Faisal et al. 2008; Churchland et al. 2006). The errors observed in our memory-guided delay task could not arise solely from noise in downstream transformations, because this would not cause the preference for gaze coding over target coding that we observed in our FEF movement responses. This finding suggests that at least some of the neural noise contributing to our gaze errors arose from non-visual activity occurring in the interval between the visual and movement burst. This could include noise

arising from functions such as target selection and attention (Basso and Wurtz 1997; Platt and Glimcher 1999), motor functions such as the mechanisms that trigger saccades at the go-signal (Churchland et al. 2006) and the cumulative noise expected to arise in the recurrent connections required to maintain working memory in the stimulus-response interval (Compte et al. 2000; Chang et al. 2012; Wimmer et al. 2014). The latter part of this proposal is consistent with the notion of memory-based spatial transformations within the FEF (Gnadt et al. 1991).

2.5.2. Effector Specificity

Our results strongly suggest that the FEF movement activity is coding for the gaze movement vector rather than the eye and head components of gaze independently. Among the effector-related models, gaze-related models (Ge and dG) were clearly preferred, with all other models statistically eliminated at the population level, with the exception of the eye-in-head displacement model (dE), which was marginal. The latter is likely because dE becomes very similar to dG when head movements are not very large (Freedman and Sparks 1997a), which was often the case in the gaze shifts that we tested, especially for ‘near’ RFs.

In an early study by Bizzi and Shiller (1970) neurons were found in the FEF that discharged exclusively during horizontal head movements, but in this study spatial coding of neurons was not analyzed (Bizzi and Shiller 1970). The only other study to address the question of gaze versus eye or head coding in the FEF during head-unrestrained gaze shifts (Knight 2012) suggested that about half (13/26) of the neurons in dorso-medial FEF code for the head movement amplitude during the saccade. However, we did not find any neuron, including

FEF neurons in the most medial portion of our recorded sites (Fig. 2.2), coding for head position or displacement, and such head-related models were always excluded at the population level. This difference could be due to task differences. In our paradigm, gaze shifts were initiated from a central range of positions and made toward the full 2-D range of the RF, we relied on endogenous variability to dissociate between eye and head contributions, accounted for noise related to initial 3-D eye and head orientations, and employed a statistical analysis that made no assumptions about linearity. Knight (2012) performed a 1-D linear analysis based on a paradigm that dissociated between head and gaze by comparing similar-sized gaze shifts starting from different initial gaze positions (which correlates to different head contributions to gaze; Freedman and Sparks 1997a,b; Knight 2012). Some of our neurons might have also coded for head movement in this paradigm; one cannot say without testing this. However, there is evidence that eccentric gaze positions are associated with head position signals (Monteon et al. 2012), and gaze position-dependent gain field modulations become more prominent at eccentric gaze positions (Andersen and Mountcastle 1983; Cassanello and Ferrera 2007; Knight 2012). Therefore, linear correlation might conflate such signals with head movement signals in a paradigm where initial gaze/head orientation correlates to head contribution to gaze. Finally, we recorded from approximately twice as many neurons and on average analyzed approximately 10 times the number of trials for each neuron.

Although position-dependent gain fields have been previously reported in the FEF in both head-restrained and head-unrestrained conditions (Cassanello and

Ferrera 2007; Knight 2012), in our dataset we did not detect significant gaze position-dependent effects. This is most likely because the initial range of positions in our dataset were not optimized to detect gain fields. It is possible however that undetected gain field modulations can account for a proportion of the noise in our RF fits, along with other non-spatial factors that we did account for such as trial-to-trial variations in attention and motivation (Basso and Wurtz 1997 ; Platt and Glimcher 1999).

Our data agrees with most studies that quantified eye-head coordination in gaze shifts evoked during FEF stimulation. Other than some exceptions (Chen 2006) the majority of FEF microstimulation studies support a gaze code (Guitton and Mandl 1978; Tu and Keathing 2000; Elsley et al. 2007; Knight and Fuchs 2007; Monteon et al. 2010, 2013). Overall, these studies suggest that the default mechanism for decomposing gaze commands into separate eye and head commands resides in the brainstem / cerebellum (Segraves 1992; Pare and Guitton 1998; Quaia et al. 1999; Sparks 2002; Isa and Sasaki 2002; Klier et al. 2007; Gandhi and Katnani 2011), but other cortical neurons appear to modulate this mechanism so that the head can contribute differently to gaze in different contexts (Constantin et al. 2004; Monteon et al. 2012).

2.5.3. Reference frames: eye-centered dominance in the FEF

To our knowledge, this is the first single-unit study to address the question of reference frame coding in completely head-unrestrained gaze shifts. Our results point to the dominance of eye-centered coding in the FEF. Our population analysis excluded all models that relied on a head-centered or space/body-

centered frame of reference (whether for coding target, gaze, eye, or head motion). This was most clear-cut in the visual code, where every model but Te was statistically eliminated. The preferred movement codes (Ge and dG) are also eye-centered in the sense that they share a coordinate origin at the fovea. The difference between these models is that Ge (final gaze position relative to the eye) has coordinate axes fixed on the retina (eye is a sphere with rotational geometry) whereas dG (gaze displacement; same as gaze position in fixation-centered coordinates) has coordinate axes fixed at the point of fixation in space (Crawford and Guitton 1997). Unfortunately, we never found a statistical preference for Ge versus dG for individual neurons or our populations, so we cannot exclude the possibility that either or both are used in the FEF. It is likely that we could not discriminate between these models because 1) our method works best at discriminating very similar models in neurons with small, closed RFs, 2) the geometric differences between dG and Ge only become pronounced for very large gaze shifts (Klier et al. 2001); and 3) in this range, we only recorded large, open movement RFs. In theory, a Ge movement code would simplify transformations both from the Te visual code and into the retina-centered codes reported in the SC (Klier et al. 2001; DeSouza et al. 2011). In contrast, dG would require position-dependent transformations between these codes, at least for very large saccades (Crawford and Guitton 1997), but might be more appropriate to drive the reticular formation burst neurons. However, testing between these possibilities would require some more experimental design, such as measuring the RFs from consistently deviated torsional eye positions

(Daddaoua et al. 2014). In general, our eye-centered results (Te for visual response and Ge/dG for movement response) agree not only with unit-recording studies in the FEF in head-restrained animals (Bruce et al. 1985; Russo and Bruce 1994; Cassanello and Ferrera 2007) but also in most other visuomotor areas (Mays and Sparks 1980; Colby et al. 1995; Russo and Bruce 1996; Tehovnik et al. 2000; Avillac et al. 2005; Mullette-Gillman et al. 2005; DeSouza et al. 2011). This suggests that if any transformations into other head- or space-centered codes occur, they occur downstream from the FEF.

One way to examine this question is through microstimulation. Microstimulation of the FEF in head-unrestrained conditions yields a continuum of eye-centered to head-centered gaze output, depending on the site of stimulation (Monteon et al. 2013). This does not necessarily contradict our current results. Theoretical studies suggest that visual RFs reveal the frame of the sensory input to the neuron, whereas microstimulation reveals the frame of reference of the target neuron population that is activated by the output of that same area (Smith et al. 2005; Blohm et al. 2009). Since the FEF projects to both the SC and reticular formation (Segraves 1992; Freedman and Sparks 1997b; Pare and Guitton 1998; Isa and Sasaki 2002; Sparks 2002; Stuphorn 2007; Walton et al. 2007), and the latter may control eye and head motion using a combination of head- and body-centered frames (Klier et al. 2007) it is not implausible that FEF neurons with eye-centered activity might *influence* head-unrestrained gaze behavior in multiple frames (Monteon et al. 2013; Martinez-Trujillo et al. 2004).

2.5.4. Role of the FEF in Spatial Transformations for Gaze Control

The schematic model in Figure 2.12 summarizes our findings and the conclusions discussed above. Visual input into the FEF, encoding target location in eye coordinates, is sent to the FEF from parietal and temporal areas such as the LIP and extrastriate visual cortex (Schall et al. 1995). This would give rise to the eye-centered target code (Te) observed in our visual data. In our memory-guided task, this target location signal enters a recurrent visual working memory network (comprised of structures such as the posterior parietal cortex (PPC), FEF, and dorso-lateral prefrontal cortex (DLPFC);

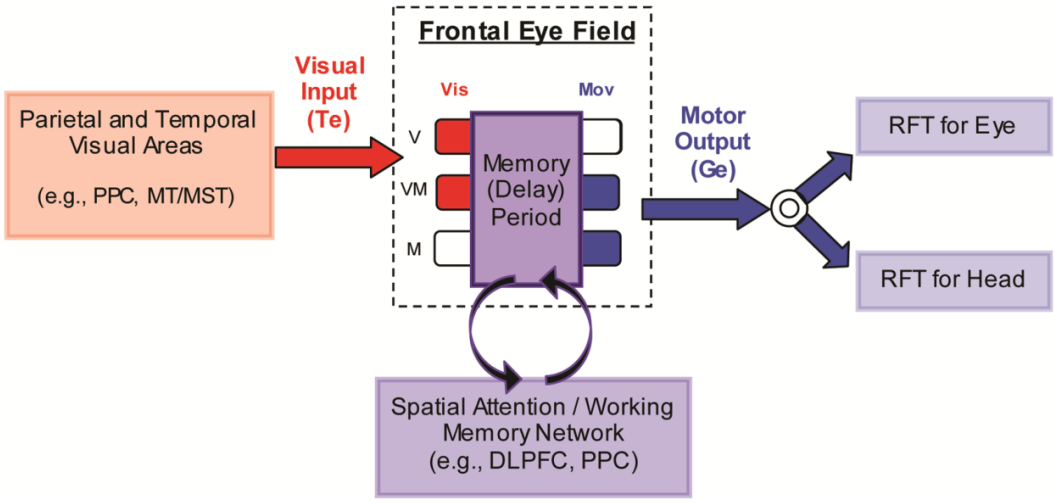

Figure 2.12: Schematic of a model for visual-to-motor transformations in the gaze system during the memory-guided gaze task. Visual signal containing target feature and location information is sent to FEF from parietal and temporal visual areas such as the PPC and MT/MST. The memory of target location is retained in eye-centered coordinates through recurrent connections with frontal and parietal areas such as the PFC and PPC, as part of the short-term memory network. This memory is retained until the go-signal is presented, after which the gaze command, coding the timing and the metrics of the impending gaze movement is generated. We propose that the distinction between target location relative to the eye (Te) in the visual response (of V and VM neurons) and gaze parameters (Ge) in the movement response (of VM and M neurons) arises from noise accumulated in the recurrent nature of the memory network and possibly produced by other 'cognitive' computations in this network. Finally, the eye-centered gaze code is 'split' downstream into eye and head movement commands with appropriate reference frame transformations (RFT) for each. PPC: Posterior Parietal Cortex; MT: Medial Temporal area; MST: Medial Superior Temporal area; PFC: Prefrontal Cortex.

Fuster and Alexander 1971; Ikkai and Curtis 2011; Funahashi 2013). As noted above, noise in these recurrent connections and possibly other cognitive / motor functions, likely causes the divergence between the visual and movement signals (Compte 2000; Faisal et al. 2008; Shenoy et al. 2013). The findings that the FEF (and likely other cortical gaze control structures) use simple eye-centered visual and movement codes suggest that this is advantageous for the other cognitive functions they control, and conversely, that the complexity of these structures is related to additional functions rather than reference frame transformations (Olson and Gettner 1995; Cohen and Andersen 2002; Hutton 2008; Purcell et al. 2012; Schall 2013).

Finally, our data suggest that in behaviors that we tested, the gaze-related output of the FEF is decomposed by default into separate signals for eye and head control downstream –each with their own reference frame transformations. This, however, does not preclude a role for frontal cortex in eye-head coordination during more complex context-dependent behaviors (Constantin et al. 2004; Monteon et al. 2012). Thus, this model fully accounts for the visuospatial transformations performed by the FEF, at least within a set of circumstances similar to those studied here.

Is this model of visuomotor transformation unique to the FEF? In other words, is this transformation happening only within the FEF? We think this is unlikely as similar neural response types and spatial codes have been observed in related structures such as the SC (Schlag-Rey et al. 1992; Munoz and Wurtz 1995; Freedman and Sparks 1997b; Everling et al. 1999; DeSouza et al. 2011), PPC

(Gottlieb and Goldberg 1999; Steenrod et al. 2013), PFC (Funahashi et al. 1991, 1993), and other cortical and subcortical areas (Schlag and Shlag-Rey 1987; Watanabe and Funahashi 2012; Funahashi 2013). Therefore, the transformation reported in this study might be occurring concurrently in a distributed network of interconnected structures, and not solely performed within the FEF (Pare and Wurtz 2001; Wurtz et al. 2001; Munoz and Schall 2004). However, this question can only be answered by similar testing in all of these structures.

Chapter 3:

Transition from Target to Gaze Coding in Primate Frontal Eye Field During Memory Delay and Memory-Motor Transformation

(Sajad et al., 2016)

Amirsaman Sajad[1-3], Morteza Sadeh[1,3,4], Xiaogang Yan[1], Hongying Wang[1], and John Douglas Crawford[1-5]

[1]Centre for Vision Research,

[2]Neuroscience Graduate Diploma Program,

[3]Department of Biology,

[4]School of Kinesiology and Health Sciences,

[5]Department of Psychology,

York University, Toronto, Ontario, Canada, M3J 1P3,

Corresponding Author:

Name: Prof. J.D. Crawford

3. 1.1. Abstract

The Frontal Eye Fields (FEF) participate in both working memory and sensorimotor transformations for saccades, but their role in integrating these functions through time remains unclear. Here, we tracked FEF spatial codes through time using a novel analytic method applied to the classic memory-delay saccade task. Three-dimensional recordings of head-unrestrained gaze shifts were made in two monkeys trained to make gaze shifts toward briefly flashed targets after a variable delay (450-1500 ms). A preliminary analysis of visual and motor response fields in 74 FEF neurons eliminated most potential models for spatial coding at the neuron population level, as in our previous study (Sajad et al., 2015). We then focused on the spatiotemporal transition from an eye-centered target code (*T*; preferred in the visual response) to an eye-centered intended gaze position code (*G*; preferred in the movement response) during the memory delay interval. We treated neural population codes as a continuous spatiotemporal variable by dividing the space spanning *T* and *G* into intermediate *T-G* models and dividing the task into discrete steps through time. We found that FEF delay activity, especially in visuomovement cells, progressively transitions from *T* through intermediate *T-G* codes that approach, but do not reach, *G*. This was followed by a final discrete transition from these intermediate *T-G* delay codes to a 'pure' *G* code in movement cells without delay activity. These results demonstrate that FEF activity undergoes a series of sensory-*memory*-motor transformations, including a dynamically evolving spatial memory signal and an imperfect memory-to-motor transformation.

3.1.2. Significance Statement

Gaze-related signals in frontal cortex are often used as an experimental model for visual working memory. However, the spatial codes employed during the delay between target-related visual activity and intended gaze-related motor activity remain unknown. Here, we show that frontal eye field delay activity (particularly in visuomovement neurons) shows a progressive transition through intermediate target-gaze codes, with a further jump to coding intended gaze position in movement neurons with no delay response. Since our analytic method is based on fitting neural activity against variable behavioral errors, this suggests that such errors accumulate during the memory delay, and further escalate during the final memory-to-motor transformation. Any of these vulnerable processes might be further degraded by diseases that affect frontal cortex.

3.2. Introduction

Primates routinely use remembered stimuli to guide spatial behavior, with varying degrees of spatial precision (Gnadt et al., 1991; White et al., 1994). This could involve a sensory-to-memory transformation, maintenance of the target in working memory, and a memory-to-motor transformation (Goldman-Rakic, 1987; Postle, 2006; Bays et al., 2011; Chatham and Badre, 2015). However, it is not known at what point in this sequence the *spatial* code for the sensory stimulus is transformed into a spatial code for movement, and likewise, when and how spatial errors in behavior arise (Gnadt et al., 1991; Stanford and Sparks, 1994; Krappmann, 1998; Opris et al., 2003; Faisal et al., 2008).

Memory-guided saccades provide an ideal experimental model for this question because many saccade-related neurons in the brainstem and cortex exhibit spatially-selective visual, memory, and / or movement responses (Funahashi et al., 1989; Bruce and Goldberg, 1985; Schall, 2015; Wurtz et al., 2001). Further, the gaze control system, which normally controls both eye and head motion, provides convenient parameters for spatial coding (i.e., target, gaze, eye, head) in various egocentric frames (eyes, head, or body) (Freedman and Sparks, 1997; Martinez-Trujillo et al., 2003; Sajad et al., 2015). Still, a complete description of the spatiotemporal transformations in the sensory-memory-motor transformation for gaze control remains elusive.

Neurophysiological studies often trained monkeys to look toward a location that is spatially incongruent with the visual stimulus in order to dissociate target (*T*)

coding in visual responses vs. intended gaze position (*G*) coding in motor responses, without addressing the intervening memory delay (Gottlieb and Goldberg, 1999; Everling and Munoz, 2000; Sato and Schall, 2003). Most studies that explored this issue during delay activity employed similar tasks to look for a discrete target-to-gaze switch (Funahashi et al., 1993; Mazzoni et al., 1996; Zhang and Barash, 2004). Other studies showed a gradual rotation of the population direction vector from the stimulus toward the instructed movement direction in Dorsolateral Prefrontal Cortex (dlPFC), or a more abrupt rotation in the mediodorsal thalamus (Takeda and Funahashi, 2004; Watanabe et al., 2009). However, no previous experiment tested if delay activity evolves across time through intermediate spatial codes (i.e., between *T* and *G*) in the visual-memory-motor transformations for saccades *toward* remembered stimuli.

Assuming that one could track such codes through time, there are several ways that a *T-G* transition could occur in memory-guided saccades (Fig. 3.1*D*). A sustained *T* code followed by a late *T-G* transition would be compatible with sensory theories of working memory (Funahashi et al.,1993; Constantinidis et al., 2001), whereas an early *T-G* transition would be compatible with motor theories of working memory (Gnadt and Andersen, 1988; Gaymard et al., 1999; Curtis and D'Esposito, 2006; Rainer et al., 1999). Alternatively, *T-G* transition could progressively accumulate during the delay (Gnadt et al., 1991; Wimmer et al., 2014). Another possibility (not shown) is that there is no transition of coding *within* any given population of cells, but rather a temporal transition of activity

from a *T*-tuned population of neurons to a *G*-tuned population (Takeda and Funahashi, 2007).

The monkey frontal eye fields (FEF), located in prefrontal cortex, are an ideal location to study this question because they are directly involved in the sensorimotor transformation for saccades and head-unrestrained gaze shifts (Bruce and Goldberg, 1985; Schall, 2015), and are part of the working memory network (Funahashi et al., 1989; O'Sullivan et al., 1995; Dias and Segraves, 1999; Sommer and Wurtz, 2001). In a recent study we exploited the variable behavior of head-unrestrained gaze shifts to show that FEF visual and motor responses encode *T* and *G* respectively (both relative to initial eye orientation) in saccades made toward remembered visual stimuli (Sajad et al., 2015). However, this previous analysis could not show when or how this transition happens, and did not explore the contributions of individual cell types. Here, we used a similar approach, but applied our analysis in steps through time to fit a continuum of intermediate *T-G* models through the entire course of a memory-guided saccade task. Since this method is based on fitting spatial models against variable behavior such as errors in final gaze direction (Keith et al., 2009; Sajad et al., 2015), this also provided a direct measure of how such errors accumulate through different phases of a memory-guided gaze shift. Further, with the use of a larger data set, we were able to categorize our cells into different memory (or non-memory) related populations, in order to understand their differential contributions through time to the *T-G* transition.

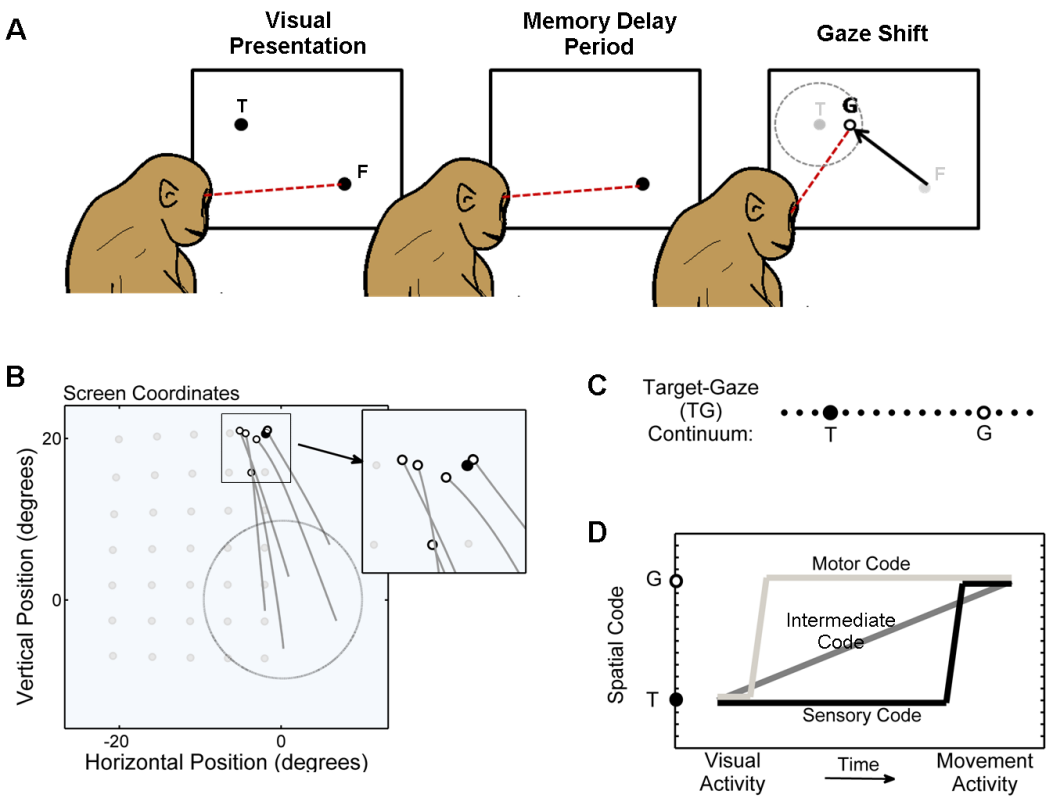

Figure 3.1. An overview of the experimental paradigm and a conceptual schematic of the possible coding schemes in the FEF. A) Activity was recorded from single neurons in the FEF while monkeys performed memory-guided gaze task with the head free to move. Monkeys initially fixated a visual stimulus (black dot labeled F) for 400-500ms. A visual stimulus (black dot labeled *T*) was then briefly flashed on the screen for 80-100ms (left panel). After an instructed delay (variable in duration; 450-850ms or 700-1500ms) the animal made a gaze shift to the remembered location of the target (gray dot labeled *T*) upon the presentation of the Go-signal. The Go-signal was the disappearance of the initial fixation target (gray dot labeled F). Inaccuracies in behavior were tolerated such that if final gaze landed within a window around the target a juice reward was provided. B) Five gaze trajectories to a single target (black circle) within a wide array of target (5 × 7 for this example session; gray dots) within the neuron's approximate RF location are shown. Initial fixation positions (tail of the trajectory) were randomly varied within a central zone (large gray circle) on a trial-by-trial basis. Final gaze positions (white circles) fell at variable positions around the target. Variability in initial and final positions (relative to different frames of reference) of target, gaze (i.e., eye in space), eye (in head), and head was used to spatially differentiate sensory and various motor parameters in various frames of reference. We exploited the variability in behavioral errors to differentiate between spatial models based on target position (*T*) and final gaze position (*G*). C) Additionally, a continuum of intermediary spatial models spanning *T* and *G* were constructed to treat spatial code as a continuous variable; this allowed us to trace changes in spatial code as activity evolved from vision to memory delay, during memory delay, and from memory delay to motor. D) shows some plausible schemes for the spatiotemporal evolution of neuronal code based on proposed theories: 1) The target code could be transformed into a gaze code early-on, and this gaze code maintained during memory (motor theory; light gray line), 2) the target code could be maintained in the memory (sensory theory; black line) and subsequently transformed into a gaze code upon movement initiation, or 3) the spatial code could gradually change from a target code to a gaze code (dark gray line).

3.3. Materials and Methods

3.3.1. Surgical procedures, identification of FEF, and behavioral data recordings

All protocols were in accordance with the Canadian Council on Animal Care guidelines on the use of laboratory animals and approved by the York University Animal Care Committee. The data were collected from two female *Macaca mulatta* monkeys (monkeys A and S). Each animal underwent surgeries for implanting the recording chamber (19mm diameter) which was centered in stereotaxic coordinates at 25mm anterior for both monkeys, and 19mm for one and 20mm lateral for the other. A recording chamber was attached over the trephination with dental acrylic (Fig. 3.2). In order to eliminate non-viable spatial models of neural coding from our analysis (see below), we needed to record head-unrestrained gaze shifts in three dimensions (3-D). To do this, two 5-mm-diameter sclera search coils were implanted in one eye of each animal and two orthogonal coils mounted on the head (Crawford et al., 1999).

3.3.2. Behavioral paradigm

Monkeys were trained to perform the classic memory-guided gaze task in completely head-unrestrained conditions (Fig. 3.1*A*). After fixating a visual stimulus presented on the screen, a second visual stimulus (target) briefly flashed for 80-100ms in the periphery cuing the gaze shift goal. However, the animal had to withhold gaze until the instruction to make gaze shift (Go-signal = disappearance of fixation target) was provided, at which time a gaze shift was made to the remembered location of the target. The Go-signal was presented at

a random time within a flat distribution that ranged 450-850ms (for 56/74 neurons) or 700-1500ms (for 18/74 neurons). Animals were allowed a relatively large reward window of 5-12° in radius (visual angles) around the target. If the animal kept gaze stable in the reward window for at least 200ms after the gaze shift, a juice reward was provided. Visual stimuli were laser-projected on a flat screen, positioned 80cm away from the subject.

Our large reward window allowed animals to produce natural (untrained) errors in final gaze direction (Fig. 3.1*B*). The variable component of these errors was necessary to dissociate the most important models (i.e., target and gaze models) described below. To quantify these we first calculated systematic gaze errors by computing the parameters of the function [dG = a1 dT + a2], separately for vertical and horizontal components, where dG was gaze displacement and dT was target displacement from initial gaze position. This revealed hypometria and vertical/horizontal offsets consistent with previous studies of memory-guided saccades (De Bie et al., 1987; White et al., 1994). Variable errors were quantified as the remaining errors that were unexplained by the systematic errors (i.e., residuals of the linear fit). Variable errors in behavior were distributed normally with SD in x-direction (SDx)= 6.2, and in y-direction (SDy) = 5.8 for animal S, and SDx = 5.9 and SDy = 5.7 for animal A. The average magnitude of the variable errors (mean ± SD) was 6.3 ± 6 degrees. As we shall see, these values were sufficient to statistically separate our target and gaze models, as were other variations in 3-D eye and head orientation for the other models tested (Sajad et al., 2015).

3.3.3. Extracellular Recording Procedures

Extracellular activity from single FEF neurons was recorded using tungsten microelectrodes (0.2-2.0 MΩ impedance, FHC). The neural signal was amplified, filtered, and stored with the Plexon MAP system for offline cluster separation using principal component analysis with the Plexon Offline sorter software. The recorded sites were considered to be within the FEF if microstimulation with a current <50 μA (70ms trains of monophasic pulses; 300μs/pulse, generated with a frequency of 300Hz) evoked a saccade while the head was restrained (Fig. 3.2*B;* Monteon et al., 2010; 2012; 2013)

The search for neuron was conducted when the animal was freely scanning the environment in a lighted room with the head free to move. When a neuron with clear and stable spiking was isolated, the experiment began. A rough estimate of the neuron's RF was first obtained using memory-guided gaze shifts to a wide spread of targets presented one at a time from a central fixation point. Then an array of gaze targets were set to cover the neuron's RF including the flanks of the RF (Fig. 3.1*B*, gray dots). Targets were positioned in a rectangular array (ranging between 4×4 to 8×8, 5-10° apart depending on the size and shape of the RF). Initial fixation positions were randomized within a central window with width ranging from 10-40° in proportion with the estimated size of the RF (example shown in Fig. 3.1*B*).

3.3.4. Data inclusion criteria (neurons and behavior)

We recorded neuronal activity from over 200 sites in the FEF of the two animals. However, since our method relies on detailed analysis of the RF of single neurons only data from sessions for which we had clear isolation of spiking data were included to eliminate any multi-unit activity from analysis. Also, only neurons for which enough trials were recorded to uniformly cover a decent extent of the RF, and showed either visual or pre-saccadic movement response types (or both) were included in the analysis. After applying our exclusion criteria a total of 77 neurons were used for analysis (57 were previously analyzed in another study). 3/77 neurons despite having clear visual and / or movement response did not exhibit any spatial tuning and thus were eliminated. So, a total of 74 neurons contributed to the results in this study. The anatomic distribution of these neurons in the recording chambers is shown in Fig. 3.2*B*.

To obtain the behavioral data, the onset of gaze shift was defined as the time when the gaze (eye in space) velocity exceeded 50°/s and the gaze end-time was marked at the time when velocity declined below 30°/s. Final gaze positions used for spatial analysis were sampled at the gaze end-time. Individual trials were excluded offline if gaze shift was clearly not directed towards the target, or the gaze error exceeded the regression line of gaze error versus retinal error by at least two standard deviations (SD) (errors in gaze end-point scale with gaze shift size). Furthermore, trials in which the subject made an anticipatory gaze

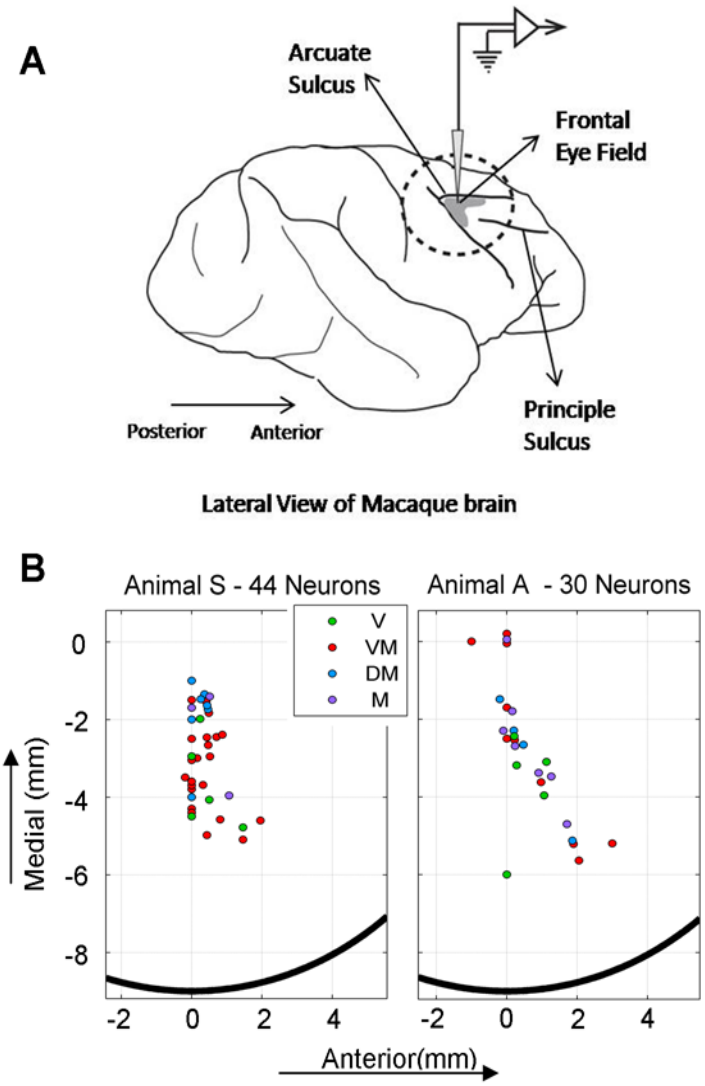

Figure 3.2. Approximate location of the FEF and the recorded sites in the two monkeys. A) shows the anatomical location of the FEF, located at the anterior bank of the arcuate sulcus. B) Sites within the FEF from which neurons were recorded in each animal are plotted (circles) in the coordinates of the recording chamber with the center (0,0) approximately located at the stereotaxic coordinates corresponding to the FEF (see Materials and Methods). The black semi-circle represents the edge of the recording chamber. The color code represents the neuron type recorded from each site. Low-threshold microstimulation at these sites evoked saccades ranging from 2 degrees (at the most lateral sites) and 25 degrees (at the most medial sites) in head-restrained conditions (Bruce and Goldberg, 1985).

shift (with reaction time < 100ms after Go-signal) were eliminated to ensure that animals waited for the go-signal (extinction of the first fixation light) to generate a

saccade. In a behavioral analysis based on the same task in the same two monkeys, it was confirmed that saccade onset correlated with the Go-signal (Sadeh et al., 2015). Finally, trials in which the gaze, eye, and head were not stable during the delay period were eliminated (for details see Sajad et al., 2015). After all trial exclusions were applied, on average, 211 trials per neuron were used for analysis.

3.3.5. Neuron classification

We categorized neurons based on the temporal profile of their response (firing rate) during visual, memory, and movement periods. Note that in this experiment each trial was unique both in terms of the starting position and the metrics of the gaze shift and a large proportion of trials were spatially spread outside of the RF hot-spot, the region where the neuron is most responsive to. Therefore, in order to provide a measure of a neuron's responsiveness we analyzed the activity of the neuron in the 10% of trials in which the neuron was most active (Spk10) which would roughly correspond to trials that fall near the center of the best-fit RF (see next section). Spk10 was calculated for different time periods and used to identify whether a neuron had visual, delay, or movement response as described below.

If Spk10 at 80-180ms after target onset (an early visual period) and/or -50 to +50ms relative to gaze onset (peri-saccadic period) was higher than 25 spikes per second (spk/s) relative to the pre-target baseline we characterized the neuron as having visual and/or movement response (Sajad et al., 2015). A neuron was deemed responsive during delay period if the average of the Spk10 during the

100ms period prior to the presentation of the Go-signal was greater than 15spk/s and was significantly higher than the trial-matched baseline (pre-target) activity levels ($p < 0.05$, Paired-sample Wilcoxon Signed-rank Test). These criteria resulted in a classification similar to that obtained by visual inspection: four classes including 1) visual (V) neurons which did not exhibit movement activity, 2) visuomovement (VM) neurons which exhibited both visual and movement responses, 3) delay-movement (DM) neurons which did not exhibit visual response but showed delay activity prior to the Go-signal, and 4) movement-only (M) neurons which only exhibited a movement response starting after the Go-signal.

3.3.6. Model Fitting Procedures

In order to systematically test between different spatial parameters, we fit spatial models to RF data for every neuron using a procedure that has now been described several times (Keith et al., 2009, DeSouza et al., 2011, Sajad et al., 2015, Sadeh et al., 2015). In brief, the RF of the neuron was plotted by overlaying firing rate data (number of spikes divided by sampling window width for each trial) over two-dimensional position data corresponding to the spatial parameter related to the candidate model, such as target position relative to the eye. The predictability power of the model for the recorded data was quantified by obtaining Predicted Sum of Squares (PRESS) residuals across all trials, which is a form of cross validation used in regression analysis (Keith et al., 2009). Specifically, the PRESS residual for a single trial was obtained by: 1) eliminating that trial from RF data, 2) fitting the remaining data points non-parametrically

using Gaussian kernels at various bandwidths (2-15°), and 3) obtaining the residual between the fit and the missing data point. The overall predictability power of the model for the recorded data set was quantified by the average of PRESS residuals across all trials for that neuron. Examples of this process will be described below. Once PRESS residuals of all tested models were obtained the spatial code was defined as the model (using the kernel bandwidth) that yielded the overall best fit to the data.

In a preliminary analysis similar to that of our previous study (Sajad et al., 2015; which used an overlapping but smaller population of neurons) we tested all of the models that have been proposed for egocentric coding in the gaze control system against the visual and movement responses of our neurons (we did not provide allocentric visual cues so such models were not tested). This included models of target location vs. gaze, eye-in-head, and head motion (both final position and displacement) in eye-centered, head-centered, and body-centered frames of reference, for a total of 11 models (as noted above, most of these tests required the use of 3-D head-unrestrained recordings). Since this replicated our previous analysis on a smaller dataset, but with slightly better statistics, we only summarize the results here.

Target location relative to initial eye orientation (*Te*) was the best model for describing our total population of visual responses, with all other models statistically eliminated (Brown-Forsythe test). Future gaze position relative to initial eye orientation (*Ge*) gave the best overall fit for our total population of motor responses, with all other models statistically eliminated except for eye-in-

head displacement and gaze displacement, which were mathematically very similar to *Ge*. Therefore, we used *Te* and *Ge* as the best representatives of visual and motor coding, abbreviated henceforth as simple *T* and *G*. Note that *G* is the visual axis in space controlled by both eye and head motion; this is still head-unrestrained data.

Note that all of these models are correlated with each other to some extent (for example, when the target is on the right, generally gaze, eye, and head move to the right). This is why it has been so difficult to separate them using standard correlation techniques (reviewed in Sajad et al. 2015). An advantage of our method is that it allows each model fit to explain all of the variations in the data that it can (even if these arise from cross-correlation), so that one then statistically compares only the data that the model cannot explain (i.e., the residuals at each point on the RF). For example, to say that *G* is statistically superior to *T* means that including errors in gaze position explains variations that cannot be accounted for by *T*, and a superior fit for *T* means that *G* errors introduce spatial variability in the fit that is not accounted for in the neural response. However, it is also possible that the ideal fit comes somewhere between *T* and *G*.

3.3.7. The Target-Gaze Continuum

Unlike previous studies, which only made a distinction between *T* and *G* as two possible spatial codes, we also considered intermediary codes between *T* and *G* by creating a quantitative *T-G* continuum between and beyond these spatial models (Fig. 3.1*D*). This is similar to the notion of intermediate reference frames

(Bremner and Andersen, 2014; Blohm et al., 2009; Avillac et al., 2005), but here we are taking intermediate codes for two different variables within the same reference frame (eye coordinates). As described in Sajad et al., (2015) these intermediate spatial models were constructed by dividing the distance between target position and final gaze position for each trial into 10 equal intervals and 10 additional intervals extended on either tail (beyond *T* and *G*). Figure 3.3*A* shows an example analysis of a visual response sampled from 80 to 180ms after target onset. The RF plots corresponding to three spatial models along the *T-G* continuum are shown in Figure 3.3A-*2*. In the RF plots, each circle represents firing rate data (diameter) for a single trial plotted over position data corresponding to the tested model (The circles are not shown in other RF plots throughout the paper). The color code represents the non-parametric fit made to all data points (at a kernel bandwidth of 4 degrees, which was the bandwidth that yielded the overall best-fit for this neuron). Below each RF plot, the PRESS residuals for all data points are shown, which provide a measure for the predictability power of the model for the data points. The mean of the PRESS residuals (mean PRESS) provided the overall predictability power of the model for our dataset. 3A-*3* shows mean PRESS (y-axis) as a function of tested spatial model along the *T-G* continuum (x-axis). The model which provides the lowest mean PRESS (marked by red arrow) is the model with the highest predictability power and thus is identified as the spatial code of the neuron. For this example visual response the best-fit model (i.e., spatial code) is the intermediate model one step away from *T* (towards *G*). Note that the RF corresponding to the best-fit

model (B, left panel) shows a relatively high degree of *spatial coherence* with high neuronal response spatially confined to a restricted region (red color). The most spatially-coherent fit would be a fit that gives the lowest overall variance in the data relative to each point on the RF, corresponding quantitatively to the lowest residuals of the fit. As the RF representation gets further from the best-fit representation (middle, and right panels) the RF becomes progressively less coherent (as visualized by size-gradient of the circles and the color map), and the magnitude of the PRESS residuals increases.

3.3.8. Time-normalization and activity sampling for spatiotemporal analysis

The specific aims of this study required a new means of analyzing data that we have not described previously: applying our spatial analysis through discrete time-steps spanning the visual, delay, and motor responses of each trial. This proved challenging because we used a variable delay period. In such a paradigm, aligning trials the standard way (with either the visual stimulus or saccade onset) results in the loss and/or mixing of activities across trials, and thus would not allow us to trace spatial coding through the entire trial across all trials (Fig. 3.3*B*). To overcome this challenge, we normalized the time between an early visual period and movement onset for all trials and applied our analysis method to RFs sampled from the time-normalized activity profile. Our analytic method thus treats time and space similarly, since the spatial codes tested in this study (i.e., the *T-G* continuum) are also obtained through normalization of errors

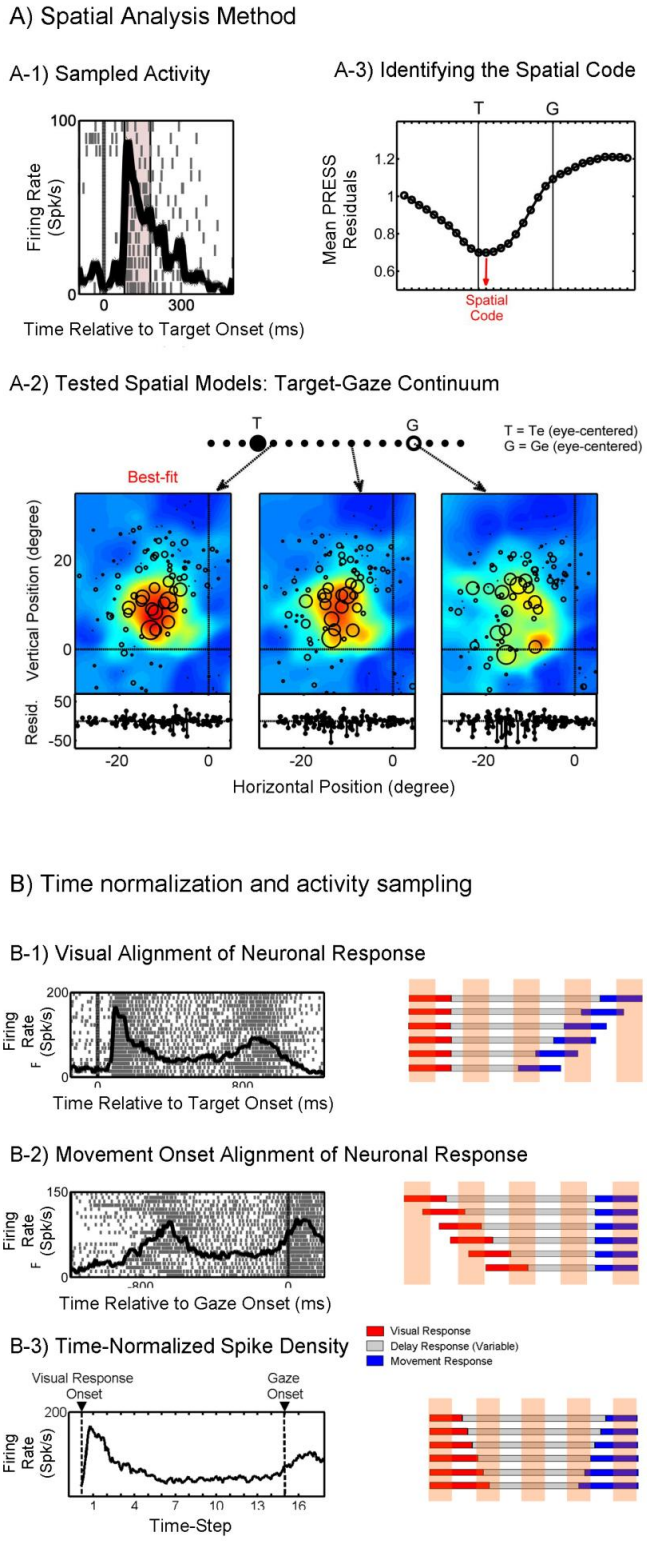

Figure 3.3. An overview of the analysis methods for identifying spatial code and sampling neuronal activity from time-normalized activity profile. ***A,*** shows an example analysis for identifying the spatial code. Here, activity from early visual response (80-180ms after target onset) was sampled for analysis (***A-1***). ***A-2,*** shows the *T*-*G* continuum and three example RF-plots are shown for the visual response corresponding to the demarked models (arrows) along the *T*-*G* continuum. *T* is the eye-centered target model and *G* is the eye-centered gaze model. In the RF plots each circle represents firing rate data (diameter) for a single trial, plotted over position data corresponding to the tested model (in this study models spanning target model, *T*, and gaze model, *G*). The PRESS residuals are shown at the bottom of each RF plot. In each RF plot, the color code (blue-red scale corresponding to low-to-high) represents the non-parametric fit made to all data points. ***A-3,*** shows mean PRESS (*y*-axis) as a function of tested spatial model along the *T*-*G* continuum (*x*-axis). For this example visual response the best-fit model or spatial code (lowest PRESS residuals) is the intermediate model one step away from *T* (towards *G*). Although ***A*** shows analysis only for a single sampling window, for the main analyses reported in this study we sampled activity at 16 half-overlapping time-steps from visual response onset until a period immediately following gaze movement onset. For this we normalized the time between visual response onset until movement onset so we could collapse all trials together for analysis. ***B,*** shows the raster and spike density plots corresponding to the classic visually- (***B-1***) and movement- (***B-2***) aligned neuronal responses as well as the time-normalized spike density (***B-3***), and illustrates activity sampling based on each of these scheme.

in behavior (i.e., the vector difference between target position and final gaze position). In order to sample neuronal activity using the time-normalized scheme, activity was sampled starting from an early visual period, which was the onset of the visual activity (mean = 87ms after target onset) for visually-responsive (V and VM) neurons and 80ms after target onset for neurons with no visual response. The duration between this early visual period and gaze movement onset was on average 895ms (± 234ms, SD) across all trials. For spatiotemporal analysis the firing rate of the neurons (spikes/sec; number of spikes divided by the sampling interval for each trial) was sampled at 16 half-overlapping windows from this time-normalized data. This choice of sampling window numbers was based on the approximate ratio of the duration of the visual response to delay period to movement response including a post-saccadic period starting from gaze onset (visual:delay:movement is approximately 3:10:3).The final (16th) time-step corresponded to an entirely post-saccadic period starting from the onset of gaze shift. Because of the time-normalization process the sampling window width scaled with the duration between visual response onset and movement onset on a trial-by-trial basis. On the 16-step time-normalized scale, the visual burst on average lasted 2.5 steps (SD = 0.81 steps), ending by the end of the third time-step in 94.5% of trials. The presaccadic duration was on average 1.35 steps (SD = 0.67), and for about 90% of the trials started after the beginning of the 14th time-step. Therefore, in the time period interleaving the first three and final three time-steps the sampled activity was largely dominated by delay activity. The sampling window width was on average 119ms (±37ms, SD) and was no less

than 50ms for any trial which ensured enough neuronal spikes captured in the sampling window to perform effective spatial analysis.

Thus, this time-normalization procedure allowed us to consider the entire sequence of visual-memory-motor responses as a continuum. It causes blurring of some other events across trials (e.g., the Go-signal), or mixing of visual and movement responses in the delay period but these possibilities are controlled for in the Results section (see Figure 3.8).

3.3.9. Testing for spatial selectivity (for single neuron, and population)

Our model-fitting approach would provide us with valid results if the sampled neuronal activity exhibits spatial selectivity. Therefore, we excluded data points both at single neuron level and at population level which did not exhibit significant spatial tuning of any kind.

To test for spatial selectivity for a sampled response for an individual neuron we compared the spatial selectivity of the best-fit representation with its random counterpart. To do this, we randomly shuffled the firing rate data (number of spikes divided by duration of the sampling window) and plotted them over the position data corresponding to the best-fit model, and repeated this procedure 100 times to obtain 100 *random* RFs. The PRESS residuals of these random RFs (and their respective mean PRESS values) were then obtained after fitting the data (non-parametrically, using Gaussian kernels) with the same kernel bandwidth that was used to fit the best-fit model, resulting in a total of 100 mean PRESS residuals. If the mean PRESS residuals for the best-fit model (PRESS

$_{best\text{-}fit}$) was at least 2SD smaller than the mean of the distribution of random mean PRESS residuals (which was normally distributed), then the sampled activity was identified as spatially-selective.

At the population level, even though at a given time-step some neurons exhibited spatial tuning, due to low signal-to-noise ratio or few number of neurons contributing to the population, our estimate for the population code would not be reliable. Therefore, we excluded population data corresponding to time-steps at which the mean spatial coherence of the population was not statistically higher from that of the pre-target baseline which presumably exhibits no spatial tuning (as no task-relevant information is available). The spatial coherence for each neuron contributing to the population spatial coherence was measured using an index:

$$\text{Coherence index} = 1 - (\text{PRESS}_{\text{best-fit}} / \text{PRESS}_{\text{random}})$$

Where $\text{PRESS}_{\text{random}}$ provided a measure of the predictability power for the random distribution (average of mean PRESS residuals over the 100 independent distributions). If $\text{PRESS}_{\text{best-fit}}$ was approximately similar to $\text{PRESS}_{\text{random}}$ then coherence index would be a value around 0. Alternatively, if $\text{PRESS}_{\text{best-fit}} = 0$ (which would only occur when the model perfectly accounted for the data) the index would be 1. The coherence index can also be used to determine the amount of variance in the neural data described by the best-fit model. In our data the range of coherence indices was from -0.07 to +0.67. We did not expect coherence index to be 1 especially because neurons in the FEF are shown to be

modulated by other non-spatial factors such as attention and reward expectancy (Schall, 2015).

3.3.10. Non-parametric fits to temporal progress of spatial code in single neurons

The spatiotemporal progression of the neuronal code was analyzed by plotting the best-fit model (y-axis) as a function of the discretely sampled time-steps (x-axis). To visualize these trends (and for the population analysis in the next section) we performed a non-parametric fit to this data for each neuron. Only data corresponding to spatially-tuned time-steps contributed to the fit. Fit values were included for every time-step whose two neighboring time-steps (both before and after) exhibited spatial tuning. The fit was discontinued for the range at which at least two consecutive time-steps were not spatially-tuned. Gaussian kernel with bandwidth of 1 time-step was used for non-parametric fitting of this data. This choice was made conservatively to avoid over-smoothing the data. As can be noted in Figures 5,6,8,9,10, the fit values closely matched the data points obtained for individual neurons. Unless stated otherwise, we used the fit values, rather than individual data points, for statistical tests reported in this study, because they were less likely to be influenced by outliers.

3.3.11. Population analysis and comparison between neuronal sub-populations

Since most theoretical papers suggest that it is neural populations, not individual neurons, that matter most for behavior (Pouget and Snyder, 2000; Blohm et al., 2009), the results presented here focus mainly on our *T-G* analysis of our entire

population of neurons as well as several sub-populations (V, VM, DM, M). The overall population coding preference across the *T-G* continuum (continuous trend-lines in Figures 4*E*, 5*B*, 6*B*, 7, 8*B*, 9*B*) at any given time-step was defined as the mean of the fits made to individual neuron data. Since the distribution of spatial code within different neuronal sub-populations did not exhibit a normal distribution, we used non-parametric statistical tests to compare between data across the population, as well as the regression analyses presented in the Results for VM and DM neurons.

3.4. Results

We recorded neurons from over 200 sites in the FEF during head-unrestrained conditions. After applying our rigorous data exclusion criteria, 74 neurons were included in the analysis (see Materials and Methods; Fig. 3.2). This is a very large number of neurons compared to other head-unrestrained studies (e.g., Freedman and Sparks 1997; Knight, 2012). However, it is not large compared to some head-restrained studies, so we limited our analysis to data that showed significant spatial tuning, and limit our conclusions to the statistically significant neural population results described below.

As described in the Materials and Methods, our preliminary data analysis corroborated the findings of the previous study (Sajad et al., 2015), i.e. that target-relative to initial eye orientation (*T*) provided a significantly preferred fit for the full population visual response and future gaze position relative to initial eye orientation (*G*) provided the best overall fit for the full population motor response.

We henceforth focus on the temporal transition along the *T-G* spatial continuum between these two events.

Figure 3.4*A* shows the activity profile of a typical neuron with visual, sustained delay, and movement responses using the standard conventions of aligning activity with either the onset of the visual stimulus (left panel) or the onset of the gaze shift (right panel). Figure 3.4*B* shows the time-normalized spike density plot corresponding to the raster and spike density plots in Figure 3.4*A*. The RF maps obtained at four representative time-steps (C1-C4) from these data are also shown. This neuron had a very sharp (small) and spatially-distinct (bound) visual RF (C1), and a similar movement RF (C4). The delay-related activity (C2, C3) exhibited similar spatial tuning, but the RF was more constricted and less spatially organized. After applying our *T-G* continuum analysis we observed a progressive shift of the best-fit model from *T* part-way toward *G* (shown by red icons above the RF plots in Fig. 3.4*C*) as activity progressed in time. This trend was often observed in our preliminary analysis and thus prompted the population analyses that follow.

3.4.1. Mixed Population Analysis

Figure 3.4*D* shows the mean, time-normalized spike density profiles of the 74 neurons that qualified for our analysis (see Materials and Methods). This reveals the typical visual response (present in 52/74 neurons), followed by activity that was statistically significant during some or all of the delay period (present in 51/74 neurons), and the typical movement response (present in 64/74 neurons) of the FEF. For our model-fitting procedure, we sampled this data through 16

half-overlapping time-steps (see Materials and Methods). The activity at each time-step was first tested for spatial tuning and then the spatial code (i.e., best-fit model) was included if the test was positive. At least 50% of neurons were spatially selective at each time-step (see histograms in Fig. 3.4*E*, bottom panel).

The mean of the individual data points at each time-step (○ ±SEM) as well as the fits made to each neuron's data points (black line) for spatially-selective responses at every time-step is shown in Figure 3.4*E* (The median was nearly identical in this dataset, not shown). Importantly, this method of illustrating the data (which we will use henceforth) provides the full spatiotemporal continuum of information coded by the population, by showing best-fits along the *T-G* continuum as a function of our 16 time-steps through the normalized evolution of the trials. These data reveal that the overall population best-fit model started from a location near *T* and monotonically and almost linearly moved towards *G* as activity evolved from dominantly vision related – through the delay activity – to movement related (R_s = 0.90, p = 2.44 × 10^{-6}, Spearman's ρ correlation) . On average, for the spatially-tuned responses the best-fit intermediate *T-G* model explained 21% of the variance in the early visual activity (1st time-step), while it decreased to approximately 12-13% during mid-delay (7-9th time-steps), and 23 % in the peri-saccadic movement period (15th time-step). Since these results were better than any of the other comprehensive list of spatial models we tested, this unaccounted variance was presumably due to non-spatial factors such as attention, motivation, and random noise.

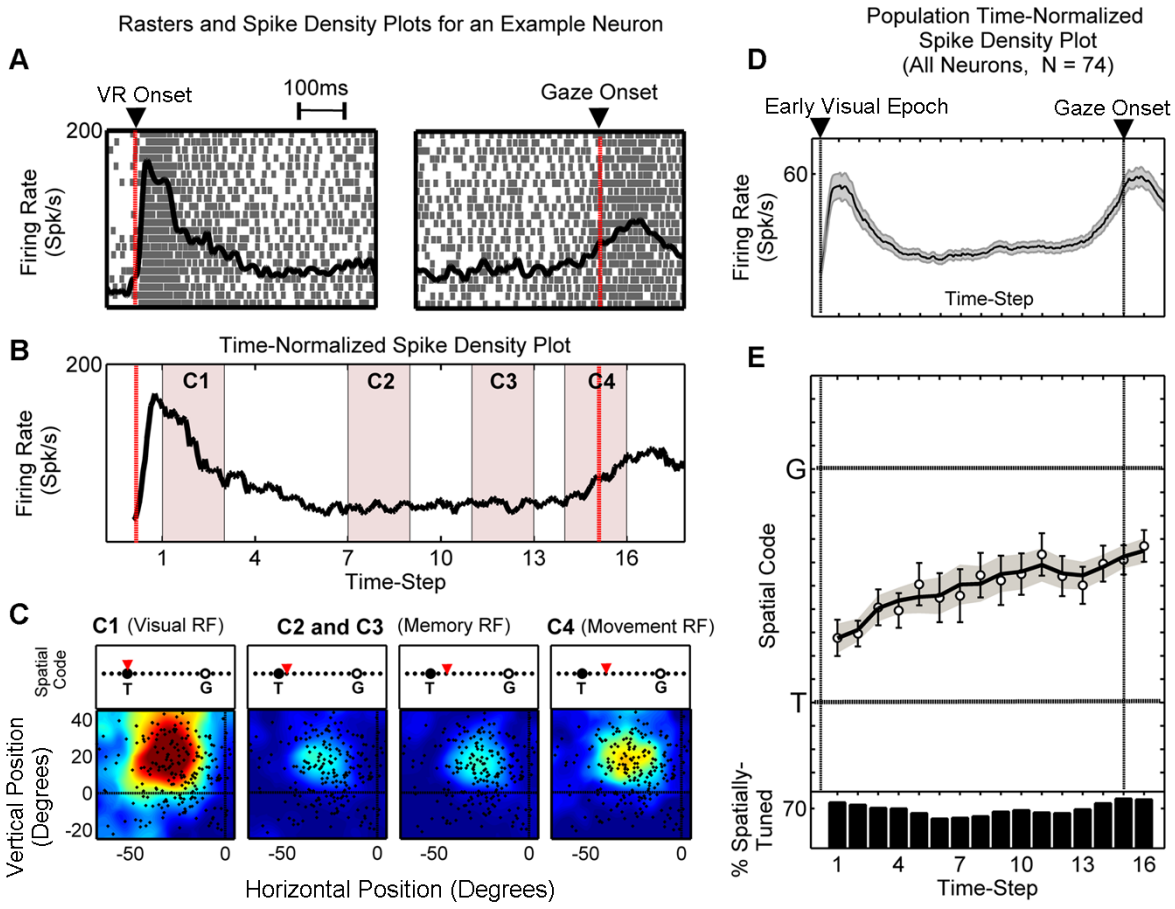

Figure 3.4. A representative neuron with visual, delay, and movement responses, and results for the overall population. ***A,*** shows the visual- (left) and movement- (right) aligned raster and spike density plots for a VM neuron with sustained delay activity. The visual response of this neuron is from 65-300ms after target onset and the movement response begins 30ms before gaze onset. ***B,*** shows the time-normalized activity profile corresponding to ***A*** with the period between visual response (VR) onset and gaze movement onset normalized for all trials. ***C,*** show the RF maps for four time-steps (***C1*** - ***C4***) sampled from the time-normalized activity profile (***B,*** light red shades) with the blue-to-red color gradient representing low-to-high neuronal activity levels. The best-fit model (i.e., spatial code) at each of these time-steps is depicted by a red triangle placed on the *T-G* continuum (panels above the RF plots). For this neuron there was a progressive but partial shift (three steps out of 10) in spatial code towards *G*. ***D,*** depicts the time-normalized spike density for the entire population (*n* = 74) including neurons with either visual or movement response or both. Neurons with movement-related activity beginning at or after gaze onset are eliminated. ***E,*** shows the mean (± SEM) of spatially-tuned best-fits at 16 half-overlapping time-steps from an early visual period (visual response onset for visually-responsive neurons, and 80ms after target onset if neuron was not visually responsive) until gaze movement onset time. The solid line shows the mean of the fits made to individual neuron data highlighting the change in the population spatial code along *T-G* continuum as activity progresses from vision to movement. The histogram in the bottom panel shows the percentage of neurons that exhibited spatial tuning (y-axis) at a given time-step (x-axis).

The *T*-to-*G* progression is not due to temporal smoothing of responses between the visual-memory transition and memory-motor transition (Figure 3.3B), because similar trends and statistics were observed when the visual and motor responses were removed entirely from the analysis (this is illustrated for VM neurons with sustained delay activity in Fig. 3.8). Framed in terms of our model-fitting method, these results mean that the population activity is initially unrelated to future gaze position errors, but as the memory interval progresses, these variable gaze errors are increasingly reflected within the population code. Separate analysis of shorter vs. longer memory intervals (not shown) yielded no difference in the results.

To examine the contribution of different cell types to this progression in spatial coding, we subdivided our population into four subpopulations, based on whether or not they had visually-evoked, delay-, or movement-related activities (see below, and Materials and Methods) and performed the same analysis for each sub-population (Bruce and Goldberg, 1985).

3.4.2. Neurons with Visual Responses (Visual and Visuomovement Neurons)

Our population of neurons with visual responses was further divided into two classes based on whether or not they also exhibited movement activity (see Materials and Methods for quantitative definitions of each neuron class). In total, we had 10 V neurons and 42 VM neurons. For these neurons, activity was sampled through time from visual response onset until a post-saccadic period staring at the onset of the gaze movement, using only the epochs that tested positive for spatial tuning.

3.4.2.1. Visual neurons

Figure 3.5*A* shows the spike density profile (top panel) and model fits through time (bottom panel) for a typical V neuron, with a strong visual response but little or no delay or movement-related activity showing typical results. This neuron only exhibited spatial tuning (see Materials and Methods) at the first four time-steps. The RF plot (in the best-fit representation) corresponding to the first time-step, which corresponds to the early visual activity is shown in Figure 3.5*A* (bottom panel) showing that this visual neuron had a small and bounded RF with sharp spatial tuning. At all four time-steps the *T*-*G* continuum analysis provided fits near the *T* model (Fig. 3.5*A*, bottom panel). Most visual neurons showed a similar trend for *T* preference in the visual response, consistent with our previous results (Sajad et al., 2015). Figure 3.5*B* illustrates the corresponding analysis for the entire V neuron population, showing the mean spike density profile (upper panel) and model fits through time using conventions similar to Figure 3.4*D* and 4E. Across the V population only the first three time-steps (corresponding to the visual transient response) exhibited significantly higher spatial coherence (lower fit residuals) than the pre-target period ($p < 0.05$; green colored data). Of the fits at these time-steps (green circles), the first were very near to *T*. The next two time-steps showed a trend to drift toward *G*, but none were significantly different from *T* ($p > 0.05$, One-sample Wilcoxon Signed-Rank Test). Although some V neurons showed declining activity during the delay period, this did not pass our population spatial tuning criteria (see Materials and Methods), and gave highly variable fits (gray shaded area) that were not further considered.

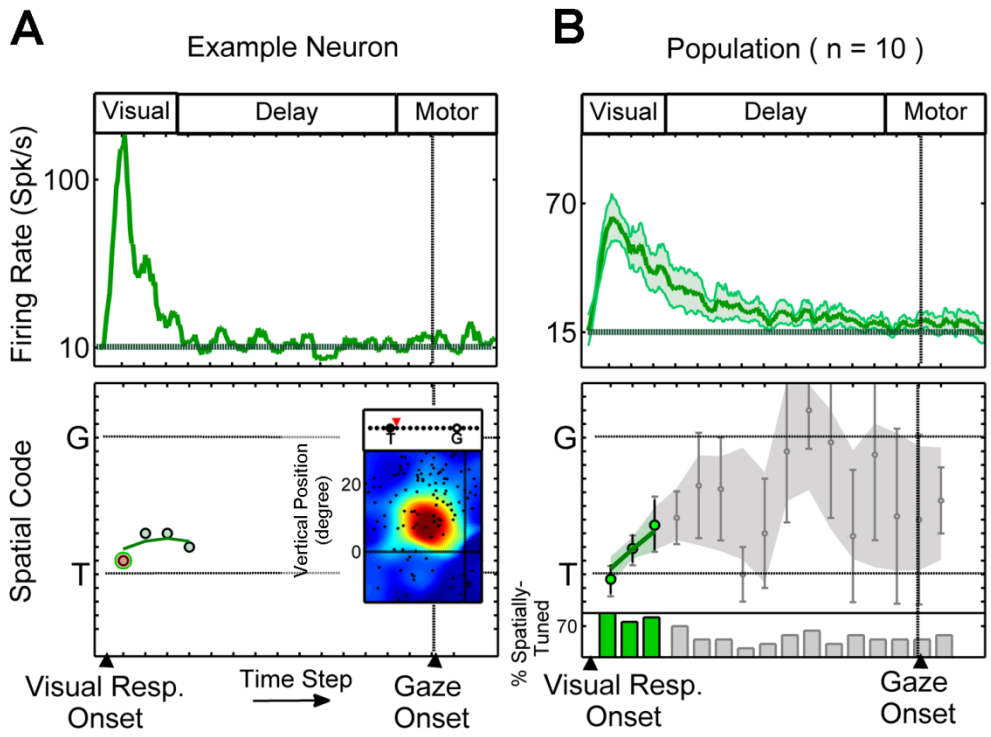

Figure 3.5. Single neuron example and population results for visual (V) neurons. ***A*,** shows the time-normalized spike density profile for an example V neuron (top panel) and the data points corresponding to the spatially-tuned time-steps across 16 half-overlapping time-steps (bottom panel). The RF plot corresponding to the highlighted time-step (first time-step in pink) is shown with the spatial code highlighted above the plot. ***B*,** shows the population time-normalized post-stimulus time histogram (mean ±SEM) and the mean (±SEM) of the spatially-tuned data points at these time-steps across the V population. Colored data points (bottom panel) correspond to time-steps at which the population spatial coherence was significantly higher than the pre-target baseline and gray shades correspond to eliminated time-steps with spatial coherence indistinguishable from pre-target baseline. The histogram shows the percentage of neurons at each time-step that exhibited spatial tuning. The baseline firing rate, calculated based on average firing rate in 100ms pre-target period, is shown by the solid horizontal lines in spike density plots (***A*** and ***B*** top panels). For reference, the approximate Visual, Delay, and Motor epochs are depicted at top of the panels.

3.4.2.2. Visuomovement neurons

A similar analysis was performed on VM neurons. VM neurons were particularly of interest in this study because they exhibited both a visual and a movement response, and unlike V neurons, a large proportion of them exhibited delay

activity (*n* = 36/42). Figure 3.6*A* (top panel) shows the time-normalized spike density plot for an example VM neuron with a large visual response followed by a delay response leading to a small movement response. This neuron exhibited significant spatial tuning at all 16 time-steps. The early visual response of this example was best described by intermediary models almost at the mid-point between *T* and *G*. However, from the third time-step onward, there was a monotonic change in the best-fit model from a model near *T* to a model near *G* (Fig. 3.6*A*, bottom panel). RF plots corresponding to the highlighted time-steps in panel A (bottom panel) are shown in panel C. Similar to the VM example shown in Figure 3.4*A*-*C*, although the RFs corresponding to the delay period are attenuated and more spatially restricted compared to the visual and movement RFs, they cover the same relative spatial position, though the spatial model that best fits each is different. The change in spatial code from *T* to *G* was present in the majority of VM neurons with delay activity: of the neurons that showed delay activity, 29/36 showed a positive increment along the *T*-*G* continuum. However, the degree of this change was variable across neurons (mean +4.65 ± 6.47 Standard deviation in *T*-*G* units). The monotonic (constant direction) change in spatial code from *T* to *G* was also observed at the population level in the VM neurons (*n* = 42) (Fig. 3.6*B*). Specifically, the mean population code in the first time-step (corresponding to early visual response) fell close to *T* (two steps towards *G* along the *T*-*G* continuum), but unlike V neurons it was significantly

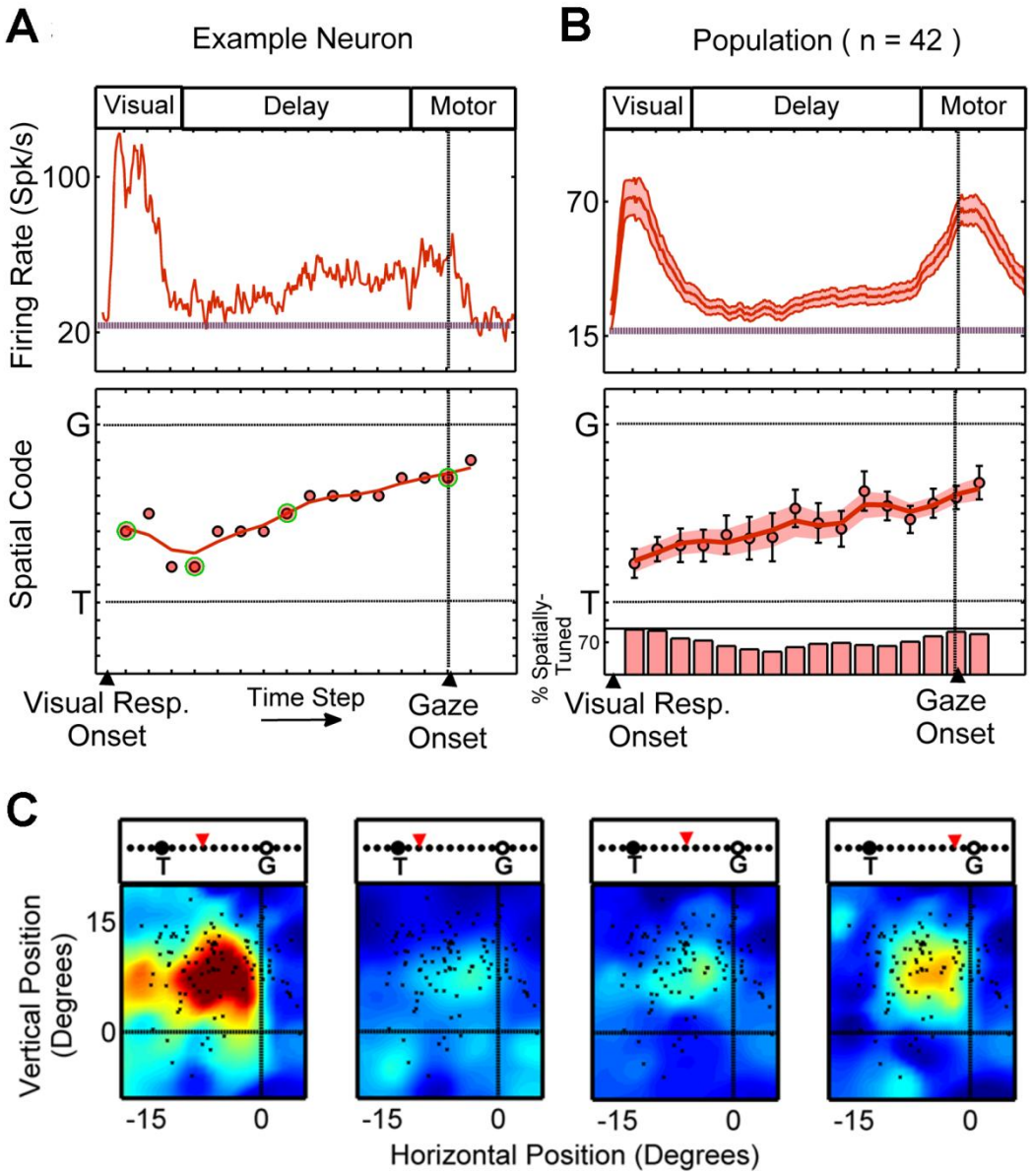

Figure 3.6. Single neuron example and population results for visuomovement (VM) neurons. ***A*** and ***B***, same conventions as Figure 3.5. ***C***, The RF plots corresponding to time-steps with highlighted data points (green boarder circles) in ***A*** (bottom panel) are shown, with the spatial code along *T-G* continuum highlighted above each plot.

different from *T* ($p = 3.2 \times 10^{-5}$, One-sample Wilcoxon Signed-Rank Test). The mean population code then progressed monotonically (almost linearly) towards *G* ($R_S = 0.91$, $p = 9.08 \times 10^{-7}$, Spearman's ρ correlation). However, at the final time-step (corresponding to a period within the movement response and just after gaze onset), it was still significantly different from *G* ($p = 3.51 \times 10^{-7}$, One-sample Wilcoxon Signed-Rank Test; Fig. 3.6*B*, bottom panel).

Figure 3.7A illustrates how the distribution of best-fits for VM neurons evolves through time. Specifically, this histogram plots the best fit *T-G* distributions for the early-visual (step 1), early-delay (step 4), mid-delay (step 9), late-delay (step 13), and perimovement (step 15) intervals. Focusing on the delay activity (middle three panels), this population did not show a bimodal distribution of *T-G* with a diminishing *T* peak while *G* codes rose. Instead, during the delay, spatially tuned VM neurons showed a broad distribution of *T-G* codes that progressively shifted toward *G* (this shift is most easily observed in the population means and medians, illustrated as vertical black and green lines).

To visualize how this occurs at the level of individual neurons, we plotted the delay code (i.e., fits to the *T-G* data, see methods) as a function of the motor code for each VM neuron that showed significant spatial tuning at all 5 time-steps (n=21). The top panel, corresponding to early-delay epoch, shows that the

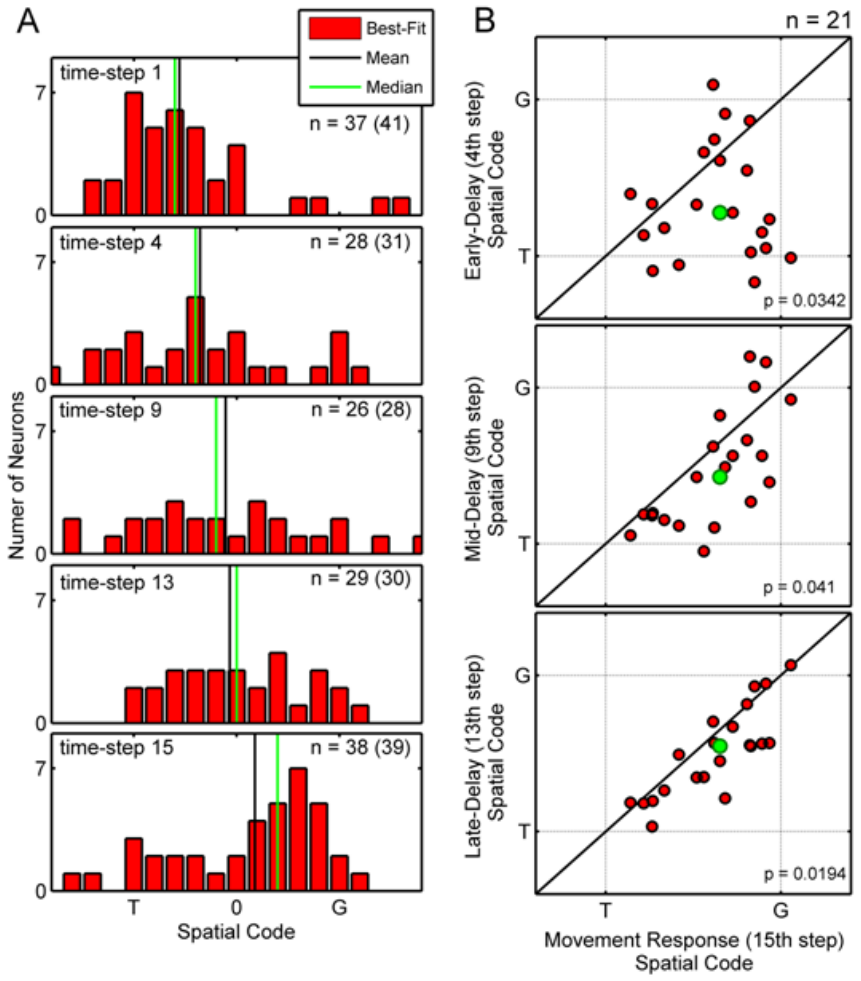

Figure 3.7. Distribution of best-fit models across the T-G continuum for VM population through 5 time-steps through visual, delay and movement responses. ***A***, shows the distribution of best-fits for VM neurons for early-visual (1st time-step from the time-normalized activity profile), early-delay (4th time-step), mid-delay (9th time-step), late-delay (13th time-step), and peri-movement (15th time-step) intervals. Only neurons with significant spatial tuning are considered. The number of neurons contributing to each distribution is indicated on each panel (the number in the brackets also includes best-fits outside of the presented range). ***B***, plots the value of the fit the T-G data at each of the delay intervals (y-axis), versus the fit value to the T-G data at the perimovement period (red dots). Here, only the 21 neurons that contributed to all five panels in ***A*** were plotted. Note the trend (from the early to mid to late delay periods) for the data points to migrate towards the line of unity, i.e. toward their movement fits.

majority of the data points were shifted below the line of unity, toward the *T*-end of the distribution. Indeed, at this point in time the distribution is not significantly different from the visual distribution (p = 0.3052, Paired-sample Wilcoxon Signed

Rank Test). However, as the activity progresses through the mid- (middle panel) and late-delay (bottom panel) intervals the data points progressively migrate upwards, finally clustering more tightly around the motor code. At the late-delay interval, this difference is significantly different from the visual fits for the same population of neurons (p = 0.0190, Paired-sample Wilcoxon Signed Rank Test). When we further reduced this population to only those cells that showed significant spatial tuning at every single time-step of the delay (n=16), 13 of these neurons showed a positive slope in the *T*-to-*G* direction during the delay period (mean slope = 0.36 *T*-*G* units per time-step, SD = 0.52 *T*-*G* units per time-step).

Collectively the results reported above support the notion that in the VM population (and most individual VM neurons) the spatial code is not stable during the delay period but rather changes through the intermediate range between *T* and *G*, starting at a point closer to a target code and ending at a point closer to a gaze code. To ensure that the *T*-*G* transition described above was not influenced by our time-normalization procedure, or temporal blurring of spatial responses across different epochs, we performed a more detailed technical analysis. For this technical analysis, we used the best possible data we could obtain from our full dataset. First, we removed any VM neurons that showed any temporal discontinuity during the delay, i.e., leaving only those that showed sustained activity throughout the entire delay period (*n* = 22).

Then, we repeated our time-normalized analysis (Fig. 3.8*A*) on these data. This yielded very similar trends and statistics to that observed for the overall

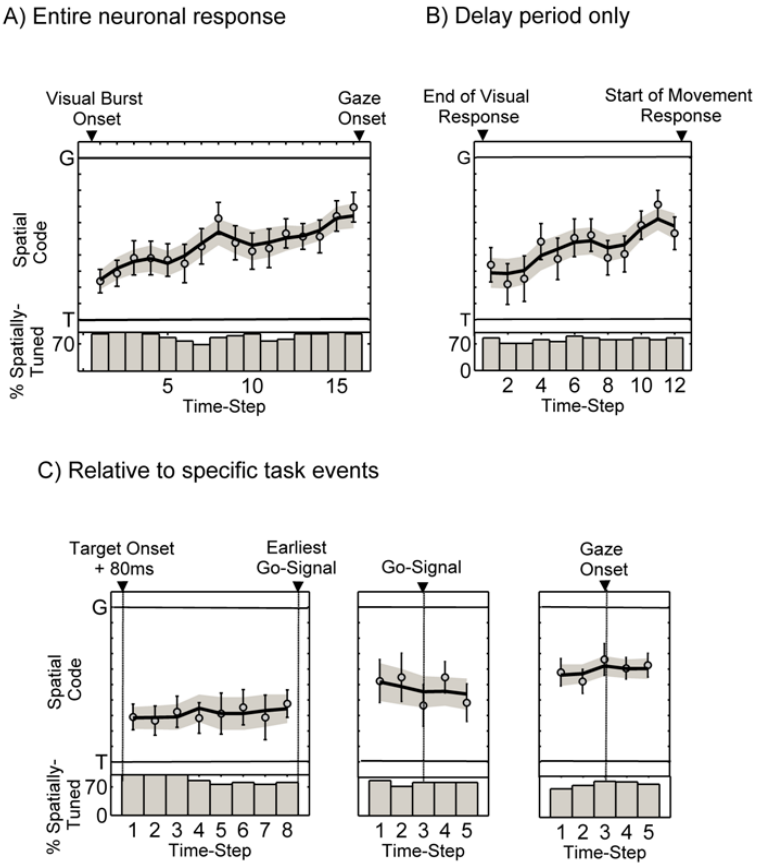

Figure 3.8. Spatiotemporal progression of neuronal code in VM neurons with sustained delay activity. ***A,*** shows the results with time-normalized activity sampling including visual and movement response using the same conventions as Figure 3.5*B* (bottom panel). ***B,*** shows the results for only the delay period, with visual and movement responses excluded. Specifically, activity was sampled from 12 half-overlapping steps from the end of visual response (on average 266ms after target onset) until the beginning of the movement response (on average 85ms before gaze onset). This duration was on average 635ms. ***C,*** shows spatial code at fixed-times intervals relative to specific task events: target onset (left), the Go-signal (middle) and gaze onset (right). For target-aligned analysis (***C***, left panel), time from 80ms after target onset and the earliest Go-signal was divided into 8 half-overlapping steps, resulting in sampling window size fixed for any session but ranging between 80 and 150ms depending on whether the earliest Go-signal appeared 450ms or 750ms relative to target onset for that session. The Go-signal-aligned analysis (***C***, middle panel) was performed using 100ms half-overlapping windows starting 150ms before to 150ms after the Go-signal. The movement-aligned analysis (***C***, right panel) was performed using half-overlapping 100ms sampling windows starting from 150ms before to 150ms after gaze onset. Notice that although there is no change in spatial code triggered by specific task events, there is a progressive change in spatial code from *T* towards *G* as we move away from time of target presentation (left panel) to the time of gaze onset (right panel) in agreement with the trend seen in ***A*** and ***B***.

population (linear progressive trend in change from a code near *T* to a code near *G*; $R_S = 0.86$, $p = 2.40 \times 10^{-5}$, Spearman's ρ correlation).

Next, we performed a similar time-normalized analysis, but excluded the visual and movement responses for every neuron (Fig. 3.8*B*). Once again a monotonic change in spatial code with a significant slope ($R_S = 0.76$, $p = 0.0038$, Spearman's ρ correlation) was observed. These results show that the progressive change in the spatial code described above (Fig. 3. 4, 6, 8*A*) is *not* due to the temporal smoothing of delay codes with visual and movement responses.

Finally, we controlled for the possibility that the *T-G* transition might have been caused by specific events within each trial, and that our time normalization technique might have blurred these events through time to create an apparently progressive *T-G* transition (see Materials and Methods, and Fig. 3.3*B*), Specifically, activity was aligned with three major task events (Fig. 3.8*C*), namely, target onset (left panel), Go-signal (middle panel), and movement onset (right panel). The target-aligned analysis (left panel) was performed from 80ms after target onset until the earliest Go-signal. In this period, (which was roughly equivalent for all trials for a given neuron irrespective of delay duration) the change in spatial code did not greatly contribute to the overall change in spatial code (Fig 8*C*, left panel). Notably, the spatial code (both mean of the individual data points and the mean of the fits) was stable both before and after Go-signal (Fig 8*C*, middle panel), suggesting that the change in spatial code was not prompted by this signal. The same observation held for gaze movement onset

(Fig 8*C*, right panel). Collectively, these control results reinforce our main result; that the spatial code during memory period changes progressively across the entire delay interval, rather than discretely under the influence of specific task events.

3.4.3. Neurons with no visual response (Delay-Movement and Movement-only Neurons)

In our population, 22 neurons exhibited movement response but lacked visual response. This movement population was further classified into two classes: Movement neurons with activity starting at least 100ms before the appearance of the Go-signal were classified as DM neurons (*n* = 12) and those with activity only appearing after the Go-signal were classified as M neurons (*n* = 10) (see Materials and Methods). Since these neuron types lacked a visual response, the first time-step used for our spatial fits (Fig. 3.9, 10) started from a fixed time (80ms) after target onset.

3.4.3.1. Delay-Movement Neurons

Figure 3.9*A* shows the time-normalized spike density plot for a representative DM neuron, with activity beginning 150ms after target onset, sustaining through the delay period, and leading into a pre-saccadic buildup towards the peak just around the time of gaze onset. This neuron first showed a spatially-tuned response at the third time-step. The RF plots corresponding to the 5th, 10th, and 15th (centered on gaze onset) time-steps are shown in Figure 3.9*C*. Although there was a sudden rise in firing rate at around the time of gaze shift, there was

no major change in the spatial code of this neuron through time. Instead, throughout the delay and motor epochs the spatial code of this neuron remained intermediate between *T* and *G*. At the population level, spatial coherence of DM neurons became significantly higher than the pre-target period at the 4th time-step and thereafter. At all these time-steps the spatial code remained at an

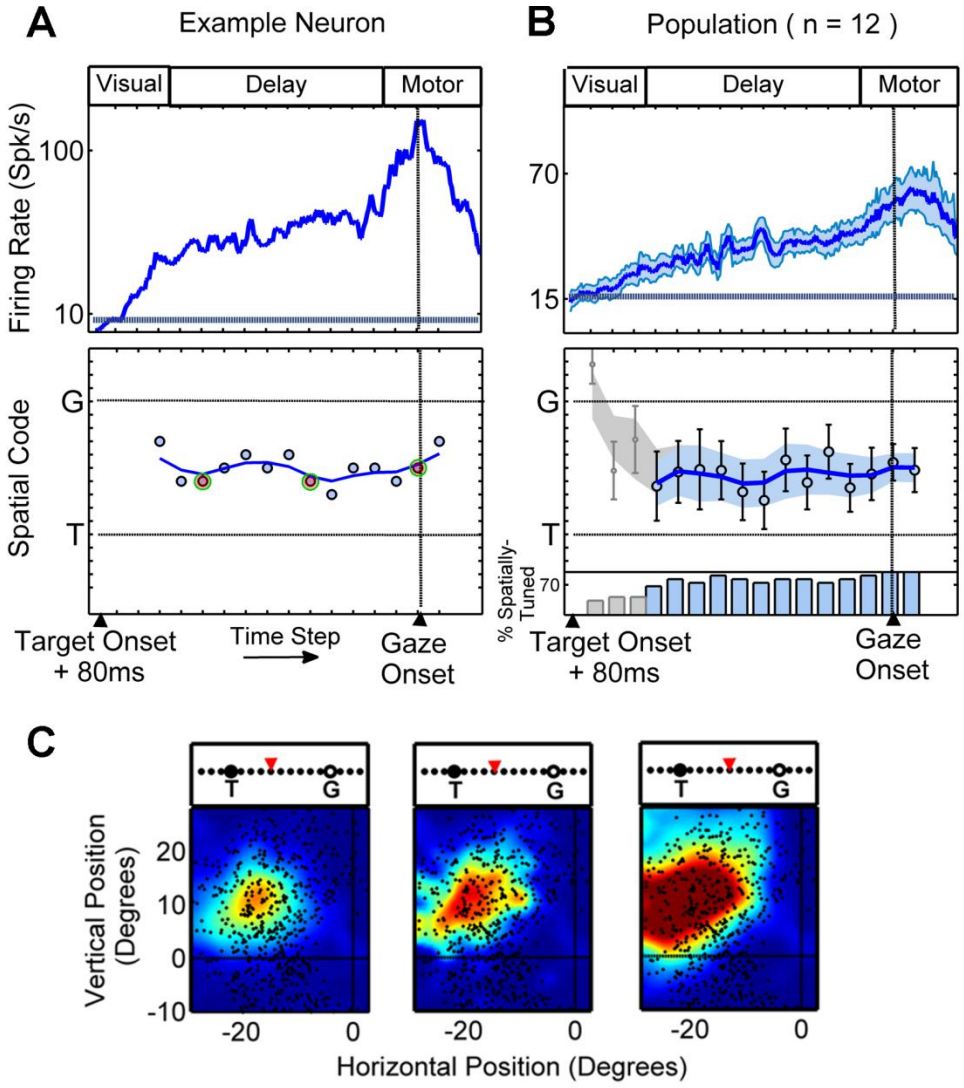

Figure 3.9. Single neuron example and population results for delay-movement (DM) neurons. ***A*** and ***B***, follow the same conventions as Figure 3.5. ***C,*** follows the same convention as Figure 3.6*C*. Since these neurons lacked a visual response neuronal activity sampling started from 80ms after target onset.

intermediate position between *T* and *G*, and significantly different from both *T* ($p = 4.88 \times 10^{-4}$) and *G* ($p = 0.0015$), even during the movement response, just after gaze onset (i.e., final time-step) (One-sample Wilcoxon Signed-Rank Test) . There was no apparent trend for change in the DM fits during the delay period (Fig. 3.9*B*). Consistent with this, there was no significant correlation between spatial code and time-step ($R_s = 0.47$, $p = 0.20$, Spearman's ρ correlation).

3.4.3.2. Movement-only neurons

Figure 3.10*A* (top panel) shows the activity of an example M neuron with activity rising just before the onset of the gaze shift (about 120ms before saccade onset). This neuron only showed spatial tuning for four time-steps around the time of gaze onset, showing a spatial code tightly centered around *G* (Fig. 3.10*A*, bottom panel). The RF plot shown here corresponds to the time-step centered at gaze onset. For the M population only the three time-steps straddling gaze onset showed significantly higher coherence index than the pre-target period (with other time-steps shown in gray; Fig. 3.10*B*). In all the time-steps in the motor epoch population spatial code was very close to *G* (less than one step short of *G* along *T*-*G* continuum) and was not significantly different from *G* ($p > 0.25$ for each time-step, One-sample Wilcoxon Signed-Rank Test).

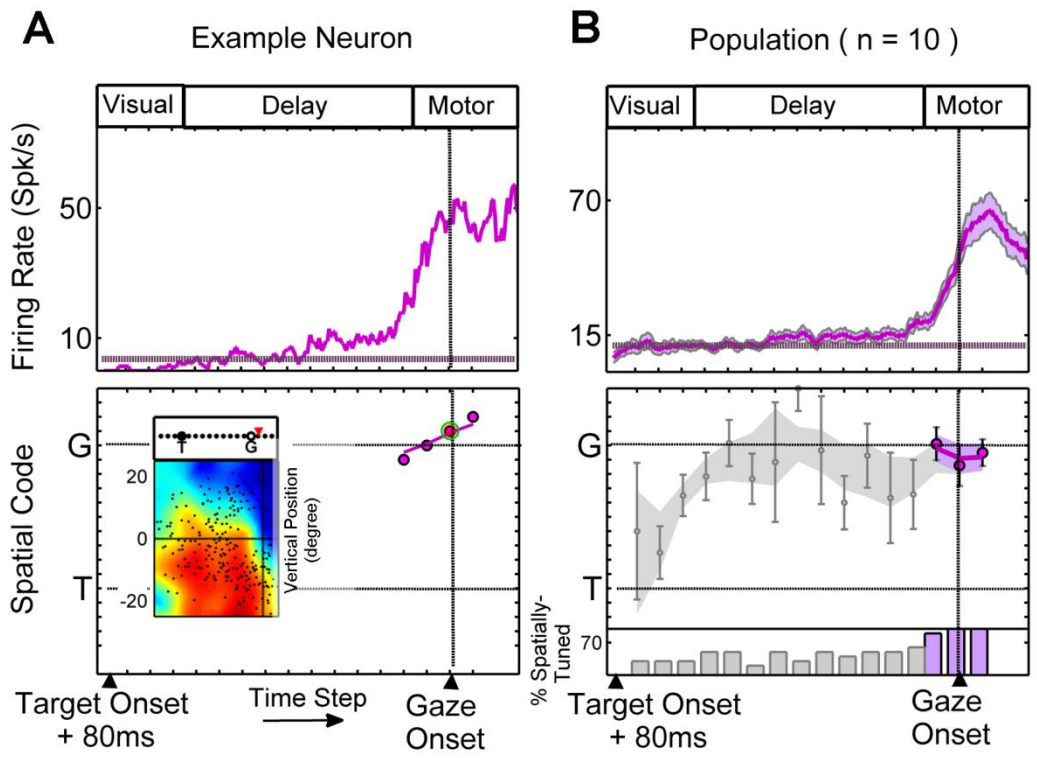

Figure 3.10. Single neuron example and population results for movement-only (M) neurons. Same conventions as Figure 3.5 are used. Since these neurons lacked a visual response neuronal activity sampling started from 80ms after target onset.

3.4.4. Summary of results and comparison of sub-populations

Figure 3.11*A* summarizes and compares the results for each of the neuron sub-populations described above, by superimposing their population means and confidence intervals within a single normalized spatiotemporal continuum plot. Based on the amount and coherence of activity in the sub-population results described above, we have divided the neuronal responses into a visual epoch (first three time-steps), the delay epoch (next 10 time-steps), and the motor epoch (final three time-steps, straddling gaze onset). During the visual epoch, V neurons start with a code very close to *T*, but tend to converge toward the VM code (V and VM were not significantly different in their three shared time-steps). Both the VM and DM populations showed an intermediate spatial code throughout the delay period, as described above. There was no statistical difference between these two populations at any shared time-steps ($p > 0.20$, two-tailed Mann-Whitney *U* test) and the slopes of the regression lines to individual data points (not shown) were not significantly different ($p = 0.87$, linear regression comparison). However, as described above only VM neurons showed a significant slope. The VM trend-line starts closer to *T*, crosses the DM line about halfway through the delay epoch, and then ends up closer to (but still significantly different from) *G*. In summary, only VM neurons showed a significantly positive *T*-*G* slope, but all spatial coding along the *T*-*G* continuum during the visual and delay epochs (in V, VM, and DM populations) was similar, and all three would have contributed to the overall population code in these epochs.

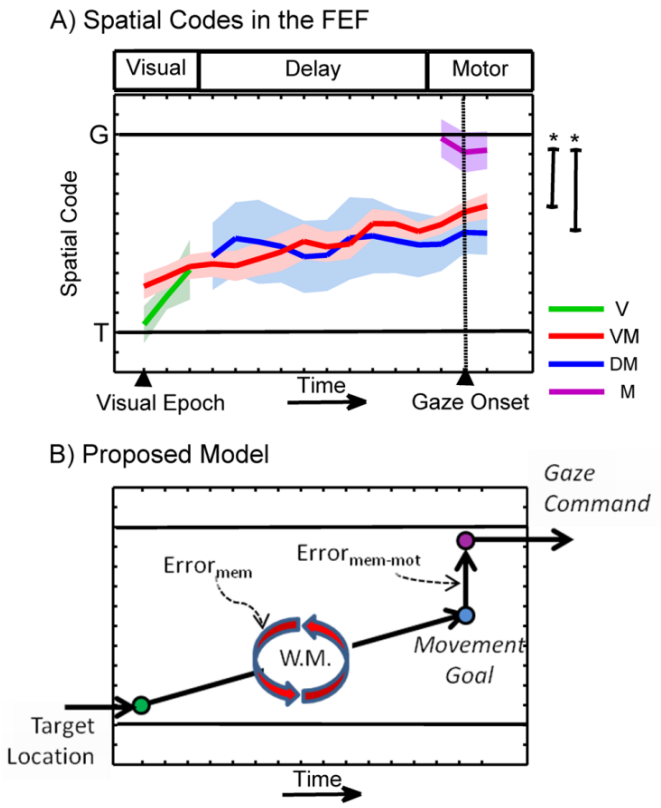

Figure 3.11. Summary of the data for different neuron types and a proposed model of the flow of spatial information within the FEF. ***A,*** shows the relationship between the spatiotemporal codes of V (green), VM (red), DM (blue) and M (magenta) neurons. Asterisks (*) denote significant differences between neuron subtypes. ***B,*** shows a schematic of the possible flow of information. Target location information enters the FEF (but may already have undergone some spatial processing in VM neurons). The spatial code is maintained in working memory (WM), but monotonically changes towards *G* due to memory-related (mem) processes. Upon the presentation of the Go-signal, the most recent memory of target location (i.e., movement goal) is relayed to the motor (mot) circuitry (comprised of M neurons) which in turn encodes the metrics of the eminent gaze shift (*G*).

The most striking difference between sub-populations occurs toward the end, during the motor epoch. Although three sub-populations are active at this point, only one (M) is not significantly different from *G*, and is significantly different from both the DM and VM neuron fits ($p = 6.16 \times 10^{-5}$ and $p = 3.49 \times 10^{-5}$ respectively, Bonferroni-corrected two-tailed Mann-Whitney *U* test; using data pooled across the three final time-steps roughly corresponding to the motor epoch). We noted that VM neurons (but not DM neurons) showed a noticeable peak in their *T-G* distribution falling between the *T-G* midpoint and *G* (Figure 3.7a, bottom panel), and wondered if these neurons contributed more to the motor output. However, when we repeated the preceding statistical comparison,

restricting the VM population to these more *G*-like codes (n = 27), the difference from M neurons was still significant (p = 0.0127, two-tailed Mann-Whitney *U* test).

To summarize, the overall impression across all four populations is of a gradual shift in coding from *T* (in the pure visual response) toward an intermediate *T-G* code (relayed between the V, VM, and DM populations), with a final discrete shift in coding toward *G* (i.e. a pure motor code) in the M population.

3.5. Discussion

This is the first study to describe the entire spatiotemporal sequence of visual-memory-motor transformations during head-unrestrained gaze shifts toward remembered visual stimuli. The current study was motivated by our previous study, which used a memory-delay task to show that 1) FEF visual activity codes target position (*T)* whereas 2) peri-saccadic motor activity codes future gaze position *(G)* (Sajad et al., 2015), but we did not show *when* or *how* this transition occurred. Further, we did not show how different cell populations contributed to this transition. Here, we addressed these questions by using a larger dataset (30% more neurons) and a new analytic method to track spatial coding along the *T-G* continuum through time. This resulted in two novel and important findings: 1) FEF delay activity (particularly in VM cells) showed a *progressive* evolution through intermediate *T-G* codes, and 2) an additional discrete jump occurred between intermediate *T-G* coding in the late delay / motor activity of VM and DM cells, to *G* coding in M-only cells during the final memory-motor transformation for saccades.

Our methodology combined several advantageous approaches: 1) head-unrestrained recordings (necessary to eliminate non-relevant spatial models in our preliminary analysis, and to provide the best behavioral estimate of frontal cortex output; Corneil et al., 2007; Paré et al., 1994; Martinez-Trujillo et al., 2003; Sajad et al, 2015), 2) a simple memory-delay saccade paradigm (avoiding the interpretive issues associated with sensory-motor dissociation tasks; Johnston et al., 2009; Hawkins et al., 2013), and 3) considering possibility for intermediate spatial codes rather than adhering to the traditional binary classification of the spatial code as sensory or motor (the significance of this will be further elaborated below). To our knowledge, this is the first time such a combination of techniques has been applied to the FEF or any other brain area to characterize the spatial codes in delay period. Although head-unrestrained recordings were critical for narrowing down our analysis to *T* and *G* (and hence the intermediate *T-G*) models, similar results would be expected in head-restrained conditions provided that there is enough variability in behavior to adequately separate *T* and *G*.

3.5.1. Intermediary codes in the delay period

Several previous studies have proposed that spatial working memory evolves through time from a sensory to motor code, when these are dissociated in some fashion (Goldman-Rakic, 1987; Gnadt et al., 1991; Fuster, 2001; Postle, 2006). Consistent with this, Takeda and Funahashi (2004) showed that the population spatial code in dlPFC progressively rotates from a sensory vector to a motor vector during a memory delay, in animals trained to rotate saccade direction

relative to visual direction. Zhang and Barash (2004) showed a reversal from 'pro' to 'anti' coding across LIP neurons in the delay preceding anti-saccades. In the current study we found that FEF delay activity showed a progressive transition from a *T* code that faithfully indicated target location, through intermediate *T-G* codes that approached, but did not quite reach coding future gaze position. This *T-G* progression was statistically significant at the neural population level, and we observed similar trends in at least some neurons. This finding differs from results of studies that spatially dissociated movement direction from the presented visual stimulus by virtue of cognitive manipulations (such as rotation or reversal) of the sensory vector (Funahashi, 1989, 1993; Takeda and Funahashi, 2002). In these studies, the sensorimotor transition involved a progressive decrease of activity in visually-tuned cells combined with a progressive increase of activity in motor-tuned cells (Takeda and Funahashi, 2004, 2007; Zhang and Barash, 2004). We did not observe this in our simpler memory-delay task, but rather a progressive change in coding along the *T-G* continuum within the same population (i.e., VM neurons), even within neurons.

To our knowledge, only one other neurophysiological study has considered the change in spatial code within one population of neurons during a memory delay. Wimmer et al., (2014) found that activity in the dlPFC showed increased correlations with variations in final gaze position during a memory-delay period. Since the *T-G* transition observed in our results signifies a progressively increased correlation of FEF delay activity with gaze errors (discussed below), it resembles previous dlPFC results (Wimmer et al., 2014). Similar results in FEF

and dlPFC are in agreement with their reciprocal connectivity and their close relationship in the maintenance of working memory (O'Sullivan et al., 1995; Sweeney et al., 1996; Offen et al., 2010). Note that the main source of the *T-G* progression within our full FEF population appeared to be VM neurons (Fig. 3.6-8). This trend was statistically significant in VM neurons, whereas, DM neurons did not show a statistically significant progression (Fig 9*B*). There is currently no clear consensus whether both classes of neurons contribute to the psychological phenomenon of working memory (Simon et al., 2002; Lawrence et al., 2005; Heinzle et al., 2007; Sommer and Wurtz, 2001). However, a survey of previous publications suggests that DM neurons might be more closely associated with motor planning, whereas VM neurons may be more closely associated with mnemonic functions (Takeda and Funahashi, 2007; Takaura et al., 2011; Markowitz et al., 2015). This notion is consistent with findings that visually-responsive neurons are responsible for retaining and updating visual memory in the superior colliculus (SC) (Sparks and Porter, 1983; Dash et al., 2015). Alternatively, it may be that all delay-responsive neurons in the gaze network are connected through an internal feedback loop for working memory, and influence each other's spatiotemporal profiles (Verduzco-Flores et al., 2009; Okamoto et al., 2007; Curtis 2006).

3.5.2. Transformations between sensory, memory, and motor codes

The second novel observation in this study was the demonstration of discrete changes in the spatial code towards G, in the transition *between* visual, memory, and motor signals. Some theoretical studies have considered spatial

transformations throughout this sequence of events (Brown et al., 2004; Faisal et al., 2008; Ma et al., 2014), and some experimental oculomotor studies have inferred from their data that additional memory-to-motor transformations must occur after the delay period (Stanford and Sparks, 1994; Opris et al., 2003). However, to our knowledge, these transformations have never been directly identified in neural signals. Here we have relied on the presumption that transformations between functional networks are inherently noisy (Alikhanian et al., 2015; Ma et al., 2014; Faisal et al., 2008) to infer the occurrence of transformations based on discrete accumulations of variable errors. Our data suggest that spatial transformations might occur upstream from VM neurons, because they already show a slightly shifted intermediate code at the start of the visual response. As described above, further transition of spatial code occurs during the memory delay, possibly due to degrading memory representations, but importantly, there is an additional transition from an intermediate *T-G* code in VM/DM neurons to a pure *G* code in M neurons at the end of the delay period (even when only compared VM vs. M neurons with preference for gaze-related models). To our knowledge, this is the first direct demonstration of a memory-to-motor transformation between cells within the same structure.

3.5.3. Conceptual Model and Sources of Variable Error

It is important to note that our model-fitting method relies on the relationship between variability in neural firing rate and variability in behavior. In particular, the *T-G* continuum reflects the degree to which neural firing rate faithfully represents target location for an idealized saccade, versus the variable errors in

actual future gaze direction. Thus, the *T-G* scores shown in Figure 3.11*A* can be interpreted as reflecting the progression of gaze error coding in different neural populations through time. With this in mind, Figure 3.11*B* schematically summarizes the possible flow of spatial signals within the FEF during our task, and how these mechanisms might contribute to gaze variations.

According to this model, both V and VM neurons receive relatively unprocessed spatial information about the location of the visual stimulus relative to the eye but VM neurons receive additional inputs from V (and perhaps other areas) containing errors that tend to shift the spatial code slightly further toward *G* along the *T-G* continuum. This spatial information is then maintained within a working memory / planning network comprised of VM and possibly DM neurons, as well as their extrinsic connections (Zelinsky and Bisley, 2015). Here, the spatial representation in VM neurons shifts through intermediary *T-G* codes throughout the delay period, presumably through the accumulation of noise in a recurrent feedback network (Burak and Fiete, 2012; Compte et al., 2000; Wang et al., 2015). Upon the presentation of the Go-signal, the retained spatial information is then disinhibited, thus producing the motor response in VM and DM neurons. At the same time, this code is relayed to the M neurons, involving an additional transformation, pushing the final motor code almost to *G*. This is consistent with the notion of noise arising in the transformation from memory to motor network (Zheng and Wilson, 2002; Alikhanian et al., 2015; Avery and Krichmar, 2015). These signals could then influence behavior through projections to the brainstem

(Kunzle et al., 1976; Segraves, 1992). For example, we have observed similar noisy gaze-related signals in the motor responses of the SC (Sadeh et al., 2015).

Overall, these observations suggest that the noisy gaze signal that we observed in the overall motor response in our previous study (Sajad et al. 2015) is not the result of a random or general degradation of visual signals, but rather arises from different sources and different types of cells that relay different signals through different synaptic networks (Lawrence and Snyder, 2005; Chatham and Badre, 2015; Markowitz et al., 2015). To simple terms, our data support a combination of the gradual progression model and late transformation models illustrated in Figure 3.1*D*.

3.5.4. Behavioral and Clinical Implications

The noise-source model shown in Figure 3.11*B* could be useful for understanding and investigating behavior in both healthy and clinical populations. It is reasonable to assume that the sources of these variable errors would be vulnerable to diseases that affect frontal cortex function (Avery and Krichmar, 2015). If so, this confirms that analysis of variable errors in memory-delay saccade task has diagnostic value for diseases that affect frontal cortex function (Ploner et al., 1999). Further, whereas most behavioral studies interpret errors from memory delay tasks only in terms of maintenance (e.g., Oyachi and Ohtsuka, 1995; D'Esposito and Postle, 1999; Wimmer et al., 2014) *or* transformations (e.g., Henriques et al., 1998; Vesia et al., 2010; Dessing et al., 2012), our study confirms that both maintenance and memory-to-motor transformations must be taken into account (Gnadt et al., 1991; Avery and

Krichmar, 2015). For example, numerous clinical studies have considered errors that arise in working memory maintenance (Minshew et al., 1999; Sweeney et al., 2007; Mazhari et al., 2010), but there is also evidence that errors arise in the gating of memory signals to action in Parkinson's and Schizophrenic patients (Avery and Krichmar, 2015; Ketcham et al., 2003; Rottschy et al., 2013). Thus, the observed errors in these patients could be interpreted as degraded states of noisy memory and memory-to-motor transformations observed here.

Chapter 4: General Discussion

The studies in this dissertation provide the first characterization of the spatial transformations in the FEF under head-unrestrained conditions. Activity from single neurons in the FEF of head-unrestrained monkeys was recorded during a memory-guided gaze task. Unlike head-restrained conditions where the desired gaze vector is virtually identical to the eye movement vector (in head) and head movements are completely ignored, head-unrestrained conditions allowed us to dissociate gaze movement into its subcomponents, namely, gaze (eye in space) vs. eye (in head) or head (in space). Also, it allowed us to dissociate eye-centered, head-centered and space/body-centered coordinate frames for a thorough investigation of the egocentric frames of reference used in the FEF. Memory-guided gaze task was used to temporally separate visual and motor responses for separate analysis. It also offered the ability to investigate the spatial code during the intervening delay period to characterize the time course for the transformations between visual and motor response. Below, I will summarize the results and conclusions of the studies in this dissertation, discuss their implications for studies in basic and clinical research and highlight some of the limitations of the study that can stimulate future research.

4.1. Study 1: Characterizing the spatial transformations in the FEF

In the first experimental chapter (chapter 2), I showed that the visual and movement response in the FEF encode different spatial parameters. Perhaps not surprisingly, the visual response preferentially encoded target position in eye-

centered coordinates. The movement response on the other hand showed preference for the endpoint of the imminent gaze shift (which deviated from target position by virtue of inaccuracies in behavior). This difference between the visual and movement response (i.e., target vs. gaze coding) was best highlighted and visualized when spatial models along a continuum between target and gaze models (T-G continuum) were considered (see Figure 2.11). These results provide the first neurophysiological evidence for difference in spatial code between the visual and movement response in a standard transformation gaze task, where the movement goal is spatially congruent with target location. In the model presented in Figure 2.12 we proposed that what separates the visual and the movement codes is the errors that incur during the memory-delay interval, likely related to memory-dependent processes (Gnadt et al., 1991).

Importantly, we ruled out most spatial models related to the displacement or position of head and eye components of gaze (note: eye displacement model was not excluded but it was rarely preferred over the eye-centered gaze models in individual neurons). Also, in our intermediate model analysis we did not observe preference for head- or space-centered spatial codes but rather observed that most visual and movement responses had reference frames closely described by the eye-frame. These results show that the transformation of gaze signal into independent eye/head codes and coordinate transformations do not occur within the FEF (Monteon et al., 2010; Bruce and Goldberg, 1985). This is consistent with the notion that the FEF encodes a signal that determines the eventual location of gaze and sends it to downstream motor circuitry for

subsequent processing necessary for generating eye-head coordinate gaze shift (Dassonville et al., 1992; Guitton and Mandl, 1978; Guitton, 1992; Monteon et al., 2010; Elsley et al., 2007; Heinzle et al., 2007).

4.2. Study 2: Investigating the time course of target-to-gaze transition

The transition from a target code to a gaze code between the visual and movement response observed in the first study (chapter 2) prompted the second study (chapter 3). Specifically, this study aimed at characterizing the time course for the target-to-gaze transition observed between the visual and movement responses in the FEF. For this I applied the T-G continuum analysis on neuronal responses sampled at discrete time-steps spanning visual and movement responses, with a focus on the intervening delay period. Importantly, the T-G continuum allowed the consideration of spatial codes between target and gaze endpoint (i.e., treats spatial code as a continuous variable). This is particularly important for studies on spatial working memory as many models have proposed drifting spatial code; something that has remained largely untested to date. (Compte et al., 2000; Ma et al., 2014; Wimmer et al., 2014). Only recently, Wimmer et al. (2014) has provided *implicit* neurophysiological evidence for such drifting spatial code in dlPFC during maintenance period by showing an increase in the correlation between changes in delay activity and the inaccuracies in the memory-guided saccade task. Here, by virtue of the T-G continuum analysis we were able to provide an *explicit* evidence for a changing spatial code (towards eventual gaze position) in the FEF during delay period. We further extended these findings by showing that the delay period is not the sole contributor to the

T-to-G transition. Specifically, we identified two additional abrupt transitions in the FEF spatial code: One between the purely sensory (target) code and that observed in the visual response of delay-responsive neurons, and one between the movement response of delay-responsive neurons and that of movement-only neurons (with no delay activity).

Noteworthy that any transition from T towards G in our study indicated accumulation of variable errors. Therefore, our results were also interpreted as evidence for a multistage accumulation of variable errors during simple memory-guided gaze task (Brown et al., 2004; O'Reilly and Frank, 2006; Gnadt et al., 1991; Krappmann 1998; Opris et al., 2003). The neurobiological origins of these errors were out of the scope of this study but the progressive change in code during delay period was in agreement with models of working memory that show gradual accumulation of correlated noise in the maintenance network (Camperi et al., 1998; Compte et al., 2000; Gold et al., 2005;Burak and Fiete, 2012; Lim and Goldman, 2013; Wimmer et al., 2014). Also, based on the presumption that neurons with delay activity are involved in maintenance while neurons without delay activity are not, the abrupt transitions were attributed to noisy transfers of activity between different functional networks (Zheng and Wilson, 2002). This fits in with models of working memory that consider encoding, maintenance, and decoding/retrieval as distinct, noisy processes that are inevitably engaged in memory-guided tasks (Woodman and Vogel, 2005; Ma et al., 2014).

The fact that codes ranging from T (in V neurons) to G (in M neurons) were observed within the FEF shows that the accumulation of variable errors is fully

reflected in FEF neuronal responses, in eye-centered coordinates (since T and G are both in this coordinate frame). But to what extent are these errors originated in the FEF and its interconnected network? It might be tempting to say that variable errors solely originate from processes that take place in eye-centered coordinates within the FEF and its circuitry. However, it is possible that the FEF, as part of the cognitive control network, carries an eye-centered copy of the most recent spatial representations (regardless of the subsequent processing stages including coordinate transformations) for effective integration with other incoming sensory information and other unprecedented cognitive operations (Cohen and Andersen, 2002; Ferrera et al., 2009; Thompson et al. 2004; Noudoost and Moore 2014). Although based on our results we cannot know definitively what the origin of these errors are, what our results clearly demonstrate is that there are distinct stages that contribute to the variable behavioural errors.

4.3. Implications for basic and clinical neuroscience

The studies in this dissertation have important implications for gaze control system, and studies that utilize this motor system as a study model for working memory, or to make inferences about brain function in patient with compromised brain function.

In our first study we show that even at the level of FEF, which is the main motor output of the cortex, for gaze control, the spatial transformations involve transforming a sensory-related signal into a desired movement goal which is yet to be transformed into specific motor commands for the eyes and the head. These results are important in understanding the series of transformations that

take place in gaze control circuitry, the interrelationship between different nodes of this pathway, and for studies that need to model the role of cortex in gaze control circuitry (Heinzle et al., 2007; Dominey and Arbib, 1992).

Our results regarding the spatial code during memory-delay interval have two implications for studies on working memory. First, we showed that the delay code is not static and can dynamically change into a code that influences the output behaviour. Secondly, we showed that there are discontinuities in the spatial representation between the delay code and the purely sensory (T) and purely motor (G) codes. These discontinuities were explained as a transfer of activity between distinct functional networks which resulted in accumulation of variable errors (since no complex transformations were needed). However in more complex tasks, such activity transfer may represent the neural substrate for the complex computations that take place in working memory tasks (O'Reilly, 2006). Therefore, working memory representations not just in the spatial domain as in this study, but in any domain, may be intermediary in nature, containing mixed attributes of both sensory and motor signals (Postle, 2006; Barak et al., 2010; Bremner and Andersen, 2014). This could reconcile the conflicting evidence for sensory vs. motor nature of working memory representations, particularly highlighted in chapter 1 and the introduction of chapter 3 (Funahashi, 2013; Curtis and D'Esposito, 2006; Postle, 2006).

Probably the most important implication of the two studies in this dissertation is that caution should be practiced when using the terms “sensory” (or “visual”) and “motor” as these are only heuristics used in relative terms. In the temporal

domain, visual activity and movement / motor activity are defined as responses that are temporally locked to visual presentation and gaze onset, respectively (e.g., Bruce and Goldberg, 1985; Funahashi et al., 1989; Mays and Sparks, 1980). But as we saw in our results even the same "visual' or "motor" response in the same brain area (FEF) can encode different spatial information depending on the neuron type (visual code in visual and visuomovement neurons; or movement code in visuomovement and movement-only neurons; Chapter 3, section 3.4.4). This raises the following question: exactly at what point should one draw the boundary between sensory and motor? Even studies that aim at answering similar questions may often define these terms differently, which could result in conflicting conclusions. For instance, in this dissertation sensory and motor-related spatial codes were separated by differences between target location and the gaze end point (as well as eye and head movement-related codes, but those were eliminated). On the other hand in visual-motor dissociation tasks reviewed throughout this dissertation, any spatial code related to movement direction is considered a movement code as long as it reflects the mental remapping of the sensory vector i.e., cognitive transformations (Everling and Munoz, 2000; Sato and Schall, 2003; Fernandez-Ruiz et al., 2007; Takeda and Funahashi, 2002; Zhang and Barash, 2000; 2004). Also in those studies (in head-restrained) an eye-centered representation of the movement goal is virtually identical to the movement vector of the eye (in head). For an effective comparison across studies it is essential to have clear definitions of these terms and to use methods that are more specific about the exact nature of the

information encoded by different neuronal responses. In this dissertation we introduced intermediary spatial model analysis that allowed us to consider spatial codes between target and gaze position. Future studies may also benefit from using indices that allow for such intermediary (hybrid) sensory-motor measures for more specific characterization of the information encoded in neuronal responses.

Aside from the clear implications for basic research, our results also have implications for clinical studies that use eye movements to understand the impairments in patients with brain lesion or other neuropsychiatric disorders (e.g., Sweeney et al., 2007; Guitton et al., 1985; Pierrot-Deseilligny et al., 1991; Ploner et al., 1999). Our findings extend our understanding of the nature of gaze-related deficits in patients with compromised frontal cortical function. A better understanding of the gaze control system and its interaction with other functional networks in the brain can render the oculomotor system a better diagnostic tool for neurological disorders and provoke the development of better treatment strategies and rehabilitation regiments that can improve the lives of affected patients (Khan et al., 2005; Levin, 1984; Guitton et al., 1985).

Our findings with respect to the multi-stage accumulation of noise in memory-guided gaze task clearly demonstrate the importance of variable errors (and not just systematic errors as usually practiced) as a tool to give insight into brain function (Avery and Krichmar, 2015). They emphasize that behavioural errors in memory-guided gaze task are accumulated not merely due to maintenance functions but in at least two additional stages (possibly related to sensory and

memory encoding and decoding). Studies that examine behavioural errors in memory-guided tasks should consider all these stages as vulnerable and noisy processes. For instance, it has been lately shown that deficiencies observed in memory-guided behaviour in Parkinson's patients is not related to maintenance in memory per se but is rather caused by impairments in decoding memory representations into specific action plans (Ketcham et al., 2003; Rottschy et al., 2013). Similar considerations should be made for any research (such as psychophysics / microstimulation / TMS studies) that studies behavioural errors in memory-guided behaviour to make inferences about memory functions of the brain.

4.4. Limitations and future directions

Below I will highlight a few limitations of the current study and propose possible experiments that can resolve these limitations.

One of the limitations of the current study is that we presented the subjects with single visual stimuli in the periphery. Therefore, it remains unknown to what extent our results can be generalized to natural conditions in which our visual field is filled with visual objects (Kayser et al., 2004; Berman and Segraves, 1994). For one, in natural conditions we can rely on both egocentric and allocentric frames of reference to encode spatial information. Also, because of our limited working memory capacity we constantly have to select "relevant" stimuli to be retained in working memory and constantly update working memory content based on our movements, modified goals, or new visual input. In the current experimental conditions, where single visual stimuli (single dots with no

meaningful features) are presented, these factors have been largely ignored. Future research needs to come up with methods that allow the investigation of brain function during tasks that involve the most natural structure of sensory input and behavioural output (Fernandes et al., 2014). The work in this dissertation set one step forward in this direction by considering FEF function during a more natural output of gaze control system: one in which both the eyes and the head contributed to gaze behaviour.

Throughout this dissertation (especially in Chapter 3) I showed that different neuron subtypes exhibited different spatial codes (even in the same activity type; e.g., movement response). However, one limitation of our study is that with the experimental methods employed here we could not identify the anatomical relationship or functional role of the recorded neurons within the FEF microcircuitry. Using techniques that can identify the projections to / from the recorded neurons can be important in understanding the neural underpinnings of information processing within and between brain areas and the specific contributions of each node in the visuomotor pathway (Cohen et al. 2009, Rey et al., Lawrence and Snyder 2005; Ninomiya et al. 2012).

Another limitation of this study, as in any study on animal models, is that it is unknown to what degree our results can be generalized to humans. Monkeys are excellent animal models for studying brain function because they are capable of performing relatively complex tasks and there is a substantial level of homology between monkey and human brain. However there are clear differences between these two species both in terms of their cognitive abilities, brain structure (Wager

and Yarkoni, 2012) , and even anatomical musculature of the gaze effectors (Farshadmanesh et al., 2012). Also, monkeys have to go through extensive training on controlled experimental tasks which are shown to alter brain activity over time (Grenewald et al., 1990). One should be wary of these limitations in interpreting the results from monkey neurophysiology experiments.

4.5 Conclusion

The studies presented in this dissertation show that while the FEF takes part in spatial transformations for gaze behaviour, it does not involve coordinate transformations nor is it involve in splitting gaze signals into independent eye and head movement commands (at least in the simple memory-guided task used in these studies). Instead, it transforms target location information to information that determine the metrics of the upcoming gaze shift. This transformation involves a sequence of stages related to early sensory processing, memory maintenance (reflected in FEF delay activity), and memory-motor transformation which involves a transfer of activity from delay-responsive neurons to movement-related neurons triggered just prior to movement. Collectively, these studies show the functional role of FEF in the spatial transformations subserving memory-guided gaze behaviour.

There are still many important questions that are unanswered related to sensorimotor transformation. First, where and how do the coordinate transformations from eye-centered coordinates to other coordinate frames take place? Also, where and how are gaze command signals decomposed into independent eye and head signals? How does the delay code in other areas

compare to that observed in the FEF? Perhaps performing similar studies (as presented in this dissertation) in other nodes of the visuomotor pathway can be a good starting step to answer these questions.

References

Adrian, E. D. (1928). The Basis of Sensations. *Norton*, New York.

Alikhanian, H., de Carvalho, S. R., & Blohm, G. (2015). Quantifying effects of stochasticity in reference frame transformations on posterior distributions.*Frontiers in computational neuroscience*, *9*.

Amemori, K. I., & Sawaguchi, T. (2006). Rule-dependent shifting of sensorimotor representation in the primate prefrontal cortex. *European Journal of Neuroscience*, *23*(7), 1895-1909.

Andersen, R. A., & Buneo, C. A. (2002). Intentional maps in posterior parietal cortex. *Annual review of neuroscience*, *25*(1), 189-220.

Andersen, R. A., & Mountcastle, V. B. (1983). The influence of the angle of gaze upon the excitability of the light-sensitive neurons of the posterior parietal cortex. *The Journal of Neuroscience*, *3*(3), 532-548.

Andersen, R. A., Bracewell, R. M., Barash, S., Gnadt, J. W., & Fogassi, L. (1990). Eye position effects on visual, memory, and saccade-related activity in areas LIP and 7a of macaque. *The Journal of Neuroscience*, *10*(4), 1176-1196.

Andersen, R. A., Brotchie, P. R., & Mazzoni, P. (1992). Evidence for the lateral intraparietal area as the parietal eye field. *Current opinion in neurobiology*, *2*(6), 840-846.

Andersen, R. A., Essick, G. K., & Siegel, R. M. (1985). Encoding of spatial location by posterior parietal neurons. *Science*, *230*(4724), 456-458.

Andersen, R. A., Snyder, L. H., Batista, A. P., Buneo, C. A., & Cohen, Y. E. (1998).

Posterior parietal areas specialized for eye movements (LIP) and reach (PRR) using a common coordinate frame. *Sensory guidance of movement*, *218*, 109-128.

Andersen, R. A., Snyder, L. H., Li, C. S., & Stricanne, B. (1993). Coordinate transformations in the representation of spatial information. *Current opinion in neurobiology*, *3*(2), 171-176.

Anderson, M. C., & Green, C. (2001). Suppressing unwanted memories by executive control. *Nature*, *410*(6826), 366-369.

Avery, M. C., & Krichmar, J. L. (2015). Improper activation of D1 and D2 receptors leads to excess noise in prefrontal cortex. *Frontiers in computational neuroscience*, *9*.

Avillac, M., Deneve, S., Olivier, E., Pouget, A., & Duhamel, J. R. (2005). Reference frames for representing visual and tactile locations in parietal cortex. *Nature neuroscience*, *8*(7), 941-949.

Awh, E., Vogel, E. K., & Oh, S. H. (2006). Interactions between attention and working memory. *Neuroscience*, *139*(1), 201-208.

Babapoor-Farrokhran, S., Hutchison, R. M., Gati, J. S., Menon, R. S., & Everling, S. (2013). Functional connectivity patterns of medial and lateral macaque frontal eye fields reveal distinct visuomotor networks. *Journal of neurophysiology*, *109*(10), 2560-2570.

Baddeley AD, Logie RH (1999) Working memory: the multiple-component model. In: Models of working memory (Miyake A, Shah P,eds), pp 28–61. Cambridge, UK: Cambridge University Press.

Baddeley, A. D. (2002). Is working memory still working?. *European*

psychologist, *7*(2), 85.

Baddeley, A. D., & Hitch, G. (1974). Working memory. *The psychology of learning and motivation*, *8*, 47-89.

Badre, D. (2012). Opening the gate to working memory. *Proceedings of the National Academy of Sciences*, *109*(49), 19878-19879.

Badre, D., & D'Esposito, M. (2009). Is the rostro-caudal axis of the frontal lobe hierarchical?. *Nature Reviews Neuroscience*, *10*(9), 659-669.

Barak, O., Tsodyks, M., & Romo, R. (2010). Neuronal population coding of parametric working memory. *The Journal of Neuroscience*, *30*(28), 9424-9430.

Barash, S., Bracewell, R. M., Fogassi, L., Gnadt, J. W., & Andersen, R. A. (1991). Saccade-related activity in the lateral intraparietal area. I. Temporal properties; comparison with area 7a. *Journal of Neurophysiology*, *66*(3), 1095-1108.

Basso, M. A., & Wurtz, R. H. (1997). Modulation of neuronal activity by target uncertainty. *Nature*, *389*(6646), 66-69.

Bays, P. M., Gorgoraptis, N., Wee, N., Marshall, L., & Husain, M. (2011). Temporal dynamics of encoding, storage, and reallocation of visual working memory. *Journal of vision*, *11*(10), 6-6.

Bisley, J. W., & Goldberg, M. E. (2003). Neuronal activity in the lateral intraparietal area and spatial attention. *Science*, *299*(5603), 81-86.

Bisley, J. W., & Goldberg, M. E. (2010). Attention, intention, and priority in the parietal lobe. *Annual review of neuroscience*, *33*, 1.

Bizzi, E. (1968). Discharge of frontal eye field neurons during saccadic and following eye movements in unanesthetized monkeys. *Experimental Brain Research*, *6*(1), 69-80.

Bizzi, E., & Schiller, P. H. (1970). Single unit activity in the frontal eye fields of unanesthetized monkeys during eye and head movement. *Experimental Brain Research*, *10*(2), 151-158.

Bizzi, E., Kalil, R. E., & Tagliasco, V. (1971). Eye-head coordination in monkeys: evidence for centrally patterned organization. *Science*, *173*(3995), 452-454.

Blatt, G. J., Andersen, R. A., & Stoner, G. R. (1990). Visual receptive field organization and cortico-cortical connections of the lateral intraparietal area (area LIP) in the macaque. *Journal of Comparative Neurology*, *299*(4), 421-445.

Blohm, G., Keith, G. P., & Crawford, J. D. (2009). Decoding the cortical transformations for visually guided reaching in 3D space. *Cerebral Cortex*,*19*(6), 1372-1393.

Bremner, L. R., & Andersen, R. A. (2014). Temporal analysis of reference frames in parietal cortex area 5d during reach planning. *The Journal of Neuroscience*, *34*(15), 5273-5284.

Brown, J. W., Bullock, D., & Grossberg, S. (2004). How laminar frontal cortex and basal ganglia circuits interact to control planned and reactive saccades.*Neural Networks*, *17*(4), 471-510.

Brown, M. R., Vilis, T., & Everling, S. (2007). Frontoparietal activation with preparation for antisaccades. *Journal of Neurophysiology*, *98*(3), 1751-1762.

Bruce, C. J., & Goldberg, M. E. (1985). Primate frontal eye fields. I. Single neurons

discharging before saccades. *J Neurophysiol*, *53*(3), 603-635.

Bruce, C. J., Goldberg, M. E., Bushnell, M. C., & Stanton, G. B. (1985). Primate frontal eye fields. II. Physiological and anatomical correlates of electrically evoked eye movements. *Journal of neurophysiology*, *54*(3), 714-734.

Bu, U., Bu, J. A., & Henn, V. (1977). Vertical eye movement related unit activity in the rostral mesencephalic reticular formation of the alert monkey.*Brain research*, *130*(2), 239-252.

Bullier, J., Schall, J. D., & Morel, A. (1996). Functional streams in occipito-frontal connections in the monkey. *Behavioural brain research*, *76*(1), 89-97.

Burak, Y., & Fiete, I. R. (2012). Fundamental limits on persistent activity in networks of noisy neurons. *Proceedings of the National Academy of Sciences*, *109*(43), 17645-17650.

Burman, D. D., & Segraves, M. A. (1994). Primate frontal eye field activity during natural scanning eye movements. *Journal of Neurophysiology*, *71*(3), 1266-1271.

Camperi, M., & Wang, X. J. (1998). A model of visuospatial working memory in prefrontal cortex: recurrent network and cellular bistability. *Journal of computational neuroscience*, *5*(4), 383-405.

Carter, C. S., Braver, T. S., Barch, D. M., Botvinick, M. M., Noll, D., & Cohen, J. D. (1998). Anterior cingulate cortex, error detection, and the online monitoring of performance. *Science*, *280*(5364), 747-749.

Cassanello, C. R., & Ferrera, V. P. (2007). Computing vector differences using a gain field-like mechanism in monkey frontal eye field. *The Journal of physiology*, *582*(2), 647-664.

Chang, M. H., Armstrong, K. M., & Moore, T. (2012). Dissociation of response variability from firing rate effects in frontal eye field neurons during visual stimulation, working memory, and attention. *The Journal of Neuroscience*, *32*(6), 2204-2216.

Chao, L. L., & Knight, R. T. (1995). Human prefrontal lesions increase distractibility to irrelevant sensory inputs. *Neuroreport*, *6*(12), 1605-1610.

Chatham, C. H., & Badre, D. (2015). Multiple gates on working memory.*Current opinion in behavioral sciences*, *1*, 23-31.

Chatham, C. H., Frank, M. J., & Badre, D. (2014). Corticostriatal output gating during selection from working memory. *Neuron*, *81*(4), 930-942.

Chen, L. L. (2006). Head movements evoked by electrical stimulation in the frontal eye field of the monkey: evidence for independent eye and head control. *Journal of neurophysiology*, *95*(6), 3528-3542.

Chen, L. L., & Walton, M. M. (2005). Head movement evoked by electrical stimulation in the supplementary eye field of the rhesus monkey. *Journal of neurophysiology*, *94*(6), 4502-4519.

Chen, X., DeAngelis, G. C., & Angelaki, D. E. (2013). Diverse spatial reference frames of vestibular signals in parietal cortex. *Neuron*, *80*(5), 1310-1321.

Chen, Y., Monaco, S., Byrne, P., Yan, X., Henriques, D. Y., & Crawford, J. D. (2014). Allocentric versus egocentric representation of remembered reach targets in human cortex. *The Journal of Neuroscience*, *34*(37), 12515-12526.

Churchland, M. M., Afshar, A., & Shenoy, K. V. (2006). A central source of

movement variability. *Neuron*, *52*(6), 1085-1096.

Cohen, B., & Komatsuzaki, A. (1972). Eye movements induced by stimulation of the pontine reticular formation: evidence for integration in oculomotor pathways. *Experimental neurology*, *36*(1), 101-117.

Cohen, J. Y., Pouget, P., Heitz, R. P., Woodman, G. F., & Schall, J. D. (2009). Biophysical support for functionally distinct cell types in the frontal eye field.*Journal of neurophysiology*, *101*(2), 912-916.

Cohen, Y. E., & Andersen, R. A. (2002). A common reference frame for movement plans in the posterior parietal cortex. *Nature Reviews Neuroscience*, *3*(7), 553-562.

Colby, C. L., & Goldberg, M. E. (1992). The updating of the representation of visual space in parietal cortex by intended eye movements. *Science*,*255*(5040), 90-92.

Colby, C. L., Duhamel, J. R., & Goldberg, M. E. (1995). Oculocentric spatial representation in parietal cortex. *Cerebral Cortex*, *5*(5), 470-481.

Collins, T., Vergilino-Perez, D., Delisle, L., & Doré-Mazars, K. (2008). Visual versus motor vector inversions in the antisaccade task: a behavioral investigation with saccadic adaptation. *Journal of neurophysiology*, *99*(5), 2708-2718.

Compte, A., Brunel, N., Goldman-Rakic, P. S., & Wang, X. J. (2000). Synaptic mechanisms and network dynamics underlying spatial working memory in a cortical network model. *Cerebral Cortex*, *10*(9), 910-923.

Constantin, A. G., Wang, H., & Crawford, J. D. (2004). Role of superior colliculus in adaptive eye–head coordination during gaze shifts. *Journal of neurophysiology*, *92*(4), 2168-2184.

Constantin, A. G., Wang, H., Martinez-Trujillo, J. C., & Crawford, J. D. (2007). Frames of reference for gaze saccades evoked during stimulation of lateral intraparietal cortex. *Journal of neurophysiology*, *98*(2), 696-709.

Constantinidis, C., & Steinmetz, M. A. (2005). Posterior parietal cortex automatically encodes the location of salient stimuli. *The Journal of neuroscience*, *25*(1), 233-238.

Constantinidis, C., Franowicz, M. N., & Goldman-Rakic, P. S. (2001). The sensory nature of mnemonic representation in the primate prefrontal cortex.*Nature neuroscience*, *4*(3), 311-316.

Robinson, D.A. (1981). Control of Eye Movements. *Handbook of Physiology, The Nervous System, Motor Control*.

Corneil, B. D., Munoz, D. P., & Olivier, E. (2007). Priming of head premotor circuits during oculomotor preparation. *Journal of neurophysiology*, *97*(1), 701-714.

McFarland, N. R., & Haber, S. N. (2002). Thalamic relay nuclei of the basal ganglia form both reciprocal and nonreciprocal cortical connections, linking multiple frontal cortical areas. *The Journal of Neuroscience*, *22*(18), 8117-8132.

Courtney, S. M. (2004). Attention and cognitive control as emergent properties of information representation in working memory. *Cognitive, Affective, & Behavioral Neuroscience*, *4*(4), 501-516.

Crawford, J. D. (1994). The oculomotor neural integrator uses a behavior-related coordinate system. *The Journal of neuroscience*, *14*(11), 6911-6923.

Crawford, J. D., & Guitton, D. (1997). Visual-motor transformations required for accurate and kinematically correct saccades. *Journal of Neurophysiology*,*78*(3),

1447-1467.

Crawford, J. D., Ceylan, M. Z., Klier, E. M., & Guitton, D. (1999). Three-dimensional eye-head coordination during gaze saccades in the primate.*Journal of Neurophysiology*, *81*(4), 1760-1782.

Crawford, J. D., Henriques, D. Y., & Medendorp, W. P. (2011). Three-dimensional transformations for goal-directed action. *Annual review of neuroscience*, *34*, 309-331.

Crawford, J. D., Martinez-Trujillo, J. C., & Klier, E. M. (2003). Neural control of three-dimensional eye and head movements. *Current opinion in neurobiology*, *13*(6), 655-662.

Cui, H. (2014). From Intention to Action: Hierarchical Sensorimotor Transformation in the Posterior Parietal Cortex. *eneuro*, *1*(1), ENEURO-0017.

Cullen, K. E., & Guitton, D. (1997). Analysis of primate IBN spike trains using system identification techniques. III. Relationship to motor error during head-fixed saccades and head-free gaze shifts. *Journal of neurophysiology*,*78*(6), 3307-3322.

Curtis, C. E. (2006). Prefrontal and parietal contributions to spatial working memory. *Neuroscience*, *139*(1), 173-180.

Curtis, C. E., & D'Esposito, M. (2003). Persistent activity in the prefrontal cortex during working memory. *Trends in cognitive sciences*, *7*(9), 415-423.

Curtis, C. E., & D'Esposito, M. (2006). Selection and maintenance of saccade goals in the human frontal eye fields. *Journal of Neurophysiology*, *95*(6), 3923-3927.

Curtis, C. E., Rao, V. Y., & D'Esposito, M. (2004). Maintenance of spatial and motor codes during oculomotor delayed response tasks. *The Journal of Neuroscience*, *24*(16), 3944-3952.

D'Esposito, M., & Postle, B. R. (1999). The dependence of span and delayed-response performance on prefrontal cortex. *Neuropsychologia*,*37*(11), 1303-1315.

Daddaoua, N., Dicke, P. W., & Thier, P. (2014). Eye position information is used to compensate the consequences of ocular torsion on V1 receptive fields. *Nature communications*, *5*.

Dash, S., Yan, X., Wang, H., & Crawford, J. D. (2015). Continuous updating of visuospatial memory in superior colliculus during slow eye movements.*Current Biology*, *25*(3), 267-274.

Dassonville, P., Schlag, J., & Schlag-Rey, M. (1992). The frontal eye field provides the goal of saccadic eye movement. *Experimental brain research*,*89*(2), 300-310.

De Bie, J., Van den Brink, G., & Van Sonderen, J. F. (2013). The systematic undershoot of saccades: A localization or oculomotor phenomenon. *Eye movements: From physiology to cognition*, 85-94.

DeSouza, J. F., Keith, G. P., Yan, X., Blohm, G., Wang, H., & Crawford, J. D. (2011). Intrinsic reference frames of superior colliculus visuomotor receptive fields during head-unrestrained gaze shifts. *The Journal of Neuroscience*,*31*(50), 18313-18326.

Dessing, J. C., Byrne, P. A., Abadeh, A., & Crawford, J. D. (2012). Hand-related rather than goal-related source of gaze-dependent errors in memory-guided reachingOrigins of gaze-dependent reach errors. *Journal of vision*,*12*(11), 17-17.

Dias, E. C., & Segraves, M. A. (1999). Muscimol-induced inactivation of monkey frontal eye field: effects on visually and memory-guided saccades. *Journal of Neurophysiology*, *81*(5), 2191-2214.

Dominey, P.F., Arbib, M. (1992). A cortico-subcortical model for generation of spatially accurate sequential saccades. *Cerebral Cortex, 2*, 153-175.

Donders, F. C. (1848). Beitrag zur Lehre von den Bewegungen des menschlichen Auges. *Holland Beitr Anat Physiol Wiss*, *1*(104), 384.

Duhamel, J. R., Bremmer, F., BenHamed, S., & Graf, W. (1997). Spatial invariance of visual receptive fields in parietal cortex neurons. *Nature*,*389*(6653), 845-848.

Edelman, J. A., & Goldberg, M. E. (2002). Effect of short-term saccadic adaptation on saccades evoked by electrical stimulation in the primate superior colliculus. *Journal of Neurophysiology*, *87*(4), 1915-1923.

Ekstrom, A. D., Arnold, A. E. G. F., & Iaria, G. (2014). A critical review of the allocentric spatial representation and its neural underpinnings: toward a network-based perspective. *Front. Hum. Neurosci*, *8*(803), 10-3389.

Elsley, J. K., Nagy, B., Cushing, S. L., & Corneil, B. D. (2007). Widespread presaccadic recruitment of neck muscles by stimulation of the primate frontal eye fields. *Journal of neurophysiology*, *98*(3), 1333-1354.

Everling, S., & Munoz, D. P. (2000). Neuronal correlates for preparatory set associated with pro-saccades and anti-saccades in the primate frontal eye field. *The Journal of Neuroscience*, *20*(1), 387-400.

Everling, S., Dorris, M. C., Klein, R. M., & Munoz, D. P. (1999). Role of primate

superior colliculus in preparation and execution of anti-saccades and pro-saccades. *The Journal of neuroscience*, *19*(7), 2740-2754.

Faisal, A. A., Selen, L. P., & Wolpert, D. M. (2008). Noise in the nervous system. *Nature Reviews Neuroscience*, *9*(4), 292-303.

Fang, Y., Nakashima, R., Matsumiya, K., Kuriki, I., & Shioiri, S. (2015). Eye-head coordination for visual cognitive processing. *PloS one*, *10*(3), e0121035.

Farshadmanesh, F., Klier, E. M., Chang, P., Wang, H., & Crawford, J. D. (2007). Three-dimensional eye–head coordination after injection of muscimol into the interstitial nucleus of Cajal (INC). *Journal of neurophysiology*, *97*(3), 2322-2338.

Farshadmanesh, F., Byrne, P., Keith, G. P., Wang, H., Corneil, B. D., & Crawford, J. D. (2012). Cross-validated models of the relationships between neck muscle electromyography and three-dimensional head kinematics during gaze behavior. *Journal of neurophysiology*, *107*(2), 573-590.

Felleman, D. J., & Van Essen, D. C. (1991). Distributed hierarchical processing in the primate cerebral cortex. *Cerebral cortex*, *1*(1), 1-47.

Feredoes, E., Heinen, K., Weiskopf, N., Ruff, C., & Driver, J. (2011). Causal evidence for frontal involvement in memory target maintenance by posterior brain areas during distracter interference of visual working memory.*Proceedings of the National Academy of Sciences*, *108*(42), 17510-17515.

Fernandes, H. L., Stevenson, I. H., Phillips, A. N., Segraves, M. A., & Kording, K. P. (2014). Saliency and saccade encoding in the frontal eye field during natural scene search. *Cerebral Cortex*, *24*(12), 3232-3245.

Fernandez-Ruiz J, Goltz HC, DeSouza JF, Vilis T, Crawford JD. (2007). Human

parietal “reach region” primarily encodes intrinsic visual direction, not extrinsic movement direction, in a visual-motor dissociation task. *Cereb Cortex*. 17:2283-2292.

Ferraina, S., Paré, M., & Wurtz, R. H. (2002). Comparison of cortico-cortical and cortico-collicular signals for the generation of saccadic eye movements.*Journal of Neurophysiology*, *87*(2), 845-858.

Ferrier, D. (1876). The functions of the brain. London: Dawsons of Pall Mall. p229.

Flanders, M., Tillery, S. I. H., & Soechting, J. F. (1992). Early stages in a sensorimotor transformation. *Behavioral and Brain Sciences*, *15*(02), 309-320.

Fogassi, L., Gallese, V., Di Pellegrino, G., Fadiga, L., Gentilucci, M., Luppino, G., Matelli, M., Pedotti, A., & Rizzolatti, G. (1992). Space coding by premotor cortex. *Experimental Brain Research*, *89*(3), 686-690.

Freedman, E. G. (2008). Coordination of the eyes and head during visual orienting. *Experimental brain research*, *190*(4), 369-387.

Freedman, E. G., & Sparks, D. L. (1997). Activity of cells in the deeper layers of the superior colliculus of the rhesus monkey: evidence for a gaze displacement command. *Journal of neurophysiology*, *78*(3), 1669-1690.

Freedman, E. G., & Sparks, D. L. (1997). Eye-head coordination during head-unrestrained gaze shifts in rhesus monkeys. *Journal of neurophysiology*, *77*(5), 2328-2348.

Frens, M. A., & Van Opstal, A. J. (1997). Monkey superior colliculus activity during

short-term saccadic adaptation. *Brain research bulletin*, *43*(5), 473-483.

Fries, W. (1984). Cortical projections to the superior colliculus in the macaque monkey: a retrograde study using horseradish peroxidase. *Journal of Comparative Neurology*, *230*(1), 55-76.

Fuchs, A. F., & Luschei, E. S. (1971). The activity of single trochlear nerve fibers during eye movements in the alert monkey. *Experimental brain research*, *13*(1), 78-89.

Funahashi S, Chafee MV, Goldman-Rakic PS. (1993). Prefrontal neuronal activity in rhesus monkeys performing delayed anti-saccade task. Nature 365:753-756.

Funahashi S. (2013). Space representation in the prefrontal cortex. Prog Neurobiol. 103:131-155.

Funahashi, S. (2015). Functions of delay-period activity in the prefrontal cortex and mnemonic scotomas revisited. *Frontiers in systems neuroscience*,*9*.

Funahashi, S., Bruce, C. J., & Goldman-Rakic, P. S. (1989). Mnemonic coding of visual space during delayed response performance: Neuronal correlates of transient memory. *Journal of Neurophysiology*, *61*, 331-349.

Funahashi, S., Bruce, C. J., & Goldman-Rakic, P. S. (1991). Neuronal activity related to saccadic eye movements in the monkey's dorsolateral prefrontal cortex. *Journal of neurophysiology*, *65*(6), 1464-1483.

Funahashi, S., Bruce, C. J., & Goldman-Rakic, P. S. (1993). Dorsolateral prefrontal lesions and oculomotor delayed-response performance: evidence for mnemonic" scotomas". *The Journal of Neuroscience*, *13*(4), 1479-1497.

Fuster JM (2009). Cortex and memory: Emergence of a new paradigm. Journal of cognitive neuroscience 21:11 (2047-2072).

Fuster, J. M. (2000). Executive frontal functions. *Experimental brain research*, *133*(1), 66-70.

Fuster, J. M. (2001). The prefrontal cortex—an update: time is of the essence. *Neuron*, *30*(2), 319-333.

Fuster, J. M., & Alexander, G. E. (1971). Neuron activity related to short-term memory. *Science*, *173*(3997), 652-654.

Fuster, J. M., & Bressler, S. L. (2012). Cognit activation: a mechanism enabling temporal integration in working memory. *Trends in cognitive sciences*, *16*(4), 207-218.

Galletti, C., Battaglini, P. P., & Fattori, P. (1993). Parietal neurons encoding spatial locations in craniotopic coordinates. *Experimental Brain Research*,*96*(2), 221-229.

Galletti, C., Battaglini, P. P., & Fattori, P. (1995). Eye Position Influence on the Parieto-occipital Area PO (V6) of the Macaque Monkey. *European Journal of Neuroscience*, *7*(12), 2486-2501.

Gandhi, N. J., & Katnani, H. A. (2011). Motor functions of the superior colliculus. *Annual review of neuroscience*, *34*, 205.

Gaymard, B., Ploner, C. J., Rivaud-Pechoux, S., & Pierrot-Deseilligny, C. (1999). The frontal eye field is involved in spatial short-term memory but not in reflexive saccade inhibition. *Experimental Brain Research*, *129*(2), 288-301.

Glenn, B., & Vilis, T. (1992). Violations of Listing's law after large eye and head

gaze shifts. *Journal of Neurophysiology*, *68*(1), 309-318.

Gnadt, J. W., & Andersen, R. A. (1988). Memory related motor planning activity in posterior parietal cortex of macaque. *Experimental brain research*,*70*(1), 216-220.

Gnadt, J. W., Bracewell, R. M., & Andersen, R. A. (1991). Sensorimotor transformation during eye movements to remembered visual targets. *Vision research*, *31*(4), 693-715.

Gold, J. M., Murray, R. F., Sekuler, A. B., Bennett, P. J., & Sekuler, R. (2005). Visual memory decay is deterministic. *Psychological Science*, *16*(10), 769-774.

Goldberg, M. E., & Bruce, C. J. (1990). Primate frontal eye fields. III. Maintenance of a spatially accurate saccade signal. *Journal of Neurophysiology*, *64*(2), 489-508.

Goldberg, M. E., & Wurtz, R. H. (1972). Activity of superior colliculus in behaving monkey. II. Effect of attention on neuronal responses. *J Neurophysiol*,*35*, 560-574.

Goldman-Rakic, P. S. (1987). Circuitry of primate prefrontal cortex and regulation of behavior by representational memory. *Comprehensive Physiology*.

Goldman-Rakic, P. S. (1995). Cellular basis of working memory. *Neuron*,*14*(3), 477-485.

Goldman-Rakic, P. S., & Selemon, L. D. (1990). New frontiers in basal ganglia research. *Trends in neurosciences*, *13*(7), 241-244.

Goodale, M. A., & Milner, A. D. (1992). Separate visual pathways for perception and action. *Trends in neurosciences*, *15*(1), 20-25.

Gottlieb, J. P., Kusunoki, M., & Goldberg, M. E. (1998). The representation of

visual salience in monkey parietal cortex. *Nature*, *391*(6666), 481-484.

Gottlieb, J., & Goldberg, M. E. (1999). Activity of neurons in the lateral intraparietal area of the monkey during an antisaccade task. *Nature neuroscience*, *2*(10), 906-912.

Grunewald, A., Linden, J. F., & Andersen, R. A. (1999). Responses to auditory stimuli in macaque lateral intraparietal area I. Effects of training.*Journal of neurophysiology*, *82*(1), 330-342.

Guitton, D. (1992). Control of eye—head coordination during orienting gaze shifts. *Trends in neurosciences*, *15*(5), 174-179.

Guitton, D., & Mandl, G. (1978). Frontal 'oculomotor'area in alert cat. I. Eye movements and neck activity evoked by stimulation. *Brain research*, *149*(2), 295-312.

Guitton, D., & Mandl, G. (1980). Oblique saccades of the cat: a comparison between the durations of horizontal and vertical components. *Vision research*, *20*(10), 875-881.

Guitton, D., & Volle, M. (1987). Gaze control in humans: eye-head coordination during orienting movements to targets within and beyond the oculomotor range. *Journal of neurophysiology*, *58*(3), 427-459.

Guitton, D., Buchtel, H. A., & Douglas, R. M. (1985). Frontal lobe lesions in man cause difficulties in suppressing reflexive glances and in generating goal-directed saccades. *Experimental Brain Research*, *58*(3), 455-472.

Hanes, D. P., & Schall, J. D. (1996). Neural control of voluntary movement initiation. *Science*, *274*(5286), 427-430.

Hanes, D. P., & Wurtz, R. H. (2001). Interaction of the frontal eye field and superior colliculus for saccade generation. *Journal of Neurophysiology*, *85*(2), 804-815.

Harris, L. R. (1980). The superior colliculus and movements of the head and eyes in cats. *The Journal of physiology*, *300*, 367.

Hawkins, K. M., Sayegh, P., Yan, X., Crawford, J. D., & Sergio, L. E. (2013). Neural activity in superior parietal cortex during rule-based visual-motor transformations. *Journal of cognitive neuroscience*, *25*(3), 436-454.

Heinzle, J., Hepp, K., & Martin, K. A. (2007). A microcircuit model of the frontal eye fields. *The Journal of Neuroscience*, *27*(35), 9341-9353.

Henriques, D. Y., Klier, E. M., Smith, M. A., Lowy, D., & Crawford, J. D. (1998). Gaze-centered remapping of remembered visual space in an open-loop pointing task. *The Journal of Neuroscience*, *18*(4), 1583-1594.

Hubel, D. H., & Wiesel, T. N. (1959). Receptive fields of single neurones in the cat's striate cortex. *The Journal of physiology*, *148*(3), 574-591.

Hutton, S. B. (2008). Cognitive control of saccadic eye movements. *Brain and cognition*, *68*(3), 327-340.

Ikkai, A., & Curtis, C. E. (2011). Common neural mechanisms supporting spatial working memory, attention and motor intention. *Neuropsychologia*,*49*(6), 1428-1434.

Irwin, D. E. (1992). Memory for position and identity across eye movements.*Journal of Experimental Psychology: Learning, Memory, and*

Cognition,*18*(2), 307.

Isa, T., & Kobayashi, Y. (2004). Switching between cortical and subcortical sensorimotor pathways. *Progress in brain research*, *143*, 299-305.

Isa, T., & Sasaki, S. (2002). Brainstem control of head movements during orienting; organization of the premotor circuits. *Progress in neurobiology*,*66*(4), 205-241.

Isoda, M., & Tanji, J. (2002). Cellular activity in the supplementary eye field during sequential performance of multiple saccades. *Journal of neurophysiology*, *88*(6), 3541-3545.

Jay, M. F., & Sparks, D. L. (1984). Auditory receptive fields in primate superior colliculus shift with changes in eye position.

Jazayeri, M., & Shadlen, M. N. (2015). A neural mechanism for sensing and reproducing a time interval. *Current Biology*, *25*(20), 2599-2609.

Johnston, K., DeSouza, J. F., & Everling, S. (2009). Monkey prefrontal cortical pyramidal and putative interneurons exhibit differential patterns of activity between prosaccade and antisaccade tasks. *The Journal of Neuroscience*, *29*(17), 5516-5524.

Kakei, S., Hoffman, D. S., & Strick, P. L. (2003). Sensorimotor transformations in cortical motor areas. *Neuroscience research*, *46*(1), 1-10.

Kayser, C., Körding, K. P., & König, P. (2004). Processing of complex stimuli and natural scenes in the visual cortex. *Current opinion in neurobiology*,*14*(4), 468-473.

Keith, G. P., DeSouza, J. F., Yan, X., Wang, H., & Crawford, J. D. (2009). A

method for mapping response fields and determining intrinsic reference frames of single-unit activity: Applied to 3D head-unrestrained gaze shifts.*Journal of neuroscience methods*, *180*(1), 171-184.

Ketcham, C. J., Hodgson, T. L., Kennard, C., & Stelmach, G. E. (2003). Memory-motor transformations are impaired in Parkinson's disease.*Experimental brain research*, *149*(1), 30-39.

Khan, A. Z., Pisella, L., Vighetto, A., Cotton, F., Luaute, J., Boisson, D., Salemme, R., Crawford, J.D., Rossetti, Y. (2005). Optic ataxia errors depend on remapped, not viewed, target location. *Nature neuroscience*, *8*(4), 418-420.

King, W. M., Fuchs, A. F., & Magnin, M. (1981). Vertical eye movement-related responses of neurons in midbrain near intestinal nucleus of Cajal.*Journal of Neurophysiology*, *46*(3), 549-562.

Klier, E. M., Martinez-Trujillo, J. C., Medendorp, W. P., Smith, M. A., & Crawford, J. D. (2003). Neural control of 3-D gaze shifts in the primate.*Progress in brain research*, *142*, 109-124.

Klier, E. M., Wang, H., & Crawford, J. D. (2001). The superior colliculus encodes gaze commands in retinal coordinates. *Nature neuroscience*, *4*(6), 627-632.

Klier, E. M., Wang, H., & Crawford, J. D. (2002). Neural Mechanisms of Three-Dimensional Eye and Head Movements. *Annals of the New York Academy of Sciences*, *956*(1), 512-514.

Klier, E. M., Wang, H., & Crawford, J. D. (2003). Three-dimensional eye-head coordination is implemented downstream from the superior colliculus. *Journal of Neurophysiology*, *89*(5), 2839-2853.

Klier, E. M., Wang, H., & Crawford, J. D. (2007). Interstitial nucleus of Cajal encodes three-dimensional head orientations in Fick-like coordinates. *Journal of neurophysiology*, *97*(1), 604-617.

Knight, T. A. (2012). Contribution of the frontal eye field to gaze shifts in the head-unrestrained rhesus monkey: neuronal activity. *Neuroscience*, *225*, 213-236.

Knight, T. A., & Fuchs, A. F. (2007). Contribution of the frontal eye field to gaze shifts in the head-unrestrained monkey: effects of microstimulation.*Journal of neurophysiology*, *97*(1), 618-634.

Koval, M. J., Lomber, S. G., & Everling, S. (2011). Prefrontal cortex deactivation in macaques alters activity in the superior colliculus and impairs voluntary control of saccades. *The Journal of Neuroscience*, *31*(23), 8659-8668.

Krappmann, P. (1998). Accuracy of visually and memory-guided antisaccades in man. *Vision research*, *38*(19), 2979-2985.

Künzle, H., Akert, K., & Wurtz, R. H. (1976). Projection of area 8 (frontal eye field) to superior colliculus in the monkey. An autoradiographic study. *Brain research*, *117*(3), 487-492.

Lappe, M. (2001). Information transfer between sensory and motor networks.*Handbook of bilogical physics*, *4*.

Lara, A. H., & Wallis, J. D. (2015). The role of prefrontal cortex in working memory: a mini review. *Frontiers in systems neuroscience*, *9*.

Lawrence, B. M., White, R. L., & Snyder, L. H. (2005). Delay-period activity in visual, visuomovement, and movement neurons in the frontal eye field.*Journal of neurophysiology*, *94*(2), 1498-1508.

Lebedev, M. A., Messinger, A., Kralik, J. D., & Wise, S. P. (2004). Representation of attended versus remembered locations in prefrontal cortex. *PLoS Biol*, *2*(11), e365.

Lee, J., & Groh, J. M. (2012). Auditory signals evolve from hybrid-to eye-centered coordinates in the primate superior colliculus. *Journal of neurophysiology*, *108*(1), 227-242.

Lee, J., & Groh, J. M. (2014). Different stimuli, different spatial codes: a visual map and an auditory rate code for oculomotor space in the primate superior colliculus. *PloS one*, *9*(1), e85017.

Leon, M.I. and Shadlen, M.N. (2003) Representation of time by neurons in the posterior parietal cortex of the macaque. Neuron, 38: 317–327.

Lerner, Y., Hendler, T., Ben-Bashat, D., Harel, M., & Malach, R. (2001). A hierarchical axis of object processing stages in the human visual cortex.*Cerebral Cortex*, *11*(4), 287-297.

Levin, S. (1984). Frontal lobe dysfunctions in schizophrenia—II. Impairments of psychological and brain functions. *Journal of psychiatric research*, *18*(1), 57-72.

Levy, R., Friedman, H. R., Davachi, L., & Goldman-Rakic, P. S. (1997). Differential activation of the caudate nucleus in primates performing spatial and nonspatial working memory tasks. *The Journal of neuroscience*, *17*(10), 3870-3882.

Liebe, S., Hoerzer, G. M., Logothetis, N. K., & Rainer, G. (2012). Theta coupling between V4 and prefrontal cortex predicts visual short-term memory performance. *Nature neuroscience*, *15*(3), 456-462.

Lim, S., & Goldman, M. S. (2013). Balanced cortical microcircuitry for maintaining information in working memory. *Nature neuroscience*, *16*(9), 1306-1314.

Linden, D. E. (2007). The working memory networks of the human brain. *The Neuroscientist*, *13*(3), 257-267.

Logie, R. H. (2014). *Visuo-spatial working memory*. Psychology Press.

Longtang Chen, L., & Tehovnik, E. J. (2007). REVIEW ARTICLE: Cortical control of eye and head movements: integration of movements and percepts.*European Journal of Neuroscience*, *25*(5), 1253-1264.

Lu, X., Matsuzawa, M., & Hikosaka, O. (2002). A neural correlate of oculomotor sequences in supplementary eye field. *Neuron*, *34*(2), 317-325.

Lynch, J. C., Hoover, J. E., & Strick, P. L. (1994). Input to the primate frontal eye field from the substantia nigra, superior colliculus, and dentate nucleus demonstrated by transneuronal transport. *Experimental Brain Research*,*100*(1), 181-186.

Ma, W. J., Husain, M., & Bays, P. M. (2014). Changing concepts of working memory. *Nature neuroscience*, *17*(3), 347-356.

Maier, J. X., & Groh, J. M. (2009). Multisensory guidance of orienting behavior. *Hearing research*, *258*(1), 106-112.

Mars, R. B., Coles, M. G., Hulstijn, W., & Toni, I. (2008). Delay-related cerebral activity and motor preparation. *Cortex*, *44*(5), 507-520.

Markowitz, D. A., Curtis, C. E., & Pesaran, B. (2015). Multiple component networks support working memory in prefrontal cortex. *Proceedings of the National*

Academy of Sciences, *112*(35), 11084-11089.

Markowitz, D. A., Curtis, C. E., & Pesaran, B. (2015). Multiple component networks support working memory in prefrontal cortex. *Proceedings of the National Academy of Sciences*, *112*(35), 11084-11089.

Martinez-Trujillo, J. C., Klier, E. M., Wang, H., & Crawford, J. D. (2003). Contribution of head movement to gaze command coding in monkey frontal cortex and superior colliculus. *Journal of neurophysiology*, *90*(4), 2770-2776.

Martinez-Trujillo, J. C., Medendorp, W. P., Wang, H., & Crawford, J. D. (2004). Frames of reference for eye-head gaze commands in primate supplementary eye fields. *Neuron*, *44*(6), 1057-1066.

Martinez-Trujillo, J. C., Wang, H., & Crawford, J. D. (2003). Electrical stimulation of the supplementary eye fields in the head-free macaque evokes kinematically normal gaze shifts. *Journal of neurophysiology*, *89*(6), 2961-2974.

Matthews, A., Flohr, H., & Everling, S. (2002). Cortical activation associated with midtrial change of instruction in a saccade task. *Experimental brain research*, *143*(4), 488-498.

Mays, L. E., & Sparks, D. L. (1980). Dissociation of visual and saccade-related responses in superior colliculus neurons. *Journal of Neurophysiology*,*43*(1), 207-232.

Mazhari, S., Badcock, J. C., Waters, F. A., Dragović, M., Badcock, D. R., & Jablensky, A. (2010). Impaired spatial working memory maintenance in schizophrenia involves both spatial coordinates and spatial reference frames. *Psychiatry research*, *179*(3), 253-258.

Mazzoni, P., Bracewell, R. M., Barash, S., & Andersen, R. A. (1996). Motor intention activity in the macaque's lateral intraparietal area. I. Dissociation of motor plan from sensory memory. *Journal of Neurophysiology*, *76*(3), 1439-1456.

McKee, J. L., Riesenhuber, M., Miller, E. K., & Freedman, D. J. (2014). Task dependence of visual and category representations in prefrontal and inferior temporal cortices. *The Journal of Neuroscience*, *34*(48), 16065-16075.

Medendorp, W. P. (2011). Spatial constancy mechanisms in motor control. *Philosophical Transactions of the Royal Society of London B: Biological Sciences*, *366*(1564), 476-491.

Medendorp, W. P., Goltz, H. C., & Vilis, T. (2005). Remapping the remembered target location for anti-saccades in human posterior parietal cortex. *Journal of Neurophysiology*, *94*(1), 734-740.

Medendorp, W. P., Goltz, H. C., Vilis, T., & Crawford, J. D. (2003). Gaze-centered updating of visual space in human parietal cortex. *The Journal of neuroscience*, *23*(15), 6209-6214.

Meredith, M. A., & Stein, B. E. (1986). Visual, auditory, and somatosensory convergence on cells in superior colliculus results in multisensory integration.*Journal of neurophysiology*, *56*(3), 640-662.

Miles, F. A., & Wallmann, J. (1993). Prefrontal neuronal activity in rhesus monkeys performing a delayed anti-saccade task. *Nature*, *365*, 753-756.

Miller, G. A. (1956). The magical number seven, plus or minus two: some limits on our capacity for processing information. *Psychological review*, *63*(2), 81.

Miller, G. A., Galanter, E., & Pribram, K. H. (1960). Plans and the structure of

behavior.

Minshew, N. J., Luna, B., & Sweeney, J. A. (1999). Oculomotor evidence for neocortical systems but not cerebellar dysfunction in autism. *Neurology*,*52*(5), 917-917.

Mohler, C. W., Goldberg, M. E., & Wurtz, R. H. (1973). Visual receptive fields of frontal eye field neurons. *Brain research*, *61*, 385-389.

Monteon JA, Avillac M, Yan X, Wang H, Crawford JD. (2012). Neural mechanisms for predictive head movement strategies during sequential gaze shifts. The Journal of Neurophysiology,108(10), 2689-707. doi: 10.1152/jn.00222.2012.

Monteon, J. A., Constantin, A. G., Wang, H., Martinez-Trujillo, J., & Crawford, J. D. (2010). Electrical stimulation of the frontal eye fields in the head-free macaque evokes kinematically normal 3D gaze shifts. *Journal of neurophysiology*, *104*(6), 3462-3475.

Monteon, J. A., Wang, H., Martinez-Trujillo, J., & Crawford, J. D. (2013). Frames of reference for eye–head gaze shifts evoked during frontal eye field stimulation. *European Journal of Neuroscience*, *37*(11), 1754-1765.

Moore, T., & Armstrong, K. M. (2003). Selective gating of visual signals by microstimulation of frontal cortex. *Nature*, *421*(6921), 370-373.

Moore, T., & Fallah, M. (2004). Microstimulation of the frontal eye field and its effects on covert spatial attention. *Journal of neurophysiology*, *91*(1), 152-162.

Mountcastle, V. B., Lynch, J. C., Georgopoulos, A., Sakata, H., & Acuna, C. (1975). Posterior parietal association cortex of the monkey: command functions for operations within extrapersonal space. *Journal of neurophysiology*, *38*(4), 871-908.

Mullette-Gillman, O.A.,, Cohen, Y. E., & Groh, J. M. (2005). Eye-centered, head-centered, and complex coding of visual and auditory targets in the intraparietal sulcus. *Journal of neurophysiology*, *94*(4), 2331-2352.

Munoz, D. P., & Everling, S. (2004). Look away: the anti-saccade task and the voluntary control of eye movement. *Nature Reviews Neuroscience*, *5*(3), 218-228.

Munoz, D. P., & Wurtz, R. H. (1993). Fixation cells in monkey superior colliculus. I. Characteristics of cell discharge. *Journal of neurophysiology*,*70*(2), 559-575.

Munoz, D. P., & Wurtz, R. H. (1995). Saccade-related activity in monkey superior colliculus. I. Characteristics of burst and buildup cells. *Journal of Neurophysiology*, *73*(6), 2313-2333.

Munoz, D. P., Dorris, M. C., Pare, M., & Everling, S. (2000). On your mark, get set: brainstem circuitry underlying saccadic initiation. *Canadian journal of physiology and pharmacology*, *78*(11), 934-944.

Munoz, D.P., Schall, J.D. (2004). Concurrent, distributed control of saccade initiation in the frontal eye field and superior colliculus. In: Hall WC and Moschovakis A, editor. The Superior Colliculus: New Approaches for Studying Sensorimotor Integration. Boca Taron (FL): CRC Press. p55-82.

Niki, H., & Watanabe, M. (1976). Prefrontal unit activity and delayed response: relation to cue location versus direction of response. *Brain research*, *105*(1), 79-88.

Ninomiya, T., Sawamura, H., Inoue, K. I., & Takada, M. (2012). Segregated pathways carrying frontally derived top-down signals to visual areas MT and V4 in macaques. *The Journal of Neuroscience*, *32*(20), 6851-6858.

O'Dhaniel, A., Cohen, Y. E., & Groh, J. M. (2009). Motor-related signals in the intraparietal cortex encode locations in a hybrid, rather than eye-centered reference frame. *Cerebral Cortex*, *19*(8), 1761-1775.

Offen, S., Gardner, J. L., Schluppeck, D., & Heeger, D. J. (2010). Differential roles for frontal eye fields (FEFs) and intraparietal sulcus (IPS) in visual working memory and visual attention. *Journal of vision*, *10*(11), 28-28.

Okamoto, H., Isomura, Y., Takada, M., & Fukai, T. (2007). Temporal integration by stochastic recurrent network dynamics with bimodal neurons.*Journal of Neurophysiology*, *97*(6), 3859-3867.

Olson, C. R., & Gettner, S. N. (1995). Object-centered direction selectivity in the macaque supplementary eye field. *Science*, *269*(5226), 985-988.

Opris I, Barborica A, Ferrera VP (2003) Comparison of performance on memory-guided saccade and delayed spatial match-to-sample tasks in monkeys. Vision Research 43:321-332.

Optican, L. M., & Robinson, D. A. (1980). Cerebellar-dependent adaptive control of primate saccadic system. *Journal of Neurophysiology*, *44*(6), 1058-1076.

O'Reilly, R. C. (2006). Biologically based computational models of high-level cognition. *science*, *314*(5796), 91-94.

O'Reilly, R. C., & Frank, M. J. (2006). Making working memory work: a computational model of learning in the prefrontal cortex and basal ganglia.*Neural computation*, *18*(2), 283-328.

O'Sullivan, E. P., Jenkins, I. H., Henderson, L., Kennard, C., & Brooks, D. J. (1995). The functional anatomy of remembered saccades: a PET

study.*Neuroreport*, *6*(16), 2141-2144.

Oyachi, H., & Ohtsuka, K. (1995). Transcranial magnetic stimulation of the posterior parietal cortex degrades accuracy of memory-guided saccades in humans. *Investigative ophthalmology & visual science*, *36*(7), 1441-1449.

Paré, M., & Guitton, D. (1990). Gaze-related activity of brainstem omnipause neurons during combined eye-head gaze shifts in the alert cat. *Experimental brain research*, *83*(1), 210-214.

Paré, M., & Guitton, D. (1998). Brain stem omnipause neurons and the control of combinedeye-head gaze saccades in the alert cat. *Journal of Neurophysiology*, *79*(6), 3060-3076.

Paré, M., & Hanes, D. P. (2003). Controlled movement processing: superior colliculus activity associated with countermanded saccades. *The Journal of Neuroscience*, *23*(16), 6480-6489.

Paré, M., & Wurtz, R. H. (1997). Monkey posterior parietal cortex neurons antidromically activated from superior colliculus. *Journal of Neurophysiology*,*78*(6), 3493-3497.

Paré, M., & Wurtz, R. H. (2001). Progression in neuronal processing for saccadic eye movements from parietal cortex area lip to superior colliculus.*Journal of Neurophysiology*, *85*(6), 2545-2562.

Paré, M., Crommelinck, M., & Guitton, D. (1994). Gaze shifts evoked by stimulation of the superior colliculus in the head-free cat conform to the motor map but also depend on stimulus strength and fixation activity. *Experimental brain research*, *101*(1), 123-139.

Pasternak, T., & Greenlee, M. W. (2005). Working memory in primate sensory systems. *Nature Reviews Neuroscience*, *6*(2), 97-107.

Pesaran, B., Nelson, M. J., & Andersen, R. A. (2006). Dorsal premotor neurons encode the relative position of the hand, eye, and goal during reach planning. *Neuron*, *51*(1), 125-134.

Pesaran, B., Nelson, M. J., & Andersen, R. A. (2010). A relative position code for saccades in dorsal premotor cortex. *The Journal of Neuroscience*,*30*(19), 6527-6537.

Pierrot-Deseilligny, C., Rivaud, S., Gaymard, B., & Agid, Y. (1991). Cortical control of memory-guided saccades in man. *Experimental Brain Research*,*83*(3), 607-617.

Platt, M. L., & Glimcher, P. W. (1998). Response fields of intraparietal neurons quantified with multiple saccadic targets. *Experimental Brain Research*, *121*(1), 65-75.

Platt, M. L., & Glimcher, P. W. (1999). Neural correlates of decision variables in parietal cortex. *Nature*, *400*(6741), 233-238.

Ploner, C. J., Rivaud-Péchoux, S., Gaymard, B. M., Agid, Y., & Pierrot-Deseilligny, C. (1999). Errors of memory-guided saccades in humans with lesions of the frontal eye field and the dorsolateral prefrontal cortex. *Journal of neurophysiology*, *82*(2), 1086-1090.

Postle, B. R. (2005). Delay-period activity in the prefrontal cortex: one function is sensory gating. *Cognitive Neuroscience, Journal of*, *17*(11), 1679-1690.

Postle, B. R. (2006). Working memory as an emergent property of the mind and brain. *Neuroscience*, *139*(1), 23-38.

Postle, B. R., & D'Esposito, M. (2003). Spatial working memory activity of the caudate nucleus is sensitive to frame of reference. *Cognitive, Affective, & Behavioral Neuroscience*, *3*(2), 133-144.

Pouget, A., & Sejnowski, T. J. (1997). Spatial transformations in the parietal cortex using basis functions. *Cognitive Neuroscience, Journal of*, *9*(2), 222-237.

Pouget, A., & Snyder, L. H. (2000). Computational approaches to sensorimotor transformations. *Nature neuroscience*, *3*, 1192-1198.

Purcell, B. A., Weigand, P. K., & Schall, J. D. (2012). Supplementary eye field during visual search: salience, cognitive control, and performance monitoring. *The Journal of Neuroscience*, *32*(30), 10273-10285.

Quaia, C., Lefèvre, P., & Optican, L. M. (1999). Model of the control of saccades by superior colliculus and cerebellum. *Journal of Neurophysiology*,*82*(2), 999-1018.

Quiroga, R. Q., & Panzeri, S. (2009). Extracting information from neuronal populations: information theory and decoding approaches. *Nature Reviews Neuroscience*, *10*(3), 173-185.

Quiroga, R. Q., Snyder, L. H., Batista, A. P., Cui, H., & Andersen, R. A. (2006). Movement intention is better predicted than attention in the posterior parietal cortex. *The Journal of neuroscience*, *26*(13), 3615-3620.

Radau, P., Tweed, D., & Vilis, T. (1994). Three-dimensional eye, head, and chest orientations after large gaze shifts and the underlying neural strategies.*Journal of Neurophysiology*, *72*(6), 2840-2852.

Rainer, G., Rao, S. C., & Miller, E. K. (1999). Prospective coding for objects in primate prefrontal cortex. *The Journal of Neuroscience*, *19*(13), 5493-5505.

Ray, S., Pouget, P., & Schall, J. D. (2009). Functional distinction between visuomovement and movement neurons in macaque frontal eye field during saccade countermanding. *Journal of neurophysiology*, *102*(6), 3091-3100.

Reinhart, R. M., Heitz, R. P., Purcell, B. A., Weigand, P. K., Schall, J. D., & Woodman, G. F. (2012). Homologous mechanisms of visuospatial working memory maintenance in macaque and human: properties and sources. *The Journal of Neuroscience*, *32*(22), 7711-7722.

Rizzolatti, G., Riggio, L., Dascola, I., & Umiltá, C. (1987). Reorienting attention across the horizontal and vertical meridians: evidence in favor of a premotor theory of attention. *Neuropsychologia*, *25*(1), 31-40.

Robinson, D. A. (1972). Eye movements evoked by collicular stimulation in the alert monkey. *Vision Research, 12(11)*, 1795-1808.

Robinson, D. A. (1978) The purpose of eye movements. Invest Ophtalmol Vis Sci 17:835-837.

Robinson, D. A. (1964). The mechanics of human saccadic eye movement. *The Journal of physiology*, *174*(2), 245.

Robinson, D. A., & Fuchs, A. F. (1969). Eye movements evoked by stimulation of frontal eye fields. *Journal of Neurophysiology*.

Romo, R., Brody, C. D., Hernández, A., & Lemus, L. (1999). Neuronal correlates of parametric working memory in the prefrontal cortex. *Nature*,*399*(6735), 470-473.

Rottschy, C., Kleiman, A., Dogan, I., Langner, R., Mirzazade, S., Kronenbuerger, M., Werner, C., Shah, N. J., Schulz, J. B., Eickhoff, S. B., & Reetz, K. (2013). Diminished activation of motor working-memory networks in Parkinson's disease. *PloS one*, *8*(4), e61786.

Russo, G. S., & Bruce, C. J. (1994). Frontal eye field activity preceding aurally guided saccades. *Journal of neurophysiology*, *71*(3), 1250-1253.

Russo, G. S., & Bruce, C. J. (1996). Neurons in the supplementary eye field of rhesus monkeys code visual targets and saccadic eye movements in an oculocentric coordinate system. *Journal of Neurophysiology*, *76*(2), 825-848.

Russo, G. S., & Bruce, C. J. (2000). Supplementary eye field: representation of saccades and relationship between neural response fields and elicited eye movements. *Journal of neurophysiology*, *84*(5), 2605-2621.

Sadeh, M., Sajad, A., Wang, H., Yan, X., & Crawford, J. D. (2015). Spatial transformations between superior colliculus visual and motor response fields during head-unrestrained gaze shifts. *European Journal of Neuroscience*,*42*(11), 2934-2951.

Sajad, A., Sadeh, M., Yan, X., Wang, H., & Crawford, J.D. (2016). Transition from target to gaze coding in primate frontal eye field during memory-delay and memory-motor transformation. *eNeuro.* **DOI:** 10.1523/ENEURO.0040-16.2016

Sajad, A., Sadeh, M., Keith, G.P., Yan, X., Wang, H., & Crawford, J.D. (2015). Visual–motor transformations within frontal eye fields during head-unrestrained gaze shifts in the monkey. *Cerebal Cortex 25*, 3932-3952.

Salazar, R. F., Dotson, N. M., Bressler, S. L., & Gray, C. M. (2012). Content-

specific fronto-parietal synchronization during visual working memory.*Science*, *338*(6110), 1097-1100.

Sato, T. R., & Schall, J. D. (2003). Effects of stimulus-response compatibility on neural selection in frontal eye field. *Neuron*, *38*(4), 637-648.

Schall, J.D. (2013). Microcircuits: decision networks. *Current Opinion in Neurobiology, 23*,269-74.

Schall, J. D. (2015). Visuomotor Functions in the Frontal Lobe. *Annual Review of Vision Science*, *1*, 469-498.

Schall, J. D., & Hanes, D. P. (1993). Neural basis of saccade target selection in frontal eye field during visual search. *Nature*, *366*(6454), 467-469.

Schall, J. D., Morel, A., & Kaas, J. H. (1993). Topography of supplementary eye field afferents to frontal eye field in macaque: implications for mapping between saccade coordinate systems. *Visual neuroscience*, *10*(02), 385-393.

Schall, J. D., Morel, A., King, D. J., & Bullier, J. (1995). Topography of visual cortex connections with frontal eye field in macaque: convergence and segregation of processing streams. *The Journal of neuroscience*, *15*(6), 4464-4487.

Schall, J. D., Purcell, B. A., Heitz, R. P., Logan, G. D., & Palmeri, T. J. (2011). Neural mechanisms of saccade target selection: gated accumulator model of the visual–motor cascade. *European Journal of Neuroscience*, *33*(11), 1991-2002.

Schiller, P. H., & Stryker, M. (1972). Single-unit recording and stimulation in superior colliculus of the alert rhesus monkey. *Journal of Neurophysiology*,*35*(6), 915-924.

Schiller, P. H., True, S. D., & Conway, J. L. (1979). Effects of frontal eye field and superior colliculus ablations on eye movements. *Science*, *206*(4418), 590-592.

Schlag, J., & Schlag-Rey, M. (1987). Evidence for a supplementary eye field. *Journal of Neurophysiology*, *57*(1), 179-200.

Schlag-Rey, M., Schlag, J., & Dassonville, P. (1992). How the frontal eye field can impose a saccade goal on superior colliculus neurons. *Journal of Neurophysiology*, *67*(4), 1003-1005.

Schmolesky, M. T., Wang, Y., Hanes, D. P., Thompson, K. G., Leutgeb, S., Schall, J. D., & Leventhal, A. G. (1998). Signal timing across the macaque visual system. *Journal of neurophysiology*, *79*(6), 3272-3278.

Scudder, C. A., Kaneko, C. R., & Fuchs, A. F. (2002). The brainstem burst generator for saccadic eye movements. *Experimental Brain Research*,*142*(4), 439-462.

Segraves, M. A. (1992). Activity of monkey frontal eye field neurons projecting to oculomotor regions of the pons. *Journal of Neurophysiology*,*68*(6), 1967-1985.

Segraves, M.A., Park, K. (1993). The relationship of monkey frontal eye field activity to saccade dynamics. *Journal of Neurophysiology*, *69*(6), 1880-1889.

Shenoy, K. V., Sahani, M., & Churchland, M. M. (2013). Cortical control of arm movements: a dynamical systems perspective. *Neuroscience*, *36*(1), 337.

Simon, S. R., Meunier, M., Piettre, L., Berardi, A. M., Segebarth, C. M., & Boussaoud, D. (2002). Spatial attention and memory versus motor preparation: premotor cortex involvement as revealed by fMRI. *Journal of neurophysiology*, *88*(4), 2047-2057.

Smith, D. T., & Schenk, T. (2012). The premotor theory of attention: time to move on?. *Neuropsychologia*, *50*(6), 1104-1114.

Smith, M. A., & Crawford, J. D. (2005). Distributed population mechanism for the 3-D oculomotor reference frame transformation. *Journal of neurophysiology*, *93*(3), 1742-1761.

Snyder, L.H. (2000). Coordinate transformations for eye and arm movements in the brain. *Current Opinion in Neurobiology, 10*,747-754.

Snyder, L. H. (2005). Frame-Up. Focus on “Eye-Centered, Head-Centered, and Complex Coding of Visual and Auditory Targets in the Intraparietal Sulcus”. *Journal of neurophysiology*, *94*(4), 2259-2260.

Snyder, L. H., Grieve, K. L., Brotchie, P., & Andersen, R. A. (1998). Separate body-and world-referenced representations of visual space in parietal cortex.*Nature*, *394*(6696), 887-891.

Soechting, J. F., & Flanders, M. (1992). Moving in three-dimensional space: frames of reference, vectors, and coordinate systems. *Annual review of neuroscience*, *15*(1), 167-191.

Sommer, M. A., & Wurtz, R. H. (2000). Composition and topographic organization of signals sent from the frontal eye field to the superior colliculus. *Journal of Neurophysiology*, *83*(4), 1979-2001.

Sommer, M. A., & Wurtz, R. H. (2001). Frontal eye field sends delay activity related to movement, memory, and vision to the superior colliculus. *Journal of Neurophysiology*, *85*(4), 1673-1685.

Sommer, M. A., & Wurtz, R. H. (2004). What the brain stem tells the frontal cortex. I. Oculomotor signals sent from superior colliculus to frontal eye field via mediodorsal thalamus. *Journal of neurophysiology*, *91*(3), 1381-1402.

Sparks, D. L. (1986). Translation of sensory signals into commands for control of saccadic eye movements: role of primate superior colliculus. *Physiological Reviews*, *66*(1), 118-171.

Sparks, D. L. (2002). The brainstem control of saccadic eye movements. *Nature Reviews Neuroscience*, *3*(12), 952-964.

Sparks, D. L., & Mays, L. E. (1980). Movement fields of saccade-related burst neurons in the monkey superior colliculus. *Brain research*, *190*(1), 39-50.

Sparks, D. L., & Porter, J. D. (1983). Spatial localization of saccade targets. II. Activity of superior colliculus neurons preceding compensatory saccades. *Journal of Neurophysiology*, *49*(1), 64-74.

Sparks, D. L., & Travis, R. P. (1971). Firing patterns of reticular formation neurons during horizontal eye movements. *Brain Research*, *33*(2), 477-481.

Sparks, D. L., Holland, R., & Guthrie, B. L. (1976). Size and distribution of movement fields in the monkey superior colliculus. *Brain research*, *113*(1), 21-34.

Sreenivasan, K. K., Curtis, C. E., & D'Esposito, M. (2014). Revisiting the role of persistent neural activity during working memory. *Trends in cognitive sciences*, *18*(2), 82-89.

Stanford, T. R., & Sparks, D. L. (1994). Systematic errors for saccades to remembered targets: evidence for a dissociation between saccade metrics and activity in the superior colliculus. *Vision research*, *34*(1), 93-106.

Stanton, G. B., Bruce, C. J., & Goldberg, M. E. (1995). Topography of projections to posterior cortical areas from the macaque frontal eye fields.*Journal of Comparative Neurology*, *353*(2), 291-305.

Stanton, G. B., Deng, S. Y., Goldberg, E. M., & McMullen, N. T. (1989). Cytoarchitectural characteristic of the frontal eye fields in macaque monkeys.*Journal of Comparative Neurology*, *282*(3), 415-427.

Stanton, G. B., Goldberg, M. E., & Bruce, C. J. (1988). Frontal eye field efferents in the macaque monkey: II. Topography of terminal fields in midbrain and pons. *Journal of Comparative Neurology*, *271*(4), 493-506.

Steenrod, S. C., Phillips, M. H., & Goldberg, M. E. (2013). The lateral intraparietal area codes the location of saccade targets and not the dimension of the saccades that will be made to acquire them. *Journal of neurophysiology*, *109*(10), 2596-2605.

Stricanne, B., Andersen, R. A., & Mazzoni, P. (1996). Eye-centered, head-centered, and intermediate coding of remembered sound locations in area LIP. *Journal of neurophysiology*, *76*(3), 2071-2076.

Stuphorn, V. (2007). New functions for an old structure: superior colliculus and head-only movements. Focus on “the role of primate superior colliculus in the control of head movements”. *Journal of neurophysiology*, *98*(4), 1847-1848.

Sugrue, L. P., Corrado, G. S., & Newsome, W. T. (2004). Matching behavior and the representation of value in the parietal cortex. *science*, *304*(5678), 1782-1787.

Suzuki, M., & Gottlieb, J. (2013). Distinct neural mechanisms of distractor suppression in the frontal and parietal lobe. *Nature neuroscience*, *16*(1), 98-104.

Sweeney, J. A., Mintun, M. A., Kwee, S., Wiseman, M. B., Brown, D. L., Rosenberg, D. R., & Carl, J. R. (1996). Positron emission tomography study of voluntary saccadic eye movements and spatial working memory. *Journal of neurophysiology*, *75*(1), 454-468.

Sweeney, J. A., Luna, B., Keedy, S. K., McDowell, J. E., & Clementz, B. A. (2007). fMRI studies of eye movement control: investigating the interaction of cognitive and sensorimotor brain systems. *Neuroimage*, *36*, T54-T60.

Sweeney, J. A., Mintun, M. A., Kwee, S., Wiseman, M. B., Brown, D. L., Rosenberg, D. R., & Carl, J. R. (1996). Positron emission tomography study of voluntary saccadic eye movements and spatial working memory. *Journal of neurophysiology*, *75*(1), 454-468.

Takaura, K., Yoshida, M., & Isa, T. (2011). Neural substrate of spatial memory in the superior colliculus after damage to the primary visual cortex. *The Journal of Neuroscience*, *31*(11), 4233-4241.

Takeda, K., & Funahashi, S. (2002). Prefrontal task-related activity representing visual cue location or saccade direction in spatial working memory tasks. *Journal of Neurophysiology*, *87*(1), 567-588.

Takeda, K., & Funahashi, S. (2004). Population vector analysis of primate prefrontal activity during spatial working memory. *Cerebral Cortex*, *14*(12), 1328-1339.

Takeda, K., & Funahashi, S. (2007). Relationship between prefrontal task-related activity and information flow during spatial working memory performance. *Cortex*, *43*(1), 38-52.

Tehovnik, E. J., Lee, K. (1993). The dorsomedial frontal cortex of the rhesus monkey: topographic representation of saccades evoked by electrical stimulation. *Experimental Brain Research, 96(3)*, 430-442.

Tehovnik, E. J., Sommer, M. A., Chou, I. H., Slocum, W. M., & Schiller, P. H. (2000). Eye fields in the frontal lobes of primates. *Brain Research Reviews*,*32*(2), 413-448.

Thompson, K. G., & Bichot, N. P. (2005). A visual salience map in the primate frontal eye field. *Progress in brain research*, *147*, 249-262.

Thompson, K. G., & Schall, J. D. (1999). The detection of visual signals by macaque frontal eye field during masking. *Nature neuroscience*, *2*(3), 283-288.

Thompson, K. G., Hanes, D. P., Bichot, N. P., & Schall, J. D. (1996). Perceptual and motor processing stages identified in the activity of macaque frontal eye field neurons during visual search. *Journal of Neurophysiology*,*76*(6), 4040-4055.

Todd, J. J., & Marois, R. (2004). Capacity limit of visual short-term memory in human posterior parietal cortex. *Nature*, *428*(6984), 751-754.

Todd, J. J., & Marois, R. (2005). Posterior parietal cortex activity predicts individual differences in visual short-term memory capacity. *Cognitive, Affective, & Behavioral Neuroscience*, *5*(2), 144-155.

Todd, J. J., Han, S. W., Harrison, S., & Marois, R. (2011). The neural correlates of visual working memory encoding: a time-resolved fMRI study. *Neuropsychologia*, *49*(6), 1527-1536.

Toni, I., Thoenissen, D., Zilles, K., & Niedeggen, M. (2002). Movement preparation and working memory: a behavioural dissociation. *Experimental brain*

research, *142*(1), 158-162.

Tsujimoto, S., & Postle, B. R. (2012). The prefrontal cortex and oculomotor delayed response: a reconsideration of the “mnemonic scotoma”. *Journal of cognitive neuroscience*, *24*(3), 627-635.

Tu, T. A., & Keating, E. G. (2000). Electrical stimulation of the frontal eye field in a monkey produces combined eye and head movements. *Journal of Neurophysiology*, *84*(2), 1103-1106.

Tweed, D. B., Haslwanter, T. P., Happe, V., & Fetter, M. (1999). Non-commutativity in the brain. *Nature*, *399*(6733), 261-263.

Tweed, D. O. U. G. L. A. S., & Vilis, T. (1987). Implications of rotational kinematics for the oculomotor system in three dimensions. *Journal of Neurophysiology*, *58*(4), 832-849.

Tweed, D., & Vilis, T. (1990). Geometric relations of eye position and velocity vectors during saccades. *Vision research*, *30*(1), 111-127.

Tweed, D., Villis, T. (1987). Implications of rotational kinematics for the oculomotor system in three dimensions. *Journal of Neurophysiology*, *58*(4), 832-849.

Van der Steen, J., Russell, I. S., & James, G. O. (1986). Effects of unilateral frontal eye-field lesions on eye-head coordination in monkey. *Journal of neurophysiology*, *55*(4), 696-714.

Van Essen, D. C., Anderson, C. H., & Felleman, D. J. (1992). Information processing in the primate visual system: an integrated systems perspective.*Science*, *255*(5043), 419-423.

Verduzco-Flores, S., Bodner, M., Ermentrout, B., Fuster, J. M., & Zhou, Y. (2009). Working memory cells' behavior may be explained by cross-regional networks with synaptic facilitation. *PloS one*, *4*(8), e6399.

Vesia, M., & Crawford, J. D. (2012). Specialization of reach function in human posterior parietal cortex. *Experimental brain research*, *221*(1), 1-18.

Vesia, M., Prime, S. L., Yan, X., Sergio, L. E., & Crawford, J. D. (2010). Specificity of human parietal saccade and reach regions during transcranial magnetic stimulation. *The Journal of Neuroscience*, *30*(39), 13053-13065.

Vilis, T., Hepp, K., Schwarz, U., & Henn, V. (1989). On the generation of vertical and torsional rapid eye movements in the monkey. *Experimental brain research*, *77*(1), 1-11.

Wager, T. D., & Yarkoni, T. (2012). establishing homology between monkey and human brains. *nature methods*, *9*(3), 237-239.

Waitzman, D. M., Ma, T. P., Optican, L. M., & Wurtz, R. H. (1991). Superior colliculus neurons mediate the dynamic characteristics of saccades. *Journal of Neurophysiology*, *66*(5), 1716-1737.

Wallace, M. T., Meredith, M. A., & Stein, B. E. (1998). Multisensory integration in the superior colliculus of the alert cat. *Journal of neurophysiology*, *80*(2), 1006-1010.

Walton, M. M., Bechara, B., & Gandhi, N. J. (2007). Role of the primate superior colliculus in the control of head movements. *Journal of neurophysiology*, *98*(4), 2022-2037.

Wang, L., Li, X., Hsiao, S. S., Lenz, F. A., Bodner, M., Zhou, Y. D., & Fuster, J. M.

(2015). Differential roles of delay-period neural activity in the monkey dorsolateral prefrontal cortex in visual–haptic crossmodal working memory.*Proceedings of the National Academy of Sciences*, *112*(2), E214-E219.

Wang, X. J., Tegnér, J., Constantinidis, C., & Goldman-Rakic, P. S. (2004). Division of labor among distinct subtypes of inhibitory neurons in a cortical microcircuit of working memory. *Proceedings of the National Academy of Sciences of the United States of America*, *101*(5), 1368-1373.

Wang, X., Zhang, M., Cohen, I. S., & Goldberg, M. E. (2007). The proprioceptive representation of eye position in monkey primary somatosensory cortex. *Nature neuroscience*, *10*(5), 640-646.

Watanabe, Y., & Funahashi, S. (2012). Thalamic mediodorsal nucleus and working memory. *Neuroscience & Biobehavioral Reviews*, *36*(1), 134-142.

Watanabe, Y., Takeda, K., & Funahashi, S. (2009). Population vector analysis of primate mediodorsal thalamic activity during oculomotor delayed-response performance. *Cerebral Cortex*, *19*(6), 1313-1321.

White, J. M., Sparks, D. L., & Stanford, T. R. (1994). Saccades to remembered target locations: an analysis of systematic and variable errors.*Vision research*, *34*(1), 79-92.

Wilson, F. A., Scalaidhe, S. P., & Goldman-Rakic, P. S. (1993). Dissociation of object and spatial processing domains in primate prefrontal cortex. *Science New York*, *260*, 1955-1955.

Wimmer, K., Nykamp, D. Q., Constantinidis, C., & Compte, A. (2014). Bump attractor dynamics in prefrontal cortex explains behavioral precision in spatial working memory. *Nature neuroscience*, *17*(3), 431-439.

Wolpert, D. M., & Ghahramani, Z. (2000). Computational principles of movement neuroscience. *nature neuroscience*, *3*, 1212-1217.

Woodman, G. F., Kang, M. S., Thompson, K., & Schall, J. D. (2008). The Effect of Visual Search Efficiency on Response Preparation Neurophysiological Evidence for Discrete Flow. *Psychological science*, *19*(2), 128-136.

Woodman, G. F., & Vogel, E. K. (2005). Fractionating working memory consolidation and maintenance are independent processes. *Psychological Science*, *16*(2), 106-113.

Wurtz, R. H., Sommer, M. A., Paré, M., & Ferraina, S. (2001). Signal transformations from cerebral cortex to superior colliculus for the generation of saccades. *Vision research*, *41*(25), 3399-3412.

Wurtz, RH. (2008). Neuronal mechanisms of visual stability. Vision Research. 48:2070–2089

Xu, B. Y., Karachi, C., & Goldberg, M. E. (2012). The postsaccadic unreliability of gain fields renders it unlikely that the motor system can use them to calculate target position in space. *Neuron*, *76*(6), 1201-1209.

Zandbelt, B., Purcell, B. A., Palmeri, T. J., Logan, G. D., & Schall, J. D. (2014). Response times from ensembles of accumulators. *Proceedings of the National Academy of Sciences*, *111*(7), 2848-2853.

Zelinsky, G. J., & Bisley, J. W. (2015). The what, where, and why of priority maps and their interactions with visual working memory. *Annals of the New York Academy of Sciences*, *1339*(1), 154-164.

Zhang, M., & Barash, S. (2000). Neuronal switching of sensorimotor transformations for antisaccades. *Nature*, *408*(6815), 971-975.

Zhang, M., & Barash, S. (2004). Persistent LIP activity in memory antisaccades: working memory for a sensorimotor transformation. *Journal of Neurophysiology*, *91*(3), 1424-1441.

Zheng, T., & Wilson, C. J. (2002). Corticostriatal combinatorics: the implications of corticostriatal axonal arborizations. *Journal of neurophysiology*, *87*(2), 1007-1017.